Design of Steam Gathering System for Menengai Geothermal Field, Kenya

Stephen Odhiambo Onyango

Faculty of Industrial Engineering, Mechanical Engineering and Computer Science
University of Iceland
2015

Design of Steam Gathering System for Menengai Geothermal Field, Kenya

Stephen Odhiambo Onyango

60 ECTS thesis submitted in partial fulfillment of a
Magister Scientiarum degree in Mechanical Engineering

Advisors
Professor Magnus Þór Jónsson
Doctor Halldor Palsson

Faculty Representative
Halldor Palsson

Faculty of Industrial Engineering, Mechanical Engineering and Computer Science
School of Engineering and Natural Sciences
University of Iceland
Reykjavik, February 2015

Design of Steam Gathering System for Menengai Geothermal Field, Kenya.
Design of Steam Gathering System for Menengai, Kenya
60 ECTS thesis submitted in partial fulfillment of a *Magister Scientiarum* degree in Mechanical Engineering.

Faculty of Industrial Engineering, Mechanical Engineering and Computer Science
School of Engineering and Natural Sciences
University of Iceland
VRII, Hjarðarhaga 2-6
107, Reykjavik
Iceland

Telephone: 525 4000

Bibliographic information:
Stephen Onyango, 2015, Design of Steam Gathering System for Menengai Geothermal Field, Kenya.
Faculty of Industrial Engineering, Mechanical Engineering and Computer Science, University of Iceland, pp. 109.

Printing: Haskolaprent, Falkagata 2, 107 Reykjavik
Reykjavik, Iceland, February 2015

Abstract

Utilizing high temperature geothermal resources for power generation requires design of steam gathering system to transport geothermal fluids. The aim of this project is develop a model that can be used to optimize the steam gathering and the re-injection systems in Menengai geothermal field. The objective function includes the capital investment and the operational cost. The constraints are the steam and water velocity and the upward slope of the two phase flow pipelines. To test the model, different scenarios are analyzed considering different location of the power plants, the separators and the re-injection system. For each scenario the variable topography distance transform is used to locate the separators and find the pipeline route. Topology design optimizes the pipe network and flow in each pipe. The geothermal area is represented by digital elevation matrix (DEM) that is a digital file consisting of the terrain elevations for ground positions at regularly spaced horizontal intervals. Variable topography distance transform (VTDT) is based on chamfer metric distance transform algorithm where the height points from the DEM is incorporated in such way that the heights are assigned to each cell. Developed model is used to size basic components of steam gathering system using Menengai geothermal field data.

Útdráttur

Nýting háhita til orkuframleiðslu krefst hönnunar á gufusöfnunarkerfi til að flytja jarðhitavökvann. Markmið þessa verkefnis er að þróa líkan sem hægt er að nota til að hámarka afköst gufusöfnunar og niðurdælingarkerfisins á Menengai jarðhitasvæðinu að meðtöldum fjárfestinga- og rekstrarkostnaði. Helstu hindranirnar er gufu- og vatnshraðinn og hækkandi halli tveggja fasa leiðslnanna. Til að prófa líkanið, eru mismunandi umhverfisaðstæður rannsakaðar með tilliti til mismunandi staðsetninga virkjananna, skilvindanna og niðurdælingakerfisins. Fyrir hvert umhverfi var svo notuð breytileg landslagsfjarlægðarbreyta til að staðsetja skilvindur og leiðslurnar. Grannfræðihönnun hámarkar nýtingu leiðslukerfisins og flæði í hverri leiðslu. Jarðhitasvæðið er sett fram með hæðarlíkani (DEM) sem er stafræn skrá sem samanstendur af landslagshæðarupplýsingum á jörðu með reglulegu láréttu millibili. Breytileg landslagsfjarlægðarbreyta (VTDT) er byggð á chamfer fjarlægðarmælieiningarbreytureikniriti þar sem hæðarpunktar í hæðarlíkaninu tákna hæð hverrar eininga. Líkanið sem þróað var er notað til að meta grunnþætti gufusöfnunarkerfisins með gögnum frá Menengai jarðhitasvæðinu.

Dedication

This work is dedicated to my late mother and my two lovely daughters, Daisy and Eileen.

Table of contents

List of Figures

List of Tables

Abbreviations/List of Variables

A = Cross-sectional area on which the stress acts (m^2)

A_p = Inside cross section area of pipe (m^2)

AHP = Analytic hierarchy process

A_p = Additional thickness due to milling and corrosion (m)

C_c = Capital cost (USD)

C_e = Annual energy cost (USD)

C = Form factor, C = 0.6 for pipe

D =Separator diameter (m)

f_G = Gas phase friction factor

f_{tp}= Two phase friction factor

GDC = Geothermal Development Company

h= Equivalent length (m)

h_c= Equivalent length of connection

h_v= Equivalent length of valve

IPP = Independent power producer

k_p = Cost of pipe (USD/m)

k_b = Cost of bend (USD/m)

k_c = Cost of connection (USD/m)

D_e = Diameter of insulation (m)

D_o = Outside diameter of pipe (m)

E = Young's Modulus

e = Seismic co-efficient.

E_w = Weld efficiency

DEM = Digital elevation matrix

D_c = Diameter of cladding (m)

d_{in},D_{in} = Pipe inside diameter (m)

f_L = Liquid phase friction factor

g = Gravitational constant (m^2/s)

H_f = Frictional head (m)

h_b= Equivalent length of bend

h_u= Equivalent length of expansion unit

i = Interest rate (%)

k_i= Cost of insulation material (USD/m)

L_{T1}, L_{T2} = Length between anchors on each axis (m)

L = Developed length of the line axis (m)

k_v= Cost of Valve (USD)

k_u= Cost of expansion unit (USD/m)

k_d= Cost of pump (USD)

L_1, L_2, L_{arm} = Length of arm (m)

L_g= Length between horizontal guide supports (ft)

L_{ANC} = Distance between two anchors (m)

LDM (k) = Local distance measure of the k^{th} element of the mask

L_p = Pipe length (m)

L_s = Distance between two supports (m)

L_{sh} = Distance between horizontal supports (m)

L_{sv} = Distance between vertical supports (m)

M_A = Sustained bending moment (Nm)

M_B = Dynamic bending moment (N/m)

$\dot{m}_{total}$ = Mass velocity (kg/s)

MWDT = Multiple weight distance transform

$\dot{m}_g$ = Mass flow rate of steam or gas (kg/s)

n_b = Number of bends

n_c = Number of connections

n_v = Number of valves

n_u = Number of expansion units

n_v = Number of valves

P = Pump power (W)

P_p = Pump pressure (Pa)

p= Design pressure (Pa)

q = Uniform load (Nm)

Q = Volumetric flow rate (m^3/s)

q_p = Pipe weight (N/m)

q_e = Insulation weight (N/m)

q_e = Cladding weight (N/m)

q_v = Medium weight (N/m)

q_s = Snow weight (N/m)

q_{jv} = Seismic vertical load (N/m)

q_w = Wind load (N/m)

q_{jh} = Seismic horizontal load (N/m)

v = Maximum wind speed (m/s).

U= Anchor distance

W = Total mass flow rate (kg/s)

V = Fluid velocity (m/s)

x = Steam quality

VTDT = Variable topography distance transform

Y= Resultant movement to be absorbed by pipe loop (m)

r = Bend radius (m)

y = Temperature dependant co-efficient

R_e = Reynolds number

S, S_h = Allowable stress at hot condition (Pa)

s = Snow factor (N/m^2)

S_A = Allowable stress range of material (psi)

t = Separator thickness (m)

T = Life time (years)

Z = Section modulus (m^3)

Δ = Expansion from A' to B' (inch)

ΔT = Temperature difference (^{o}C)

ΔH= Elevation difference between end and start of pipe (m)

Δ_{pl}= Pressure drop for the installation (Pa)

ρ_g = Steam density (kg/m^3)

ρ_l = Liquid density (kg/m^3)

ρ_s = Density of steel (kg/m^3)

ρ_e = Density of steel (kg/m^3)

ρ_h = Homogenous density (kg/m^3)

ρ_c = Density of insulation (kg/m^3)

ρ_w = Wind pressure (N/m^2)

ρ_v = Density of medium (Kg/m^3)

μ_L = Liquid dynamic viscosity

μ_G = Gas dynamic viscosity

ϵ = Absolute pipe roughness

μ_{tp} = Two phase dynamic viscosity

α = Seventh power law void fraction

α_p = Co-efficient of thermal expansion (1/^{o}C)

$\varphi_U^2\, n_u h_u$ = Two - phase multiplier for expansion units.

$\varphi_B^2\, n_b h_b$= Two - phase multiplier for bends

$\varphi_V^2\, n_v h_v$ = Two - phase multiplier for valves.

$\varphi_C^2\, n_c h_c$ = Two - phase multiplier for connections.

ε = Void fraction

σ= Surface tension

η = pump efficiency

Acknowledgements

This project will not have been complete without my supervisor, Professor Magnus Þor Jónsson, your continuous guidance and help has been the key in the completion of this project. You spent most your valuable time to help and your patience is highly appreciated. A lot of thanks also goes to Halldor Palsson for his guidance and help during the project.

I want to thank UNU-GTP and in particular the director, Ludvik for giving me the chance to pursue my studies in Iceland. To all staff UNU-GTP and ISOR, thank you so much for assistance offered. I also thank GDC management and manager Geothermal Resource Management (GRM), Mr. Cornel Ofwona for giving me time off to attend the studies. To my colleagues in GRM and my fellow MSc colleagues at UNU-GTP, your contributions and encouragements are highly appreciated.

To my late mother, I wish you were alive today to witness this far I have reached. It has not been easy without you. My lovely daughters Daisy and Eileen, thank you so much, you have missed fathers love for better period of your lives. To my wife Victoria, thank you for being the father and mother of our daughters during this period. Thank you for your understanding and patience. Lastly to God Almighty all praise and glory be onto your name.

1 Introduction

The Kenyan Government has rolled out a 40 month programme to generate 5,000 MW to make Kenya sufficient in its energy requirements and to meet the country‘s desire to attain universal access by 2020 (10 year energy sub-sector report). Geothermal resources have been identified as one of the contributors and about 2,000 MW are expected to be generated from geothermal power. Out of this, Geothermal Development Company (GDC) will contribute over 1,000 MW from geothermal power only. The country have made major gains in this regard following the recent commissioning of 140 MWe Olkaria IV power plant. Accelerating geothermal development has been adopted to ensure the wider objective of universal access is attained.

Kenya have over ten high temperature geothermal fields with a potential of over 10,000 MW. Menengai geothermal field is one of the high temperature geothermal fields located within the Kenya rift valley. It is located about 30 km from Nakuru town. Menengai geothermal field has a potential of over 700 MWe. (Ofwona, 2004). Field development is being carried by state owned Geothermal Development Company (GDC). Menengai is the third geothermal field to be developed in Kenya after Olkaria and Eburru. Figure 1 shows the location of Menengai geothermal field within the Kenya rift valley.

Drilling started in February 2011 by the Geothermal Development Company Limited (GDC).The first well (MW-01) was discharged in April 2011. Several deep geothermal wells have been drilled in the field and some of the wells discharge tested. Production drilling for the first 105 MWe power plant is ongoing and the plant is expected to be commissioned by 2015. This will be the first geothermal power plant in the Menengai geothermal field. The power plants will be operated by Independent Power Producers (IPPs) while steam gathering system and reservoir management will be sole responsibility of GDC.

With the production drilling for the first 105 MWe currently ongoing in Menengai Geothermal field, it is considered important by the Geothermal Development Company (GDC) to find the cost effective and efficient way of transporting geothermal fluid to the power plants and re-injection wells. The Menengai geothermal field is expected to generate over 400 MWe of power during the first phase of geothermal field development. In order for GDC to assure IPPs of reliable steam supply, GDC has started construction of the steam gathering system. However it will be important for the company to find a decision making tool to advise on the design of basic steam gathering equipment in future. It is on this basis that a model is made that can advise on the optimal pipeline route, optimum pipe diameter and thickness, correct separator location and size and the optimal power plant site. Since all wells to be used in this study have been discharge tested, some assumptions on mass flow and production enthalpies will be made for wells that will be drilled in the same well platforms as the tested wells.

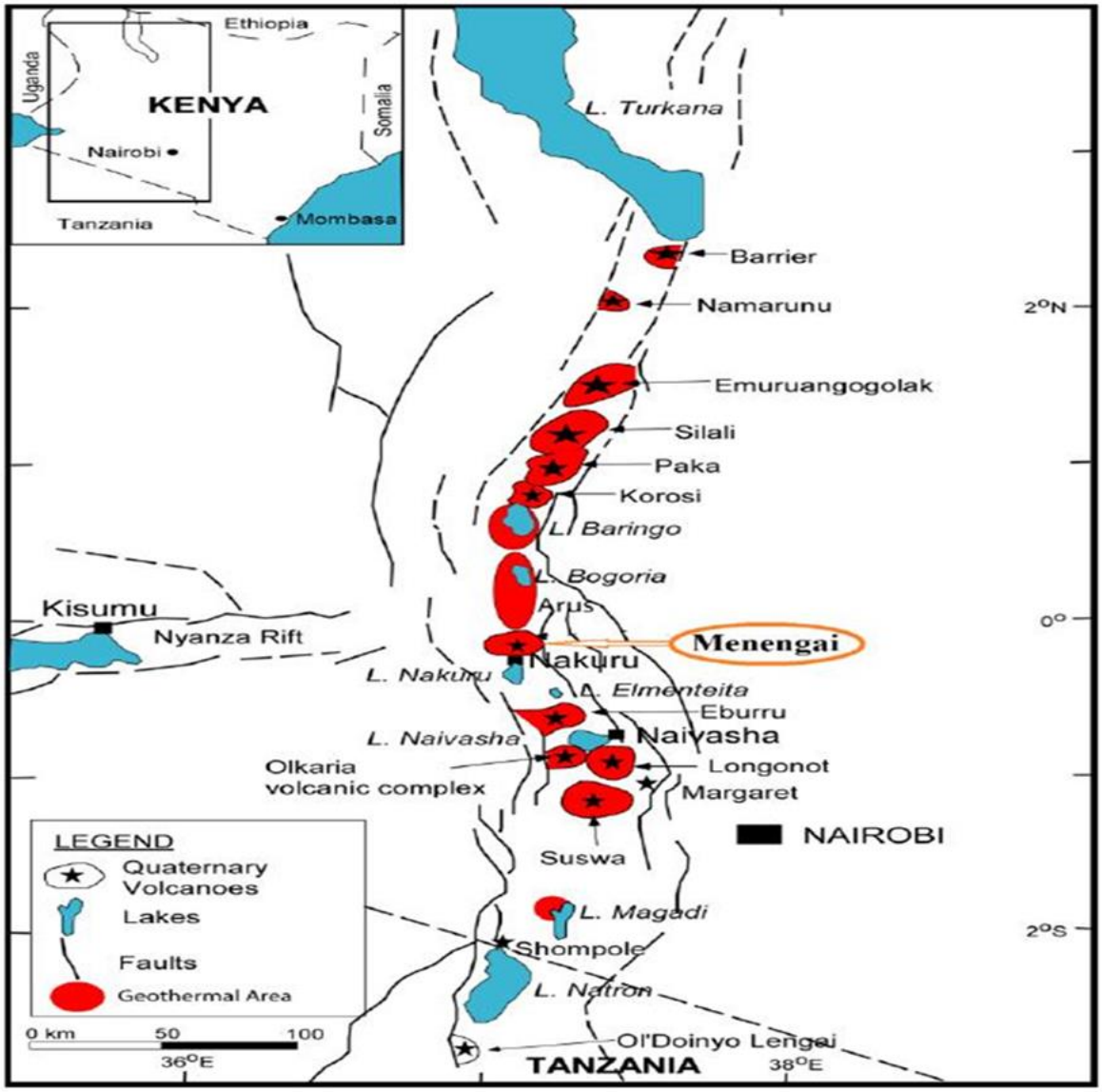

Figure 1: Location of Menengai geothermal field.

Menengai geothermal field is characterized by lava flows, several areas have rough terrain that may pose challenges in finding optimal pipeline route, optimal separator and power plant location. Effort is however made to find areas with relatively moderate terrain that are not far away from the production wells for separator and power plant placements. Reliable and cost effective steam gathering arrangement is crucial for any geothermal project development, emphasis is placed in finding the most cost effective way of designing the steam gathering system.

1.1 Motivation

Steam gathering system contributes about 10 % of the overall cost of geothermal field development. Cost effective steam gathering system arrangement is thus essential for any geothermal project development in the world. GDC has an obligation to supply steam to all IPPs within the Menengai and any other geothermal field under its development. In order to achieve this, a good tool have to be developed to guide the company on selecting the best

pipeline arrangement to ensure it meet its primary objective of steam supply. This therefore requires for a model that can be used to design and size basic steam gathering system equipment. The objective of this study is thus to develop a decision making tool to be used in finding optimal pipeline route across the landscape, optimize pipeline and separator dimensions, locate the best separator station for a group of geothermal wells and lastly give the best power plant location for set of wells or separator stations. The Digital elevation matrix (DEM), location of wells, mass output from tested wells and possible plant locations will be the initial inputs in the model. There exists no such a tool and this will form the basis of preliminary design and with relevant improvements will serve as a guide for future designs within Menengai and other geothermal fields.

1.2 Objectives of the study

The main objectives of this study are to develop decision making tool that can be used to:

- Obtain optimal pipeline route across landscape in Menengai geothermal field.
- Optimize topology design for different pipeline arrangements and layout.
- Predict single phase and two phase pressure drops.
- Select pipeline and separator dimensions for Menengai geothermal wells.
- Optimize the best separator station placement for two-phase wells.
- Optimize the best power plant location for power generation.
- Obtain the total cost of steam gathering system for Menengai geothermal project.

Models are developed to meet the objectives while taking cost effectiveness of the design into account throughout the design process.

1.3 Literature review

Geothermal pipeline design concepts has evolved over the years. In particular, geothermal pipe line route selection has been studied extensively and algorithms developed for finding optimal pipe routes. Distance transform algorithms have been used in pipeline route selection. One of these algorithms is Variable topology distance transform (VTDT). Variable topology distance transform (VTDT) was introduced by De Smith (2005). Kristinsson (2005) used the VTDT to obtain shortest route for geothermal pipelines. Kjærnested (2011) extended the works of Kristinsson (2005) and De Smith (2005) to incorporate the visual effect optimization codes to the VTDT algorithms. The method developed by Kjærnested (2011) was applied on a geothermal field in Iceland giving good results. Multiple weight distance transforms (MWTD) was suggested by Kristinsson (2005) to be used for optimal separator and power plant location. Kjærnested (2011) used this algorithm to place separators and power plant in Hverahlið geothermal field. VTDT algorithm will be used in this study to find optimal distances across landscape within Menengai geothermal field. This study also incorporates weighting criteria for multiple wells to obtain the best separator location.

Pressure loss in pipelines carrying two-phase flow is complex to estimate due to different flow regimes that may occur in the pipe during flow. Several models for predicting pressure loss in pipelines carrying two-phase flows however exists. Most of these models are

analytical and empirical though they have been applied in two-phase pressure drop estimations. According to Thome (2006), several comparisons on the methods have been made and suggestions made for the conditions for using the methods. Gronerud (1972) and Muller-Steinhagen and Heck correlations seems to give best fit with experimental data for two phase frictional pressure drop estimations, (Thome, 2006). Though some methods applied here for estimating two-phase frictional pressure drop models differ when tested with measured data with values of up to 50%, their application will be limited to estimation and comparison with the selected two-phase frictional pressure drop models.

Separators are classified as either vertical or horizontal (DiPippo, 2007) based on orientation. Deciding on vertical or horizontal is however a matter of choice of the designer since both have proved better performance in terms of operation. Vertical cyclone separators were first used in Waireki, New Zealand in 1951 and to date have been used in other countries. Vertical cyclone separators have reported efficiencies of up to 99.99% in Cerro Prieto, Mexico. This has been the separator of choice in geothermal power plants in Kenya.

In any design process, the designers always try to achieve optimal or near optimal solutions to the design problems. Several methods exists for finding the optimal power plant location for a group of wells. MWDT have been suggested by Kristinsson (2005) as a tool for optimising plant location. Analytic hierarchy process (AHP) have been used since its discovery in 1980 by several companies to assist in complex decision making. Several companies have used AHP in solving complex problems. This study uses AHP to optimise the best location for power plant for the Menengai geothermal field. The problem with AHP may lie in giving weights to the evaluation criteria as they have to be decided by the designer.

1.4 Geothermal steam gathering system design

High temperature geothermal resources are found in few areas around the world with active tectonic activity. Most of the resources are developed for power generation and other direct use applications. To utilise these high temperature fluids, fluids have to be transported from deep down the well to the points of use. This therefore calls for design of system of pipes and other equipment to transport and make the fluid suitable for specific application. Fluid flowing from a geothermal well can be single phase (single water or single steam) or two phase (mixture of water and steam). Steam gathering system can therefore be defined as network of pipes from production wells to separator stations, separator stations to power plants and injection wells, separator stations and accompanying control equipment to ensure safe operation. Pipe network and separator stations will be the main focus of this study. Steam gathering system for flash geothermal power plant can therefore be divided into the following parts, namely:

- Production and injection wells;
- Pipelines;
- Steam separators.

All these parts need careful design to ensure efficiency of the entire gathering system. Piping system is required to transport fluids between the points. All pipes in the system have supports, anchors and expansion loops to absorb thermal expansion of the pipe due to temperature difference during installation and operation.

Production and injection wells –geothermal well is a structure of pipes that transports hot fluids from the reservoir to the surface. Most geothermal wells are drilled to depths between 2000 m to 3000 m. Production wells discharge hot fluids that are used for power generation and forms the starting point for fluid utilisation. Injection wells are used to dispose separated water and used water back to the geothermal reservoir. System of pipes transport geothermal fluid from the production wells and to injection wells. The fluid from the geothermal well can therefore be defined by its temperature, pressure and enthalpy. The fluids discharged by a geothermal well can be single phase or two-phase. Re-injection wells are normally located far from production zone within the geothermal field.

Pipes- transport of fluid from one point to another occurs through a pipe line. Piping system includes pipe, fittings (e.g. elbows, reducers, branch connections, etc.), flanges, valves and pipe supports. Suitable route for the pipeline should be obtained to help reduce pressure drop. Two phase pipelines should be designed in most cases to go downhill to avoid plug and slug flow regimes for two-phase flows with low steam ratio. Pressure drop in brine pipelines is controlled to eliminate brine pumping where necessary however it may not be as important since the fluid is being disposed. Pressure loss in steam pipes may affect the overall power capacity of the plant and the turbine inlet pressure. The design of this part of the system entails careful selection of pipe diameter and fluid velocity to minimise total pipeline cost. Steam pipes are relatively bigger compared to water pipes due to low density of steam. The main concern in steam pipe design is the pressure drop. Pressure drop is inversely proportional to pipe diameter, larger pipes have less pressure drop and vice-versa. Installing larger pipes will lead to expensive pipelines that may be uneconomical in the long term. When separators are located close to the power house, the length of steam pipelines will be shorter and when separators are located at well pads, the pipe length might be longer and may result in higher steam pressure drop. A compromise between cost and pressure drop in steam pipes is sometimes necessary. Where separator is located away from the plant, steam traps are fitted in pipelines to remove any condensate formed inside the pipeline. Moisture removers may also be placed close to the power plant to ensure steam entering the turbine is dry. Selection of pipe material for particular application is necessary so as to reduce the chances or rate of corrosion of the pipe material. Pipes are insulated to reduce heat loss, steam pipelines should have less insulation as this will make some steam condense inside the pipeline and help wash and dissolve carryover brine from the separator that can be drained away using drain pots. Higher pressure drop in steam pipelines results in super-heated steam at the end of the pipe, this leads to evaporation of brine carryover from the separator making dissolved solids in brine to form dust that will be trapped in the turbine blades if not removed. These dust will form scales on the turbine blades making it less efficient. Steam pipes should therefore be designed to have less insulation and low pressure drop.

Separators-When geothermal well produce mixture of steam and water (two-phase fluid), the two phases need to be separated from each other. A separator is required to separate the two phases. The separation of the phases occurs due to large density difference between steam and water. Separators can be classified by orientation as either vertical or horizontal (DiPippo, 2007). The separators can be located at the power house, at satellite stations in the field or at the wellheads. Good separator should have high separator efficiency and high outlet steam quality. In geothermal power plants, additional moisture removers are always required to ensure the steam that enters the turbine is dry. The design of these moisture removers and quite similar to the design of separators.

Other parts of the gathering system like well head equipment, control instruments, rock mufflers, brine settling ponds, control valves all form part of the steam gathering design. However these items will not be part of this study.

1.5 Model development process

The chosen software for this study is python programming language however excel is used in topology design as it gives better results using evolutionary algorithms. Python is used as the software of choice for it is free and hence the model can easily be run on any standard pc and updated as need be in the future. All calculations in python are also written in excel to check the accuracy of python calculations.

For any design process, some design data are required. In this study, data gathering forms foundation of the model. Locations of geothermal wells, mass output form the wells, well pressures and production enthalpies are prerequisite. Digital elevation model (DEM) for the geothermal area and other maps are also required. Weather data and pipe material properties have to be defined. The cost of pipe and other works required to install the pipes are also defined. The accuracy of the results of this model relies on the accuracy of the data used as inputs into the model.

This tool starts by obtaining the optimal pipeline route for single and two phase pipes. This is calculated using VTDT algorithm incorporating constraints. The input to VTDT is digital elevation matrix (DEM) and well coordinates. The output gives pipe route and total pipeline length. Pipe line lengths are organized into a distance table to find the best topology for the pipe network by an excel solver code which uses genetic algorithm to find an optimal solution. Distance table and mass flow from each well/platform are the inputs into this module. The output gives the total pipeline length for the wells under consideration and the flow in each pipeline. Elevation difference between start and end of pipe for static pressure drop estimation is also calculated in this step.

The output from topology design forms the basis for diameter optimization. Model to optimise pipe diameter for single phase and two phase flows takes mass flow and pipeline length from topology design. Other fluid properties are calculated based on separation pressure and flow enthalpy or quality. Pipe diameter for two phase flows and steam pipelines requires the knowledge of pressure drop. Lines of code that estimates pressure drop calculates pressure drop for all pipe diameters that are within the defined recommended velocity ranges (25 – 40 m/s for steam and two phase pipelines, DiPippo, 2007). Pipe wall thickness, mechanical stress analysis and total pipeline cost are then calculated for all the pipe diameters selected.

Separator location is optimised using VTDT algorithm, the best place chosen for a group of two phase wells forms the input for separator design and cost. Mass flow, separation pressure and enthalpy are required for sizing and steel price per kilo is used in estimating the cost of material and fabrication of the separator. These prices are however estimates and not actual.

Optimization of power plant location code requires comparison of each criterion for all alternatives and criteria matrix. The code then finds the location with the highest overall

score. AHP process applied looking at three different alternatives considered for power plant placement on five evaluation criteria.

The process is summarised in Figure 2 below where each box represents blocks of codes. The model outputs are the desired values such as total cost of the steam gathering system for all the scenarios considered. The outputs are the results of the main objectives of this study.

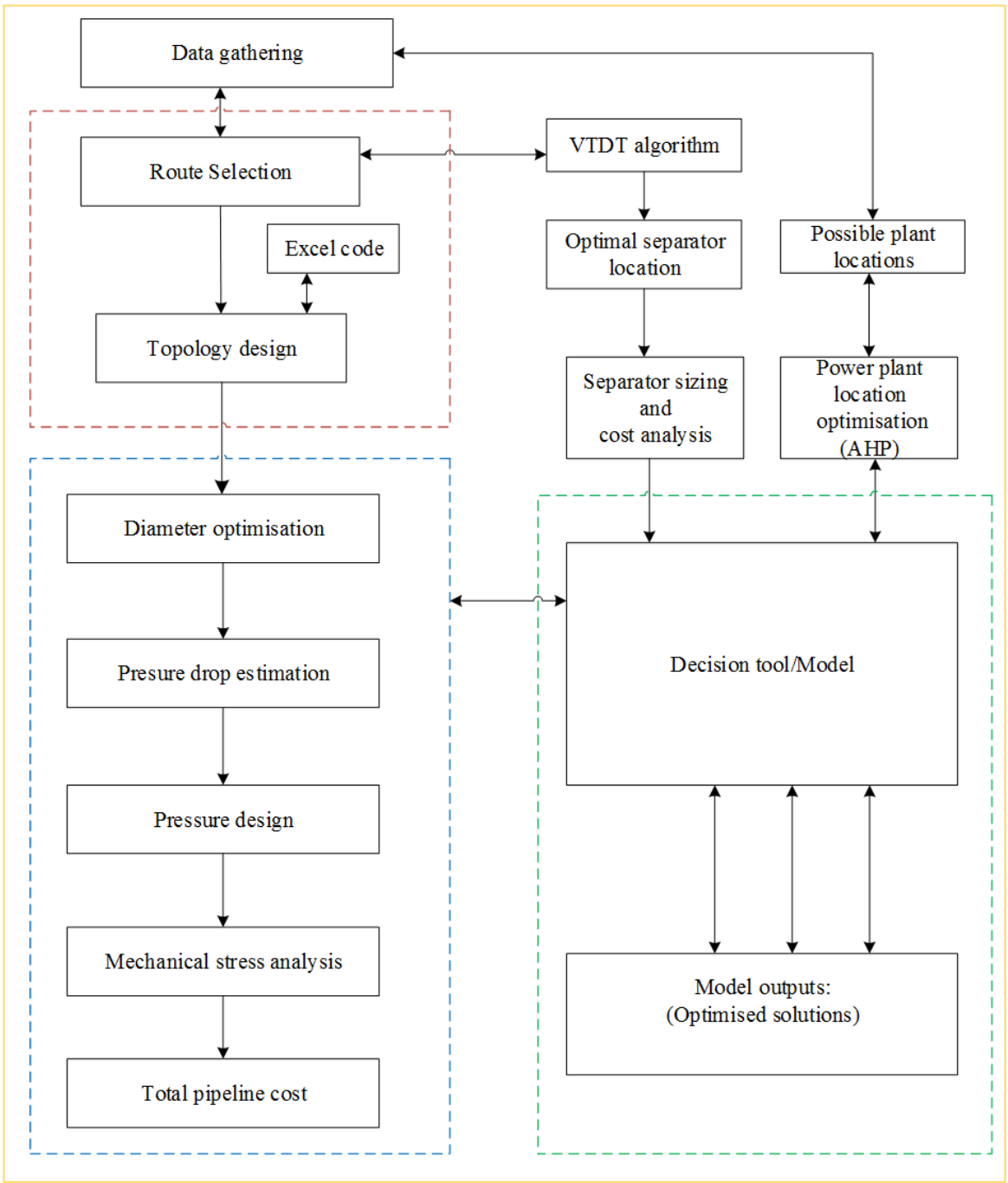

Figure 2: Sketch of modelling process

2 Pipeline design process

Piping is a system of pipes used to transport fluids (liquids and gases) from one location to the other. A standard design process for geothermal fluid pipelines involves the following steps (Mohitpour, Golshan and Murray (2000)):

- Topology and route selection;
- Demand and flow analysis;
- Pipe diameter optimization, minimize the total cost due to head loss;
- Thickness and pressure classes;
- Thermal stress analysis, anchors, expansion loops and expansion units;
- Pump size and arrangement.

Pipe lines can be buried underground or erected above ground. Buried pipelines are not considered in this study. The problem with pipe design is to find pipeline configuration and size within the constraints, which is safe and economical (Henriquez and Aguirre).

2.1 Pipeline route selection and topology design

2.1.1 Pipeline route selection

Route selection is a process of identifying constraints and maintaining the function and economic feasibility of projects. (Þorleikur, 2014). Distance transforms and cost modelling are some of the methods that can be used for geothermal pipeline route selection. Longer pipeline routes results in expensive projects and may also lead to reduced revenue due excessive pressure drop in steam pipelines. The following factors and constraints must be considered prior to selecting the most attractive pipe route, (Mohitpour, Golshan, Murray, 2000):

- Public safety;
- Pipeline integrity;
- Environmental impacts;
- Restricted proximity to existing facilities;
- Cost efficiency.
- Land use constraints

There are different process and design criteria for geothermal pipeline routing. The criteria depend on the fluid that is being transmitted through the pipeline whether it is water, steam or two-phase. One of these methods is distance transforms (DT). Distance transforms is used to obtain optimal paths across the landscape in Menengai geothermal field. The landscape is represented by digital elevation matrix (DEM), and constraints included in the algorithm.

Distance transforms

Distance transforms (DT) is an image processing algorithm. A standard distance transform works with a digital binary image that consists of object points and non-object points. For each non-object point in an image, distance transform obtains the distance from that point to the closest object point. The ability of a distance transform to generate distance isolines is the most important property of distance transform. It is from this property that the possibility of using distance transforms for route optimization arises. (Kjærnested, 2011). When utilizing a distance transform algorithm, exact Euclidean distances are used to generate the distance isolines. This is in essence the a global operation and unless the digital picture is very small, calculating the exact Euclidean distances can be computationally intensive and inefficient, therefore it is more efficient to compute local distances and propagate them over the entire image to estimate the global distances (Smith, 2004) .Chamfer matrices of different sizes have been used but a 5x5 chamfer is used in the distance transform for finding optimal pipeline route in this study. Table 1 below shows an example of a 5x5 chamfer matrix. The letters a-c represents the incremental distances in the chamfer matrix. A 5 X 5 fractional chamfer is used in this study.

Table 1: 5 X 5 chamfer matrix

2b	c	2a	c	2b
C	b	a	b	C
2a	a	x	a	2a
C	b	a	b	C
2b	c	2a	c	2b

Distance transform provide fast method for estimation of Euclidean distance from every cell of a square to the nearest cell in the target set. Standard distance transform algorithms involves two-pass scan of rectangular or square lattice dataset: forward scan from top left to bottom right, and backward scan from bottom right to top left. Several distance transform algorithms exists and some have been applied in geothermal pipeline route selection, separator location and power plant location.

Distance transform algorithms are used on digital elevation models (DEM) which are digital representation of ground topography. Identifying and selecting appropriate route is not only economical but has also environmental and social benefits. Poorly selected pipeline route can have undesirable consequences e.g. excessive pressure drop, high cost and in some cases loss of life. The specific distance transform used in this study is variable topography distance transform (VTDT). The algorithm finds optimal paths across landscape which in this case is represented as the digital elevation model. Restrictions such as maximum allowable incline for two-phase flows, non-accessible areas are incorporated into the input file and can be easily modified if necessary.

Variable topography distance transforms

Variable topography distance transform (VTDT) can be used to find shortest distance in cells in 3 dimensional landscape by introducing constraints. Each cell have latitude, longitude and altitude values assigned to it. The height difference between cells make it possible for slope between two adjacent cells to be calculated by the algorithm. A variable topography distance transform algorithm offers away to obtain the shortest path by using distance transforms on

digital elevation models and introducing constraints. The central function in VTDT algorithm is given by:

$$slope = \frac{DEM(k) - DEM\ (0)}{LDM(k)}$$

$$if\ ((d_k + LDM\ (k)) < d_0)\ \&\&\ (slope < slopemax)$$

$$then:\ d_0 = d_k + LDM(k)$$

Digital elevation model is a 2-D matrix where every element H_{ij} represents the height in the corresponding surface location (*i,j*). The gradient constraint is implemented in variable topography distance transform by the condition:

$$if\left(H_{i+m,j+n} - H_{ij} < \Delta H_c \text{ and } \alpha_{i+m,j+n} < \alpha_c\right) \text{then } d_{i,j} = min\left(d_{i+m,j+n} + c_{m,n}, d_{i,j}\right)\ else\ d_{i,j} = d_{i,j}$$

Where the height ($H_{i+m,j+n}$) and the slope ($\alpha_{i+m,j+n}$) is calculated from the altitudes of the cells in question from the DEM. The critical values of height difference (ΔH_c) and slope (α_c) are user defined. (Jónsson, 2014).The central function in VTDT algorithm used in this study is modified to incorporate other objectives so as to find optimal separator location for multiple wells. The weighted distances from the wells are used for to find the optimal location for separator station. Maximum incline upwards and height difference are also some of the constraints in VTDT and are user defined. The inputs into VTDT are digital elevation matrix, location of wells, constraints and the coordinates of restricted area(s).

2.1.2 Topology design

Topology design for pipeline network gives the optimal distance between the wells and separator stations, re-injection wells, or power plant. The total distance computed is the optimal distance for all pipeline lengths for the entire system analysed. The input for the topology design model is the output from distance transform organised into a distance table. The method uses genetic algorithms and finds the best arrangement given a set of distances between wells. Flow in each pipeline is also computed by the code as some pipes join based on the scenario considered. The topology model is implemented and optimised in excel. Solver add-in in is used to get the optimised solution for given pipe network. The objective of this is to find the minimum length for a given pipe line network under certain conditions. List of decision variables are defined depending on the number of points a pipe can go to. Integer constraints are placed on decision variables and the model calculates if it is best to have single pipe from each well-pad to the separator or if pipe from one well (s) can be connected together into a bigger pipe to the separator station, power plant or re-injection wells. This approach is used to get the best arrangement for two phase and single phase pipelines (steam and brine pies). The flow in each pipe arrangement is also optimised in excel and is used in subsequent calculations in python.

Topology design is carried out considering all possible power plant locations scenarios and the result are pipe lengths between wells, the total pipeline length and the flows in each of the pipelines. The topology design results are used as input in pipe diameter, pressure drop and pressure design.

2.2 Pipe diameter optimization

The main design objective is to minimize the total cost and at an acceptable pressure drop. The dimension design for pipelines requires the knowledge of total mass flow of the geothermal fluid, flow pressure and temperature. The optimized parameters are the recommended velocity inside the pipelines and pressure drop within the entire pipeline length. Optimizing pipe diameter for brine flows is quite straightforward while steam pipelines and two phase are relatively complex because excessive pressure drop is not desirable as no pumping can be used to compensate for pressure loss.

2.2.1 Single phase flows

Brine leaves the separator at saturated conditions and if pressure in any point within the pipe is less than the saturation pressure, brine flashes into steam. This must be avoided by careful route selection and diameter optimisation. The re-injection wells are in most cases located at lower elevations than the separators to ensure positive hydrostatic head inside the brine pipelines. To optimize pipe diameter for single-phase flow (water), the recommended velocity inside the pipe and the total updated cost have to be considered. The total updated cost method is used for brine pipe diameter optimisation. The pipe diameter with the lowest total updated cost is the optimum diameter. The total updated cost (C_t) is given by the equation 1:

$$C_t = C_c + C_p + (C_o + C_e)(1 - 1/(1+i)^T)/i \quad (1)$$

Where C_p and C_o are pump installation and pump and pipe maintenance costs respectively. The capital cost (C_c) is given by the equation:

$$C_c = L_p k_p + n_b k_b + n_c k_c + n_u k_u + n_v k_v + n_d k_d + L_p k_i \quad (2)$$

The annual energy cost (Ce) is obtained by:

$$C_e = k_e O_h P \quad (3)$$

The pump power (P) is calculated using the equation:

$$P = g\rho H_f Q/\eta \quad (4)$$

In order to calculate friction head (H_f), the velocity (V) and the second equivalent length L_e must be determined. The velocity of the fluid is obtained by the equation:

$$V = Q/\left(\frac{\pi D_{in}^2}{4}\right) \quad (5)$$

The second equivalent length (L_e) is calculated using the equation:

$$L_e = L_p + n_b h_b D_{in} + n_c h_c D_{in} + n_u h_u D_{in} + n_v h_v D_{in} \quad (6)$$

To determine the friction factor (f), the Reynolds number (R_e) should be calculated. Based on the value of the Reynolds number, the friction factor should be calculated from equations 7 and 8 (DiPippo, 2007).

$$R_e \leq 2100, \quad f = 64/R_e \tag{7}$$

$$R_e > 5000, \quad f = 0.25/\left(Log_{10}\left[\frac{\epsilon}{3.7D_{in}} + \frac{5.74}{R_e^{0.9}}\right]\right)^2 \tag{8}$$

Friction head is thus calculated using the equation:

$$H_f = f\,V^2\frac{L_e}{2\,g\,D_{in}} \tag{9}$$

The pump pressure (P_p) can therefore be calculated by the equation:

$$P_p = (\Delta Z + H_f)\rho\, g \tag{10}$$

The total updated cost will be the main parameter for selection of optimum diameter for brine pipelines. Pipe diameter with minimum total updated cost is selected. Figure 3 shows an examples of total updated cost method. It shows a plot of total updated cost verses pipe diameter. The optimum pipe diameter is 550 mm nominal diameter.

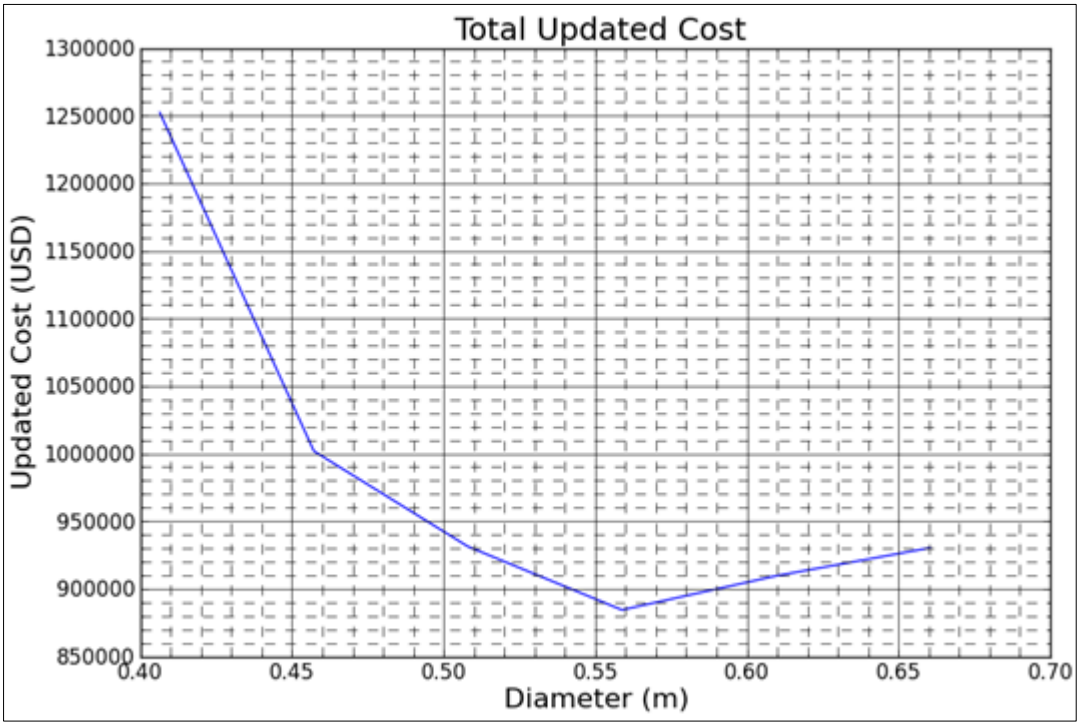

Figure 3: Total updated cost method for brine pipe lines. Pipe length is 500 m, mass flow is 300 kg/s and energy price is 0.22 USD/kWh

The steam pipe diameter is sized based on velocity, pressure drop and capital cost. Low velocity results in low pressure drop but this leads to large diameter pipes which are

expensive. On the other hand, high steam velocity gives smaller diameter pipes but with very high undesirable pressure drop. To select an optimum diameter for steam pipes, a compromise is made between pressure drop and capital cost. Figure 4 shows two plots that can be used to select the diameter of steam pipe based on the pressure drop. The plots are of pipe line cost verses diameter and pressure drop verses diameter.

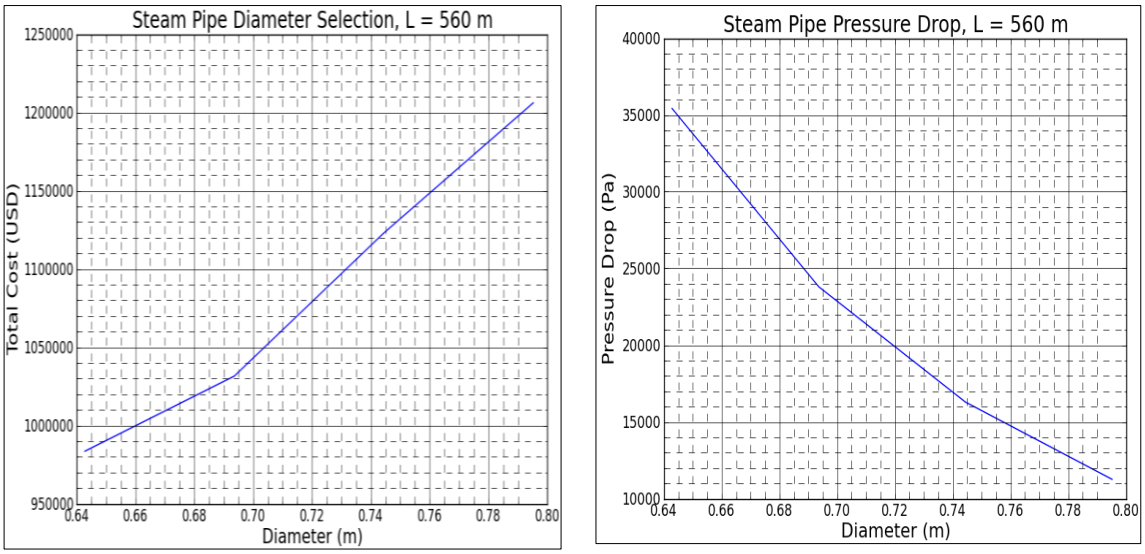

Figure 4: Plot of cost verses diameter on the left and pressure drop verses diameter on the right.

2.2.2 Two phase flows

Two-phase flows are flows where there is simultaneous flow of steam and water. Though in most cases there exist three phases (water, steam and gas), the gas phase is always a very small fraction of the total flow and is disregarded in the calculations. Selecting optimum pipe diameter for transporting two-phase fluids require careful considerations so as to avoid undesirable flow regimes (plug and slug) in the pipeline. These undesirable flow regimes (slug and plug) may damage the pipeline or result in expensive maintenance of pipe and piping components. The maximum recommended velocity of steam (40 m/s) and reasonable pressure drop are two parameters that are used to select the diameter for pipelines carrying two-phase flows. The pressure drop in two phase pipeline consists of momentum, static and frictional pressure drop terms. The diameter is selected so as to always have annular flow regime inside the pipeline carrying two-phase flows. The selected pipe diameter is a compromise between cost and pressure drop. The smallest diameter with the acceptable pressure drop is chosen. Flow regime maps are used to predict the flow type for the selected diameters.

2.3 Pressure drop

Pressure drop in geothermal pipelines is of concern for both two phase and single phase fluids. It is thus important to minimise pressure drop as much as possible. Calculating pressure drop in pipelines carrying single phase fluids is simple and straight forward but two-phase fluids pressure drop require complex calculations. Several approaches are

however available for estimating pressure drop in pipelines carrying two phase geothermal fluid. Actual pressure drop can however be only established through actual measurements.

2.3.1 Single phase pressure drop

Single phase pressure drop is relatively easy to estimate and equations are available for estimating the pressure drop. Pressure drop in steam pipelines can result in reduction of power output from the power plant as it will lower the turbine inlet pressures. On the other hand, pressure drop in brine pipelines may result to flashing inside the pipeline resulting to undesirable flow regimes. Pressure drop in brine pipelines should not be allowed to go below the saturation pressure at the separation temperature. The total pressure drop in single phase pipelines comprises the frictional and static pressure drop. The static pressure drop is a function of elevation difference between the end and start of the pipe. The frictional pressure drop is however a function several variables such as fluid velocity (v), pipe inside diameter (d_{in}), pipe roughness (ε), the Reynolds number (Re). In this study, the pipe diameter is optimised so as to reduce the total pressure drop in single phase pipelines. Single phase pressure drop is given by the equation:

$$\Delta P = \left(\Delta Z + H_f\right)\rho\, g \qquad 11$$

Since the separation pressure of 7 bar-a and turbine pressure of 6 bar-a are used as the required design conditions, the pressure loss in steam pipelines can be allowed up to 1 bar-a. Steam pipe diameters with more than 0.2 bar-a pressure drop are not selected and are only considered when the pipeline length is extremely long. This is to purposely ensure the steam inlet to the turbine does not go below the set turbine inlet pressure.

2.3.2 Two phase pressure drop

Two phase pipelines must be designed as efficiently as possible so as to avoid undesirable flow regimes in the pipeline (plug and slug). Pressure drop in the two phase pipelines influences the separation pressure which in turn determines the turbine inlet pressure and how well the geothermal resource can be utilised. There are many theories and correlations available for predicting two phase pressure drop but most of them have been developed using smaller pipes which may not be the case for geothermal applications.

Two phase pressure drop consists of frictional term, gravitational (elevation change) and momentum change. Two main parameters used extensively in two phase pressure drop calculations are mass velocity and void fraction. Several models have been proposed for calculations of the void fraction which will be discussed here. The most widely used void fraction definition is the cross –sectional average void fraction, which is based on the relative cross-sectional areas occupied by the respective phases. (Engineering data book III, Void fraction in two phase flows, page 17-2). Two phase frictional pressure drop is modelled as a single phase pressure drop but with correction factor. The correction factors are discussed in details and applied in the estimation of the frictional pressure drop for pipelines carrying two phase flows. It is important to have a knowledge of flow regime inside the two phase pipe as some friction multipliers depends on the type of flow regime.

Two phase flow regime maps

The complex interaction between the phases in two-phase flow forms an overall outlook of the flow each time, and this overall outlook is categorized into different flow regimes. These flow regimes have been categorized by visual inspection of the flow. The number of flow regimes that can exists in a two phase flow is not exactly known due to the fact that the shift between regimes can become very unclear. A flow regime is a subjective and qualitative concept; therefore, it is not possible to incorporate it into mathematical equations as a parameter. The simplest classification of flow regimes is to use three regimes: separated flow, intermittent flow and distributed flow. Flow regime maps are used to determine the likely flow regime in a pipeline carrying two phase flows. Most of the common flow regime maps available are developed using smaller pipe diameter pipes than the pipes used in carrying two phase geothermal fluids. The most common way to determine the flow regime of a two-phase flow is by using the so called empirical flow regime maps. Empirical flow regime map maps are plots of the transition lines between each flow regime with regard to some flow parameters. These plots are correlated from measurements of the two-phase flow, coupled with some flow regime identifying techniques (Thome 2006). (For original references see *engineering data book III* (Thome, 2006)). An example of classification of flow regimes in a pipe carrying two phase is as shown in the Figure 5 below. Several flow regime maps were used to classify flow regimes in pipelines carrying two-phase flows. The maps are digitised in Matlab and re-plotted so that the equations for lines defining different flow regimes could be implemented in Python.

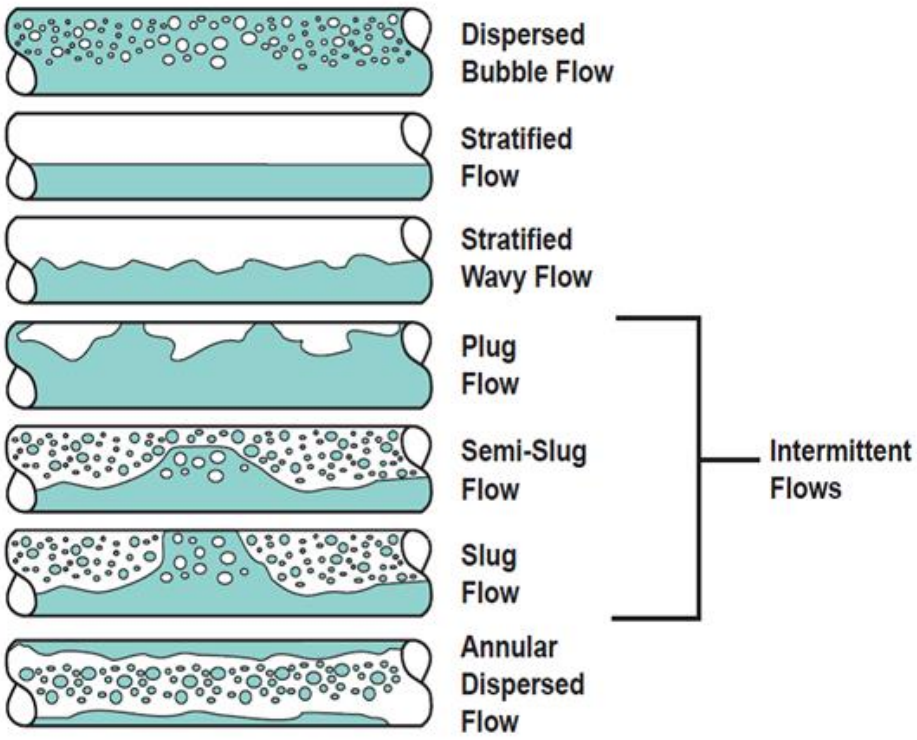

Figure 5: Two-phase flow regime classification

Several flow regime maps were used to classify the two-phase flows for the Menengai pipelines. Some of the maps used are described below.

Baker map

This map is plotted with G/λ against L/ψ where G and L are mass fluxes of the gas and liquid phases respectively while λ and ψ are found using the following equations. (Thome, 2006). This is the widely used map used in two phase flow regime determination.

$$\psi = \left(\frac{0.0724}{\sigma_L}\right).\left(\frac{\mu_L}{0.0009}\left(\frac{1000}{\rho_L}\right)^2\right)^{1/3} \quad 12$$

$$\lambda = \left(\frac{\rho_G}{1.2} .\frac{\rho_L}{1000}\right)^{1/2} \quad 13$$

Weisman map

This map used mass flux as a parameter in obtaining the axes. The x-axis of this map is mass flux of water while the y-axis is the mass flux of air. The map used in this study is adapted from Weisman 1983.

Mandhane map

The map uses volumetric flux as a parameter in obtaining the axes. The x-axis of this map is liquid volumetric flux while the y-axis is the gas volumetric flux. The map used in this study is adapted from Weisman 1974.

Breber et al map

This map is divided into square regions which makes it relatively simple to use for flow regime prediction. The map uses the *Martinelli* number and the *Wallis* factor as the axes, The *Wallis* factor is defined by the equation (Thome, 2006)

$$j^* = \frac{G_L.x}{\sqrt{d\,.g\,.\rho_g(\rho_L - \rho_g)}} \quad 14$$

The *Martinelli* number *(X)* is defined as

$$X = \left(\frac{1-x}{x}\right)^{0.9} \left(\frac{\rho_g}{\rho_L}\right)^{0.5} \left(\frac{\mu_L}{\mu_g}\right)^{0.1} \quad 15$$

Taitel and Duckler map

This map have x-axis given by Martinelli parameter (X) while y-axis is calculated using either one of the following equations:

$$Fr_G = \frac{\dot{m}_G}{[\rho_G(\rho_L - \rho_G)d_{in}g]^{1/2}} \quad 16$$

Where Fr_G is the Froude number for gas phase, the other two parameters T and K are obtained from the equations 17 and 18;

$$T = \left(\left(\frac{dp}{dz}\right)_L\right) / \left(g(\rho_L - \rho_G)\right)^{0.5} \quad 17$$

$$K = Fr_G Re_L^{0.5} \quad 18$$

All the above flow regime maps were used to predict the regime for the designed pipelines. Since the pipelines used in this study are relatively bigger compared to the pipe used for flow regime determinations for particular maps, the results may not be necessarily be correct for the real pipelines. Figure 6 below shows Baker and Weisman 1983 flow regime maps with plots of Menengai wells. The maps predict dispersed flow regimes.

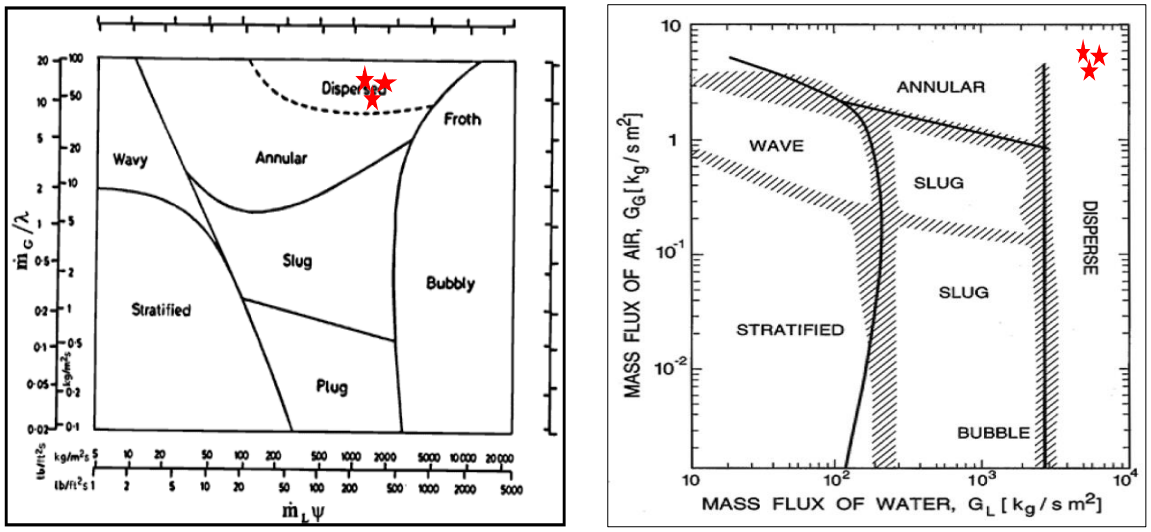

Figure 6: Baker map on the left and Weisman 1983 map on the right. The red stars are plots for Menengai wells. Both maps predict dispersed flow regimes.

Two phase pressure drop models

Two-phase flow models can categorised as either homogenous or separated flow models. Homogeneous flow models assumes that water and steam phase flow with the same velocity while separated flow assumes that water and steam phases travel at different velocities. Both these models require calculation of the void fraction, this the ratio of the area occupied by steam to the total area of the pipe cross-section.

Homogeneous flow model

Homogeneous flow of two phase geothermal fluid assumes equal velocities for both liquid and steam phases in the pipeline. The properties of the liquid and steam phases are averaged and used for estimation of pressure drop in the two phase pipelines. In this flow model, homogeneous void fraction equation is used. Pressure drop estimation using homogeneous flow is done and comparison made with other pressure drop estimation methods. The total pressure drop in homogenous flow model is the sum of static pressure drop (elevation head), momentum pressure drop (acceleration) and frictional pressure drop. The homogeneous flow

void fraction is given by equation 19. The void fraction can then be used to estimate the cross sectional areas occupied by the gas and liquid phases.

$$\varepsilon_h = \frac{1}{1 + \left(\frac{1-x}{x}\right)\frac{\rho_g}{\rho_l}} \quad 19$$

To estimate friction pressure drop using homogenous flow model, the following parameters are determined so as to find the frictional head loss. The two phase viscosity is calculated using the equation

$$\mu_{tp} = x\mu_G + (1-x)\mu_L \quad 20$$

Homogenous density is calculated by the equation:

$$\rho_h = \varepsilon_h\rho_G + (1-\varepsilon_h)\rho_L \quad 21$$

Homogenous flow Reynolds number is thereby given by:

$$R_e = d_{in}\dot{m}_{total}/\mu_{tp} \quad 22$$

Two phase friction factor for homogenous flow model is thus given by equation 23:

$$f = \frac{0.079}{{R_e}^{0.25}} \quad 23$$

The homogenous friction pressure drop can thus be described by the equation:

$$\Delta P_{friction} = \frac{2fL{\dot{m}_{total}}^2}{d_{in}\rho_h} \quad 24$$

For all frictional pressure drop calculations, the pipe inside diameter is optimised by restricting the maximum velocity of two phase to 40 m/s. The minimum allowed velocity is 25 m/s. The momentum pressure gradient per unit length for homogenous flow model is given by the equation:

$$\left(\frac{dp}{dz}\right)_{momentum} = d\frac{(\dot{m}_{total}/\rho_h)}{dz} \quad 25$$

The static pressure drop is given by:

$$\Delta P_{static} = \rho_h\, g\Delta H \quad 26$$

The total two-phase pressure drop for homogenous model is thereby calculated by equation 27:

$$\Delta P_{total} = \Delta P_{static} + \Delta P_{friction} + \Delta P_{momentum} \quad 27$$

Separated flow models

Total pressure drop for separated flow model is similar to equation 26. This model depicts two distinct pipelines each carrying equivalent single phase fluid. To obtain the area of the pipe occupied by each phase, knowledge of void fraction is necessary. Void fraction is the ratio of area occupied by steam to the total pipe area. Several correlations for void fraction calculations are available for separated flows models, these correlations are classified as either analytical or empirical.

Analytical void fraction models

In this category, two models are considered, Zivi kinetic energy model for annular flow and Levi momentum model are used. The models derived by Zivi are presented below, the first method assumes no liquid entrainment in the gas phase while the second correlation assumes liquid entrainment in the gas phase;

1. Zivi correlation for no liquid entrainment

The equation for the void fraction (ε) is given by:

$$\varepsilon = \frac{1}{1 + \left(\frac{1-x}{x}\right)\left(\frac{\rho_g}{\rho_l}\right)^{2/3}} \tag{28}$$

2. Zivi equation for liquid entrainment is given by the expression, where $e = 0.7$

$$\varepsilon = \frac{1}{1 + e\left(\frac{1-x}{x}\right)\left(\frac{\rho_g}{\rho_l}\right) + (1-e)\left(\frac{1-x}{x}\right)\left(\frac{\rho_g}{\rho_l}\right)^{2/3}\left[\frac{1 + e\left(\frac{1-x}{x}\right)\left(\frac{\rho_g}{\rho_l}\right)}{1 + e\left(\frac{1-x}{x}\right)}\right]^{1/3}} \tag{29}$$

3. The Levi momentum model gives the following expression for the void fraction correlation. In his correlation, Levi assumed that momentum is exchanged between the phases constantly as *x, e,* ρ_g/ρ_l vary, such that the flow tends to maintain an equality of sum of the frictional and static head losses in each phase.

$$\boldsymbol{x} = \frac{\varepsilon(1-2\varepsilon) + \varepsilon\sqrt{(1-2\varepsilon)^2 + \varepsilon\left[2\frac{\rho_L}{\rho_G}\,(1-\varepsilon)^2 \;+\; \varepsilon(1-2\varepsilon)\right]}}{2\frac{\rho_L}{\rho_G}\,(1-\varepsilon)^2 \;+\; \varepsilon(1-2\varepsilon)} \tag{30}$$

Empirical void fraction equations

Several correlations for empirical void fractions are briefly described here below:

1. Smith separated flow model assumes the momentum fluxes in the two phases are equal. It also assumes separated flow consisting of a liquid phase and a gas phase with fraction *e*

of liquid entrained in gas. The simplified expression for Smith separated flow void fraction is given by the expression:

$$\varepsilon = \frac{1}{1 + 0.79\left(\frac{1-x}{x}\right)^{0.78}\left(\frac{\rho_G}{\rho_L}\right)^{0.58}} \quad 31$$

2. Lockhart Martinelli

Void fraction equation is given by the expression:

$$\varepsilon = \frac{1}{1.0 + 0.28\left(\frac{1-x}{x}\right)^{0.64}\left(\frac{\rho_G}{\rho_L}\right)^{0.36}\left(\frac{\mu_L}{\mu_G}\right)^{0.07}} \quad 32$$

3. Seventh power law void fraction

This void correlation is derived from the analysis of two-phase flow velocity distribution using seventh power law. The average velocity of the equivalent single phase flow is used to determine the wall friction factor and hence the two phase pressure drop.

$$\frac{1-\alpha}{\alpha^{7/8}} = \left[\left(\frac{1}{x} - 1\right)\left(\frac{\rho_g}{\rho_f}\right)\left(\frac{\mu_f}{\mu_g}\right)\right]^{7/8} \quad 33$$

4. Drift flux void fraction model

This model was developed by Zuber and Findlay (1965) however it has been modified by Wallis (1965) and Ishii (1977). The expression shows that the void fraction is a function of mass velocity, while the previous theories does not factor this. The expression is given by:

$$\varepsilon = \frac{x}{\rho_G}\left[C_o\left(\frac{x}{\rho_G} + \frac{1-x}{\rho_L}\right) + \frac{\bar{U}_{GU}}{\dot{m}}\right]^{-1} \quad 34$$

Where $\dot{m}$ is the mass velocity, the parameter $\bar{U}_{GU}$ is defined by (Rouhani and Axelsson (1970). (Engineering data book III)

$$\bar{U}_{GU} = 1.18(1-x)\left[\frac{g\sigma(\rho_L - \rho_G)}{\rho_L^2}\right]^{1/4} \quad 35$$

And C_o is defined by

$$C_o = 1 + c_o\,(1-x) \quad 36$$

The constant (c_o) is 0.12

Other void fractions models

There are some other void fraction models used in this study, the three of them are given by the following equations, (Heimisson, 2014).

1. Turner and Wallis model (1965) is given by the expression:

$$\varepsilon = \left[1 + \left(\frac{1-x}{x}\right)^{0.72} \left(\frac{\rho_G}{\rho_L}\right)^{0.4} \left(\frac{\mu_L}{\mu_G}\right)^{0.08}\right]^{-1} \quad 37$$

2. Thome model (1964) is given by the equation:

$$\varepsilon = \left[1 + \left(\frac{1-x}{x}\right) \left(\frac{\rho_G}{\rho_L}\right)^{0.89} \left(\frac{\mu_L}{\mu_G}\right)^{0.18}\right]^{-1} \quad 38$$

3. Baroczy model (1966)

This model for void fraction is defined by:

$$\varepsilon = \left[1 + \left(\frac{1-x}{x}\right)^{0.74} \left(\frac{\rho_G}{\rho_L}\right)^{0.65} \left(\frac{\mu_L}{\mu_G}\right)^{0.13}\right]^{-1} \quad 39$$

Two-phase friction pressure drop

Void fraction and mass velocity are the major parameters used in determination of two phase frictional pressure drop. Frictional pressure drop in two-phase flows is typically predicted using separated flow models. The first of these analyses was performed by Lockhart and Martinelli (1949) and then followed by many others (Thome, 2006). The basic equations of the separated flow model are not dependent on the particular flow configuration adopted. It is assumed that the velocities of each phase are constant, in any given cross-section, within the zone occupied by the phase. Models for the calculation of the correction factor Φ^2 is given in general form as:

$$\Delta P_{fric}^{two\ phase} = \Phi^2\ \Delta P_{fric}^{single\ phase} \quad 40$$

If the single phase is liquid, then the factor should approach 1. It should also approach a relevant scaling value for gas only flow. (Palsson, 2013). Some of the approximations are discussed below: Correlations by Friedel, Muller-Steinhagen and Heck and Gronnerud give reliable results for estimations of friction pressure drop when compared with actual measurements. (Thome, 2006).

1. Friedel (1979) correlation

This is one example of rather complex correction factor for two-phase friction pressure drop. The friction multiplier is given by the equation:

$$\Delta P_{fric} = \Delta P_L\ \Phi_{fr}^2 \quad 41$$

Where ΔP_L is calculated for the liquid-phase flow as:

$$\Delta P_L = 4\, f_L \left(\frac{L}{d_{in}}\right) \dot{m}_{total}{}^2 \left(\frac{1}{2\,\rho_L}\right) \quad 42$$

The liquid friction factor (f_L) and the Reynolds number (R_e) are obtained from equations 43 and 44 respectively.

$$f_L = \frac{0.079}{R_e{}^{0.25}} \quad 43$$

$$R_e = d_{in}\dot{m}_{total}/\mu_L \quad 44$$

The two phase multiplier is thus given by:

$$\Phi_{fr}^2 = E + \frac{3.24\, F\, H}{Fr_H^{0.045}\, We_L^{0.035}} \quad 45$$

The Dimensionless parameters Fr_H , E , F and H are given by equations 46 to 49:

$$Fr_H = \frac{\dot{m}_{total}{}^2}{g d_{in} \rho_H^2} \quad 46$$

$$E = (1-x)^2 + x^2\, \frac{\rho_L\, f_G}{\rho_G\, f_L} \quad 47$$

$$F = x^{0.78}(1-x)^{0.224} \quad 48$$

$$H = \left(\frac{\rho_L}{\rho_G}\right)^{0.91} \left(\frac{\mu_G}{\mu_L}\right)^{0.19} \left(1 - \frac{\mu_G}{\mu_L}\right)^{0.7} \quad 49$$

The liquid phase Weber number (We_L) is given by the equation:

$$We_L = \frac{\dot{m}_{total}{}^2 d_{in}}{\sigma \rho_H} \quad 50$$

The Froude number (Fr_H) and the Weber (We_L) number are the two main dimensionless numbers used in the Friedel approximation. The method is recommended when the ratio of $\left({}^{\mu_L}/_{\mu_G}\right)$ is less than 1000.

2. Lockhart and Martinelli correlation

The method of Lockhart and Martinelli (1949) is the original method that predicted the two-phase frictional pressure drop based on a two phase multiplier for the liquid-phase, or the vapour-phase respectively, as:

$$\Delta P_{fric} = \Delta P_L\, \Phi_{Ltt}^2 \quad 51$$

$$\Delta P_{fric} = \Delta P_G \, \Phi_{Gtt}^2 \quad (52)$$

The gas phase pressure drop is calculated by the equation:

$$\Delta P_G = 4 f_G \left(\frac{L}{d_{in}}\right) \dot{m}_{total}{}^2 \, x^2 \left(\frac{1}{2 \rho_G}\right) \quad (53)$$

The liquid phase friction pressure drop is similar to gas phase friction factor but using liquid physical properties. The corresponding two-phase multipliers for the liquid-phase and vapour-phase are given as:

$$\Phi_{Ltt}^2 = 1 + \frac{C}{X_{tt}} + \frac{1}{X_{tt}^2}, \text{ for } Re_L > 4000 \quad (54)$$

$$\Phi_{Gtt}^2 = 1 + CX_{tt} + X_{tt}^2 \text{ , for } Re_L < 4000 \quad (55)$$

X_{tt} is the Martinelli parameter for both phases in the turbulent regimes defined as:

$$X_{tt} = \left(\frac{1-x}{x}\right)^{0.9} \left(\frac{\rho_G}{\rho_L}\right)^{0.5} \left(\frac{\mu_L}{\mu_G}\right)^{0.1} \quad (56)$$

The value C in the equation depends on the flow regimes of the liquid and vapor phases and can be found in Engineering data book III(Thome, 2006).

3. Chisolm correlation

Chisolm correlation is an extensive empirical method applicable to a wide range of operating conditions. Chisolm two-phase frictional pressure drop gradient is given as:

$$\left(\frac{dp}{dz}\right)_{fric} = \left(\frac{dp}{dz}\right)_L \Phi_{Ch}^2 \quad (57)$$

The frictional pressure gradients for the liquid ($\left(\frac{dp}{dz}\right)_L$) and gas ($\left(\frac{dp}{dz}\right)_G$) phases are:

$$\left(\frac{dp}{dz}\right)_L = 2 f_L \left(\frac{\dot{m}_{total}{}^2}{\rho_L \, d_{in}}\right) \quad (58)$$

$$\left(\frac{dp}{dz}\right)_G = 2 f_G \left(\frac{\dot{m}_{total}{}^2}{\rho_G \, d_{in}}\right) \quad (59)$$

The friction factors for gas and liquid phases are calculated using their respective dynamic viscosities for turbulent flow regimes. For laminar flow regime (Re < 2000) the friction factor is calculated using the equation:

$$f = 16/Re \quad (60)$$

The Chisolm two phase multiplier is then calculated as:

$$\Phi_{Ch}^2 = 1 + (Y^2 - 1)\left[B\, x^{(2-n)/2}\,(1-x)^{(2-n)/2} + x^{2-n}\right] \quad 61$$

Where n is the exponent from the friction factor expression of Blasius (n= 0.25) and the parameter Y is given by:

$$Y^2 = (dp/dz)_G/(dp/dz)_L \quad 62$$

Chisolm parameter is a function of mass velocity and parameter Y. Calculation for parameter B can be found in Engineering data book III (equations 13.2.33 to 13.2.35).

4. Grönnerud correlation

The Grönnerud correlation is given by the equation:

$$\Delta P_{fric} = \Delta P_L\, \Phi_{gd} \quad 63$$

His two phase multiplier is thus given by:

$$\Phi_{gd} = 1 + \left(\frac{dp}{dz}\right)_{Fr}\left[\frac{(\rho_L\ /\rho_G\ )}{(\mu_L\ /\mu_G\ )^{0.25}} - 1\right] \quad 64$$

The frictional pressure gradient depends on the Froude number and is given as:

$$\left(\frac{dp}{dz}\right)_{Fr} = f_{Fr}\ [x + 4(x^{1.8} - x^{10}\ f_{Fr}^{0.5})] \quad 65$$

If $Fr_L \geq 1$, then the friction factor f_{Fr} =1, or if $Fr_L < 1$, then

$$f_{Fr} = Fr_L^{0.3} + 0.0055\left(ln\frac{1}{Fr_L}\right)^2 \quad 66$$

The parameter (Fr_L) is given by the equation:

$$Fr_L = \frac{\dot{m}_{total}^2}{g d_{in}\, \rho_L^2} \quad 67$$

The correlation is applicable to vapour qualities from 0 ≤ x ≥ 1.

5. Bankoff correlation

Bankoff multiplier is an extension of homogenous model , His two phase frictional gradient is expressed as:

$$\left(\frac{dp}{dz}\right)_{fric} = \left(\frac{dp}{dz}\right)_L\ \Phi_{Bf}^{7/4} \quad 68$$

The liquid phase pressure gradient is obtained and the Bankoff two-phase multiplier (Φ_{Bf}) is calculated as:

$$\Phi_{Bf} = \frac{1}{1-x}\left[1-\gamma\left(1-\frac{\rho_G}{\rho_L}\right)\right]^{3/7}\left[1+x\left(\frac{\rho_L}{\rho_G}-1\right)\right] \quad 69$$

Where:

$$\gamma = \frac{0.71 + 2.35\frac{\rho_G}{\rho_L}}{1+\left(\frac{1-x}{x}\right)\left(\frac{\rho_G}{\rho_L}\right)} \quad 70$$

6. Muller-Steinhagen and Heck correlation

This correlation proposed a two-phase friction pressure gradient that in essence is an empirical interpolation between all liquid flow and all vapor flow. It is given by:

$$\left(\frac{dp}{dz}\right)_{fric} = G(1-x)^{1/3} + Bx^3 \quad 71$$

Where G is a factor given by:

$$G = A + 2(B-A)x \quad 72$$

The parameter A is the frictional pressure gradient for liquid flow $(dp/dz)_L$ while B is the frictional pressure gradient for all gas flow $(dp/dz)_G$.

7. Zhao 2000 correlation

The average liquid-phase velocity and the wall friction factor were first introduced to predict two-phase pressure drop using the techniques developed for single-phase flows. Zhao et al. (2000) extended the idea to pseudo flow since the flow has the same boundary layer velocity distribution as the two-phase liquid layer. A correction factor was introduced in determining the liquid-phase velocity ($\bar{V}_l$).

$$\bar{V}_l = 1.1(1-x)\frac{W(1-x)}{\rho_l(1-\alpha)A} \quad 73$$

Where $1.1(1-x)$ = A correction factor mainly for entrainment. The average velocity of the equivalent single-phase flow ($\bar{V}$)can be calculated using the equation:

$$\frac{\bar{V}_l}{\bar{V}} = \frac{\left(1-\sqrt{\alpha}\right)^{8/7}\left(1+\sqrt[8/7]{\alpha}\right)}{(1-\alpha)} \quad 74$$

The mixture density (ρ_{tp}) can be calculated by the equation:

$$\rho_{tp} = \rho_g\alpha + \rho_l(1-\alpha) \quad 75$$

The two-phase dynamic viscosity if defined by:

$$\mu_{tp} = \mu_g x + \mu_l(1 - x) \quad (76)$$

From the average velocity of the equivalent single-phase, the Reynolds number and the two-phase friction factor can be calculated using the equation:

$$R_e = d_{in}\dot{m}_g/\mu_{tp} \quad (77)$$

The friction factor (f_{tp}) is then given by:

$$f_{tp} = \frac{0.316}{Re^{0.25}} \quad (78)$$

The combined momentum and frictional pressre drop due to pipe length can be calculated by (Zhao et al., 2000):

$$\Delta P_L = \frac{f_{tp}\,\rho_l\,\bar{V}^2}{2\,d_{in}(1 - AC)}.L \quad (79)$$

AC is the acceleration correction and is given by the equation:

$$\text{AC} = \dot{m}_g/\rho_g\, pA^2\alpha \quad (80)$$

8. Chisolm and Liard correlation

Equations 81 to 82 are used for estimating two phase frictional pressure drop:

$$\Delta P_{fric} = \Delta P_L\, \Phi_{CL} \quad (81)$$

$$\Phi_{CL} = 1 + \frac{C}{X} + \frac{1}{X^2} \quad (82)$$

Where X is the Martinelli parameter and parameter X^2 is given by:

$$X^2 = \frac{f_l\,(1 - x)^2\,\rho_g}{f_g\,x^2\,\rho_l} \quad (83)$$

Where f_l and f_g are friction factors for liquid and gas phases respectively flowing alone in the pipe. If both phases are turbulent (very likely), C = 21.

9. Beckers correlation

This is pressure dependent friction correction factor. The factor is given by the equation:

$$\Delta P_{fric} = \Delta P_G\, \Phi_{Be} \quad (84)$$

Where Φ_{Be} , is the two-phase multiplier for the Becker's approximation and is given by:

$$\Phi_{Be} = 1 + 2400\left(\frac{x}{p}\right)^{0.96} \quad (85)$$

Where *p* is the liquid pressure;

Pressure drop in bends and other installations

Due to complexity of two phase flows, modelling two phase flows through bends is a difficult task. Empirical correlations for predicting two phase pressure drop in bends and other installations are however available. Three of such empirical approximations are presented below, (Mundakir and Lee).

1. Chisolm B-type multiplier, 1980

The multiplier for pressure loss in bends is given by:

$$\varphi^2_{\mathrm{BLO}} = 1 + \left(\frac{\rho_{\mathrm{l}}}{\rho_{\mathrm{g}}} - 1\right)(\mathrm{B\,x}(1-\mathrm{x}) + \mathrm{x}^2) \quad (86)$$

Parameter B is defined by equation 87 as:

$$\mathrm{B} = 1 + 2.2/(\mathrm{K_{BLO}}\,(2 + \tfrac{\mathrm{r}}{\mathrm{D_{in}}})) \quad (87)$$

And $\mathrm{K_{BLO}}$ is expressed as:

$$\mathrm{K_{BLO}} = 1.6\,\mathrm{f\,h} \quad (88)$$

The general pressure drop (Δ_{pI}) for bends, expansion units, valves and connections is therefore given by:

$$\Delta_{\mathrm{pI}} = \frac{\mathrm{f}\rho_{\mathrm{tp}}\overline{\mathrm{V}^2}}{2}\,(\varphi^2_{\mathrm{B}}\,\mathrm{n_b h_b} + \varphi^2_{\mathrm{C}}\mathrm{n_c h_c} + \varphi^2_{\mathrm{U}}\mathrm{n_u h_u} + \varphi^2_{\mathrm{V}}\,\mathrm{n_v h_v}) \quad (89)$$

2. Chisolm B-type multiplier, 2000

The 2000 multiplier is similar to 1980 multiplier but with a correction factor. The multiplier is given by:

$$\varphi^2_{\mathrm{BLO}} = \frac{1}{(1-x)^2}\left\{1 + \left(\frac{\rho_{\mathrm{l}}}{\rho_{\mathrm{g}}} - 1\right)(Bx(1-x) + x^2)\right\} \quad (90)$$

The multiplier is substituted into equation 89 to obtain pressure drop due to bends and other installations.

3. A Palidowa (1992) Correlation

Palidowa correlation is given by the equation:

$$\varphi_{GO}^2 = [\varphi + A(1 - \varphi)x](1 - x)^{0.333} + x^{2.276} \quad 91$$

Where φ is given by the equation:

$$\varphi = \frac{\rho_g}{\rho_l} \left(\frac{\mu_l}{\mu_g}\right)^{0.25} \quad 92$$

And A is a constant equal to 2.7.

Total two phase pressure drop

Total pressure drop for two-phase flows is given by the equation:

$$\Delta P_{total} = \Delta P_{static} + \Delta P_{friction} + \Delta P_{momentum} + \Delta P_I \quad 93$$

2.4 Mechanical design of pipes

2.4.1 Pipe thickness and pressure class

Pipe thickness calculation requires the knowledge of the operating pressure conditions. The objective is to find the minimum pipe wall thickness necessary to resist the design pressure over the entire pipeline lifetime. According to ASME B31.1, the nominal pipe thickness (t_n) is larger or equal to the required pipe thickness (t_m) according to the equation 94.

$$t_n \geq t_m = \frac{p\, D_o}{2\,(S\, E + p\, y)} + A \quad 94$$

3 mm is added to the minimum wall thickness in order to get required wall thickness, this carters for corrosion allowance, plate allowance and manufacturing allowance. Well pressure can be optimised to give the maximum flow. This however is difficult when wells in the same field have different closing pressure. The operating pressure can be set depending on the well head pressures of the wells used. The design pressure is calculated by adding the some margin to the operating pressure. This is the maximum pressure the pipeline is expected to withstand during its entire lifetime.

2.4.2 Mechanical stress analysis

Loads acting on pipeline

Any piping system is subjected to a number of loadings during its lifetime. These loadings can be one or combination of the following loads: internal and/ or external pressure, temperature, weight of piping and contents (the weight of the pipe, fittings, valves, insulation and cladding, the weight of the conveyed fluid, the weight of the test fluid), climatic loads (wind and snow load), dynamic effects due to the fluid (water hammer, forces from safety valves and rupture disks), movement of the ground and buildings, vibrations from

machinery, earthquakes. The loads that act on a pipe can generally be categorised as either sustained or occasional.

Sustained load criteria

The following condition must be fulfilled for the distance between supports based on sustained loads.

$$\frac{P\ D_o}{4\ t_n} + 0.75\ i\ \left(\frac{M_A}{Z}\right) \leq\ S_h \tag{95}$$

Section modulus (Z) is given by:

$$Z = \frac{\pi}{32}\left(\frac{D_o^4 - D_{in}^4}{D_o}\right) \tag{96}$$

Vertical sustained loads

Vertical sustained loads (q_{sv}) include pipe weight (q_p), piping components weight, insulation weight (q_e) and cladding material weight (q_c) and can be calculated from the equations:

$$q_{sv} = q_p + q_e + \ q_c \tag{97}$$

$$q_p = \ \pi\ g\ \rho_s\ \left(\frac{D_o^2 - D_{in}^2}{4}\right) \tag{98}$$

$$q_e = \ \pi\ g\ \rho_e\ \left(\frac{D_e^2 - D_o^2}{4}\right) \tag{99}$$

$$q_c = \ \pi\ g\ \rho_c\ \left(\frac{D_c^2 - D_e^2}{4}\right) \tag{100}$$

Occasional loads

When occasional loads act upon a pipeline, the following conditions must be fulfilled:

$$\frac{P\ D_o}{4\ t_n} + (0.75\ i)\ \left(\frac{M_A}{Z}\right) + \ (0.75\ i\ )\left(\frac{M_B}{Z}\right) \leq\ kS_h \tag{101}$$

k= 1.20 if load is less than 1% of operational time
k= 1.15 if load is less than 10% of operational time
k= 1.00 if else

Vertical occasional loads

Vertical occasional loads (q_{dv}) consist of transported medium weight (q_v), snow weight (q_s) and seismic loads (q_{jv}) and is calculated as:

$$q_{dv} = q_v + q_s\ +\ q_{jv} \tag{102}$$

$$q_v = \pi\, g\, \rho_v \left(\frac{D_{in}^2}{4}\right) \quad (103)$$

$$q_s = 0.2\, S\, D_c \quad (104)$$

$$q_{jv} = 0.5\, e\, q_o \quad (105)$$

$$q_o = q_v + q_p + q_e + q_c \quad (106)$$

Horizontal occasional loads

Horizontal occasional loads (q_{dh}) is the maximum value of wind (q_w) or seismic load (q_{jh}) that can be calculated.

$$q_{dh} = \max [q_w, q_{jh}\ ] \quad (107)$$

$$q_w = C\, \rho_w\, D_c \quad (108)$$

$$\rho_w = v^2 / 1.6 \quad (109)$$

$$q_{jh} = e\, q_o \quad (110)$$

2.4.3 Bending moments

The pipe is assumed to be a simple beam, thus, the bending moment for sustained load and dynamic load is calculated using equations 111 and 112 respectively:

$$M_A = q_{sv} \frac{L_s^2}{8} \quad (111)$$

$$M_B = \sqrt{(q_{dv}^2 + q_{dh}^2)} \cdot \left(\frac{L_s^2}{8}\right) \quad (112)$$

2.4.4 Length between supports

Based on the bending moments and other conditions set above, the distance between supports is chosen so as to satisfy certain design conditions. The distance between supports (L_s) is calculated by;

$$L_s^2 \leq \frac{\left[k\, S_h - \frac{P\, D_o}{4\, t_n}\right]\left[\frac{\pi}{4}(D_0^4 - D_{in}^4)\right]}{\left[D_o(0.75\, i)\left\{(q_{sv}) + \left(\sqrt{q_{dv}^2 + q_{dh}^2}\right)\right\}\right]} \quad (113)$$

Deflection (δ) equation is used to determine if the deflections are within range for pipelines installed outside the plant based on the length between supports calculated. It is determined by:

$$\delta = \frac{2.07\ q\ L^3}{384\ E\ I} \tag{114}$$

Moment (I) is given by:

$$\mathrm{I} = \frac{\pi(D_o^4 - D_{in}^4)}{64} \tag{115}$$

Length between vertical (L_{sv}) and horizontal (L_{sh}) supports

Supports placed on expansion loop within the pipeline can be termed as vertical or horizontal. The supports are selected so as to satisfy the equation 116.

$$(0.75\ \mathrm{i}) \left\{ (\mathrm{q_{sv}\ L_{sv}^2}) + \left(\sqrt{(\mathrm{q_{dv}\ L_{sv}^2})^2 + \left(\mathrm{q_{dh}\ L_{sh}^2}\right)^2} \right) \right\} \leq \left(k\ S_h - \frac{\mathrm{P\ D_o}}{4\ \mathrm{t_n}} \right) 8\mathrm{Z} \tag{116}$$

2.4.5 Thermal expansion of pipeline

Pipe installation often takes place in ambient conditions while the pipeline operates at elevated temperatures. This brings about expansion of the pipe material due to the temperature difference. The pipe expansion (ΔL) in a pipe of length L is given by the equation:

$$\Delta \mathrm{L} = \alpha\ \mathrm{L}\ \Delta \mathrm{T} \tag{117}$$

The thermal strain (ε_x) is given by:

$$\varepsilon_x = \Delta \mathrm{L}/\mathrm{L} = \alpha\ /\Delta \mathrm{T} \tag{118}$$

Thermal stresses (σ_x) and load on anchors (F) can be calculated by:

$$\sigma_x = \mathrm{E}\ \varepsilon_x \tag{119}$$

$$\mathrm{F} = \mathrm{A}\ \sigma_x \tag{120}$$

Expansion loops

Expansion loops absorbs thermal expansion of the pipeline. Expansion loops can be either u-shape or change of direction type. The following criteria must be met for expansion loop design. The sketches of the expansion loop types are attached in the appendix (**Error! Reference source not found.** and **Error! Reference source not found.**.)

$$\frac{\mathrm{D_o\ Y}}{(\mathrm{L} - \mathrm{U})^2} \leq 208.3 \tag{121}$$

Two expansion loops designs (U-shape and zigzag) are considered in this study namely;

Change of direction (zigzag) expansion loop

Design of change of direction expansion loop is given by equations 122 to 126;

$$Y = \alpha \Delta T . \sqrt{(L_{T1}^2 + L_{T2}^2)} \quad 122$$

$$L = L_1 + L_2 \quad 123$$

$$U = \sqrt{L_1^2 + L_2^2} \quad 124$$

$$L_{ANC} = \sqrt{(L_{T1}^2 + L_{T2}^2)} \quad 125$$

Assuming $L_1 = L_2 = L_{arm}$, the above equation simplifies to equation 126:

$$L_{arm} \geq \sqrt{\frac{D_o \alpha \Delta T L_{ANC}}{71.477}} \quad 126$$

U-shape expansion loop

One of the method used to estimate the loop size is the M.W Kellogg method. M.W Kellogg method uses the Kellogg chart to calculate the loop's size as follows (Kellogg, 1956). The x-axis of this chart is K_2 and isolines for K_1 run across the chart. Dimensions of the loop are obtained by getting the values of K_1 and K_2 and multiplying them by L. The Kellogg chart is attached in the appendix. The distance between guide horizontal supports to the loop (L_C) is calculated as:

$$L_C = \frac{1}{2} L (1 - K_1) \quad 127$$

The y-axis of the chart is obtained by:

$$y_{axis} = \frac{L^2 S_A}{10^7 D_o \Delta} \quad 128$$

The expansion loop dimensions for all pipe configurations are done for both the above methods.

3 Separator placement, design and power plant location

Separation process is very crucial in geothermal flash power plants. Vertical separators can also be referred to as cyclone separators. Cyclone separators are considered in this study with special emphasis on vertical Weber type cyclone separator. Webre type separators with top outlet are more preferable as they give better accessibility to separator inside wall; this makes crack inspection on the inner walls easy and efficient. Top outlet separators also ensure increased efficiency and lower pressure drop (Foong, 2005). Creep water from the vessel wall are trapped and removed. For more details on removal of creep water, see Foong, (2005). Vertical cyclone separators with spiral two phase inlet are considered in this study due to their enhanced efficiency.

3.1 Separator placement

Separators are located at lower elevations than the wells to avoid running two-phase pipelines uphill as this may cause undesirable flow regimes inside two-phase pipelines. It is difficult to have all wells share common separator station as most geothermal sites are located in slopes of volcanoes and in rough terrain thus making it difficult to move all two phase pipelines downhill. Locating separators close to two-phase wells results in low pressure drop in two phase pipelines while having separators close to power plants will lead to higher pressure drops. Low pressure drop in two-phase pipelines results into less steam at high pressure as the amount of water that flashes into steam is less and vice versa. Both high and low pressure drop scenarios may be beneficial based on the reservoir pressures of the geothermal resource being considered.

Optimal separator location is desirable when it can handle group of wells together from the same well pad or from multiple well pads. The optimized separator location for group of wells is obtained using weighted distances in VTDT algorithm. It is however difficult to get some wells connected to a central separator station due to difficulty in topology and restrictions placed in pipelines carrying two phase flows. In such cases a suitable site should be selected for the placement of the individual separator.

3.1.1 Separator placement optimisation

Obtaining best place for central separator requires some weight functions to be incorporated into the VTDT algorithm. Introduction of weights into VTDT algorithm to find near optimal separator location forms one of the main improvements made to variable topology distance transforms and is one of the main achievements of this study. Several weights are introduced and with each weighting criteria, different locations for separator station placement is obtained. The weights includes mass ratio of well flow to total mass flow from all the wells, steam quality and pipeline length. Wells with higher mass flow are given higher weights

than those will less mass flow. Wells with low steam quality are also given higher weights, this is due to the fact that the water phase is higher than steam phase and its more likely to have undesirable flow regimes in those pipelines hence the separator location should be closer to those wells than the ones with higher steam quality. The results of all these will be discussed and how they affect the overall placement of the separator. Including weights in VTDT algorithm for separator placement optimization for geothermal power development can therefore be utilised and decision made on the usefulness of the approach based on the total pipeline lengths from the wells.

3.2 Separator design

The input parameters in separator design are: total flow of two-phase flow into the separator or the steam outflow, the well fluid total enthalpy and the separation pressure/temperature. The process from the well through the separator process is assumed to be isenthalpic. The state of at the separator outlets are considered to be saturated water and saturated steam. Figure 7 below shows a separation process on pressure-enthalpy diagram.

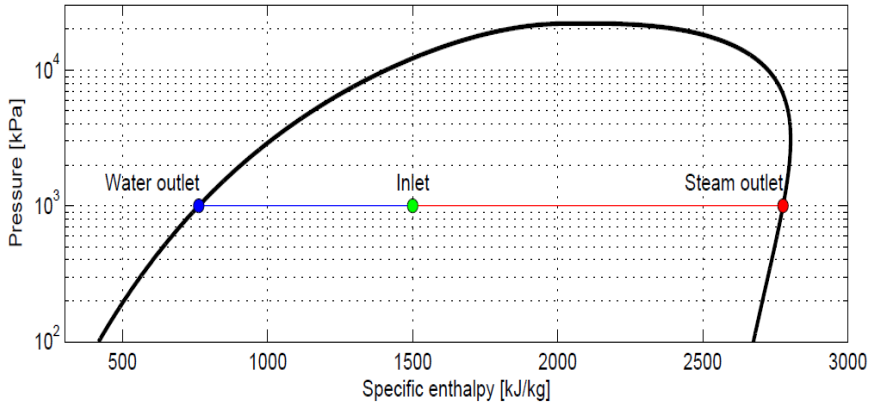

Figure 7: Separation process on p-h diagram

The model output are parameters such as separator size (diameter and height), separator thickness and separation efficiency. Care is taken to size the separator correctly while also ensuring high separation efficiency.

3.2.1 Separator dimensions

Three approaches are considered for finding the appropriate separator dimensions. Lazalde Crabtree, Bangma and spiral inlet guidelines are used for separator sizing (Munggang, 2102). The inlet pipe to the separator (D_t) should be equal to the steam pipe (D_e) and the liquid outlet pipe (D_b). Separation pressure, flow enthalpy and total mass flow in the separator are major parameters in determining the size of the separator. Some of the recommended design guidelines for cyclone separator are summarised in Table 2.

Table 2: Cyclone separator design guidelines (DiPippo, 2007)

Parameter	Separator
Maximum steam velocity at 2-phase inlet pipe	45 m/s
Recommended range of steam velocity at the 2-phase inlet pipe	25 – 40 m/s
Maximum upward annular steam velocity inside cyclone	4.5 m/s
Recommended range of upward annular steam velocity inside cyclone	2.5 – 4.0 m/s

Figure 8 is the sketch of vertical separator.

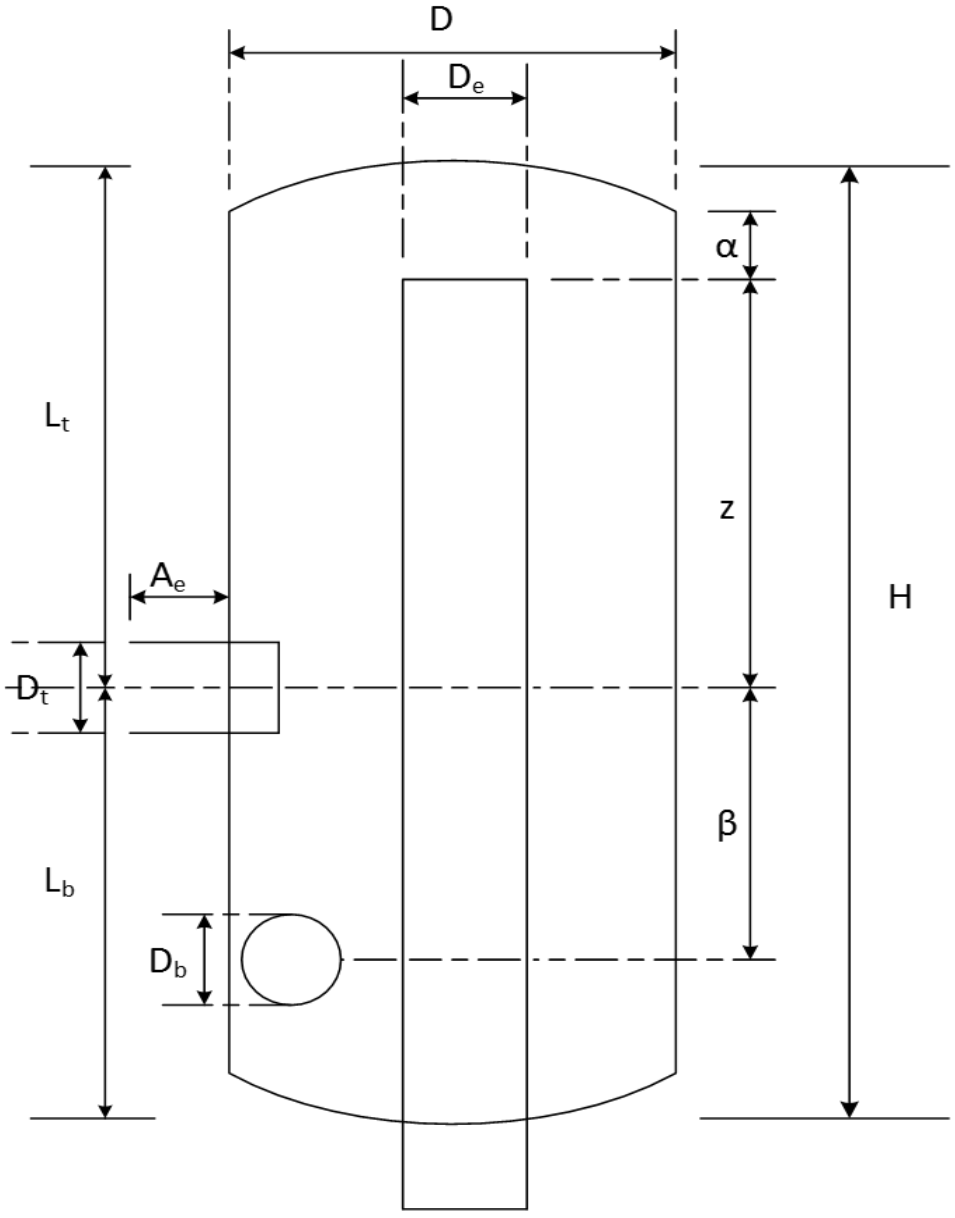

Figure 8: Sketch or vertical geothermal separator

Table 3 shows a summary of design guidelines by Bangma, Lazalde and Spiral-inlet design.

Table 3 : Vertical separator design guidelines (Munggang, 2102).

Parameter	Bangma Design	Lazalde-Crabtree Design	Spiral-inlet design
D	3 D_t	3.3 D_t	2.95 D_t
D_e	0.8 D_t	1 D_t	1 D_t
D_b	1 D_t	1 D_t	0.7 D_t
α	3.25 D_t	0.15 D_t	0.28 D_t
β	3 D_t	3.5 D_t	3.2 D_t
Z	3 D_t	5.5 D_t	5.8 D_t
L_T	7 D_t	6.475 D_t	6.8 D_t
L_B	4.5 D_t	4.975 D_t	4.9 D_t

Care is necessary so as to try as much as possible to take separator dimensions that are practical in construction point of view. This is due to the fact that vertical cyclone separators are used as the separator of choice in the study and very tall separators may pose installation challenges.

3.3 Separator efficiency

The overall separator efficiency is a product of annular (entrainment) and centrifugal efficiency. Computation for separator efficiency is implemented using the guidelines by Lazalde Crabtree. Efficiency is measured by the amount of brine carryover in steam. The outlet steam quality have been reported to be as high as 99.99 % at Cerro Prieto, Mexico. The sizing of all separators considered in this study are done such that the efficiency is always greater than 99%.

3.4 Separator vessel wall thickness

Separation pressure is very critical parameter in separator thickness determination. Low separation pressures are desirable to accommodate any future decline in pressures in production wells and also to increase steam quality. On the other hand, high separation pressures result in low steam output but high-pressure steam. Separator vessel wall thickness is given by equation 129: This equation is assumed to be the same as the pipe thickness equation.

$$t = \frac{p\,D}{2SE - 0.2\,p} + A \qquad 129$$

The thickness of the separator should be sufficient enough to resist the pressure at the separator working conditions.

3.5 Power plant location

Location of power plant affects directly the pipelines length and therefore total pipeline cost. It as well influences pressure drop between the turbine inlet and the separator stations. Analytic Hierarchy Process (AHP) is applied to optimize the power plant location. AHP was introduced in 1980 by Thomas Saaty and it reduces complex decisions to a series of pairwise comparisons. AHP is a process for developing a numerical score to set priorities and make a decision. The AHP can be implemented in three consecutive steps; computing the vector of criteria weights, computing the matrix of option scores and ranking the options (Saaty, 1980). AHP helps decision maker with complex decision making and aid in making the best decision. Alternatives are considered in AHP and criteria used in evaluating the suitability of the different alternatives being considered. In AHP, the best option may not necessarily optimise each evaluating criteria, but it gives the option with the best overall score for the evaluating criteria. Each evaluating criterion is weighted according to pairwise comparison of the criterion. The option with the highest score is chosen as the best after evaluating all the criteria.

The objective of this part of the study is to select the best location for the power plant. Based on the knowledge of the area and the wells already drilled and tested, three (3) areas are identified as potential power plant placement sites (Onyango, 2012). Identification of the three possible locations areas are informed by the available wells and may not necessarily be the best location for future wells that may be drilled in Menengai geothermal field. The evaluation criteria used in this study are carefully chosen and weighted based on their perceived importance. Alternatives are evaluated and the best alternative used in other calculations and also compared with other alternatives on the basis of the total project cost. Three alternatives identified are;

- Area A: This is area around MW-01 to MW-07 (171065,9977308, 1980)
- Area B: Area around MW-11 and heading towards MW-02
- Area C: Area around campsite. (175669,9979235,1840)

Figure 9 shows the three identified areas A, B and C. that will be used in this study as possible power plant locations.

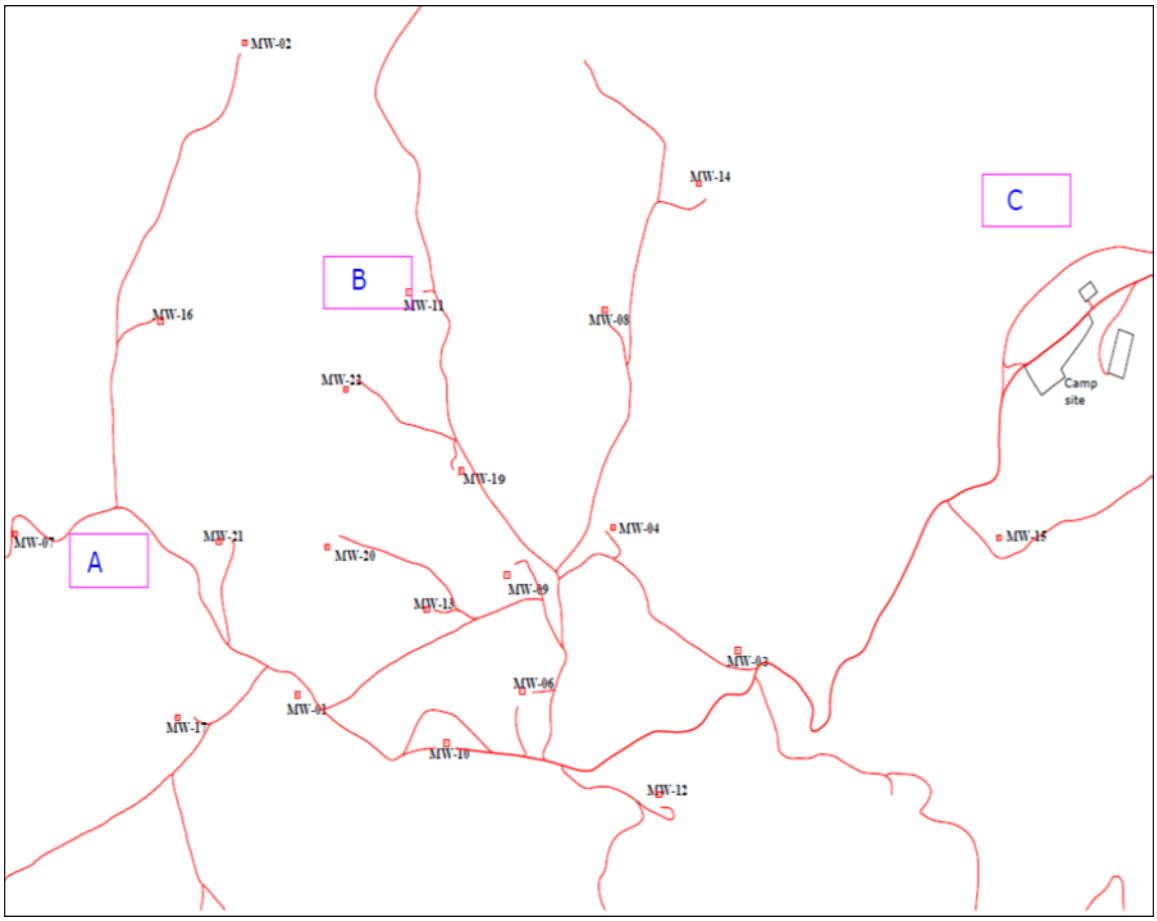

Figure 9: Section of Menengai geothermal field showing possible plant locations

Constraints on possible location for the power plants are determined by the distance from the possible productive wells. The criteria set for power plant location are;

- Land availability
- Distance from production wells
- Distance from re-injection wells
- Pipeline cost
- Number of the wells in Areas

These criteria are evaluated for all the three potential plant sites and the site with the highest total score chosen.

4 Analysis and optimization: Case study - Menengai geothermal field

Construction of 3 X 35 MW power plants is on-going at Menengai geothermal field. The separation pressure for the plants is 7 bar-a. Steam gathering system construction is currently underway for the three power plants.

4.1 Project data

Several data are required as an input to the model. Brief overview of the data is presented here below. Some of the data are not readily available and appropriate assumptions will be made where necessary. The following are the assumptions made;

- The mass flow rate, average enthalpy and well head pressures of planned wells are the same with the already tested wells in the well pads considered.
- The re-injection wells used will have the capacity to take all the brine from separator stations.
- Condensate is re-injected together with the brine
- Distance from wellhead to separator for individual separator is 50 m for all wells
- Only the costs of pipe, bends, valves, connections, insulation, cladding, and their installations along with welding costs are taken into account.
- The steel prices used are estimates and not actual prices
- SI units are used in all calculations
- Insulation thickness of 100 mm is used in all pipeline configurations
- The separation pressure for two phase wells is 7 bara.

4.1.1 Well test data

Well production data are obtained after various other disciplines i.e. geo-scientific research and drilling operations are carried out. All these are crucial as they from the early stages of the well data gathering and acquisition and steam field development. Brief discussion on the early field development work is outlined below.

Geo-scientific work are carried out during the early stages of field development to guide on the best places to site wells that might be productive enough to support power generation. These include geophysical exploration, geochemical exploration, geological exploration, heat-loss surveys and environmental surveys. The data obtained in these surveys are integrated and locations which have better chances of producing hot geothermal fluids targeted for drilling.

Drilling of a geothermal well follows geo-scientific exploration and is the step that proves the viability of the geothermal resource. Well drilling in Menengai takes four stages, drilling 26'' hole, drilling 17 ½'' hole , drilling 12 ¼ '' and lastly 8 ½''. Production casing lies in the 12 ¼ '' hole while 8 ½'' is cased with 7'' slotted liners. The depth of the wells ranges from over 2000 m to about 3000 m. Injection tests are carried out in the wells immediately after drilling to locate permeable zones within the well and also to predict possible productivity of the well.

Heating temperature and pressure profiles are regularly carried out to show how the well is recovering from the effects of drilling and also to determine if the temperatures inside the well is sufficient enough to warrant well discharge. Temperature at the casing shoe is expected to be around 200ºC before discharge is attempted. Well discharge data is obtained after many months of horizontal discharge tests and some data obtained during the tests will be used as input to the model. Lip pressure method by Russell James is used for horizontal discharge test data acquisition. Temperature and pressure profiles of some wells used in this study are attached in the appendix. A summary of drilled and tested wells are given in the Table 4 below and shown in Figure 10.

Table 4: Summary of wells some drilled and their properties

Well ID	Easting (m)	Northing (m)	Elevation (m)	Mass flow (t/hr)	Enthalpy (kJ/kg)		No of wells per pad
MW-01	171847	9976849	2064	230		2000	3
MW-01A	171847	9976849	2064	200			
MW-02	171597	9979478	1898		Re-injection well		
MW-04	173355	9977522	2085	80		1400	2
MW-06	172920	9976864	2102	75		2600	2
MW-07	170499	9977497	1942		Re-injection well		
MW-09	172848	9977331	2105	82		2600	4
MW-10A	172559	9976654	2108	50		1600	3
MW-12	173573	9976446	2106	70		1700	
MW-13	172464	9977193	2052	50		2600	3
MW-19	172629	9977753	2078	70		2000	4
MW-20	171989	9977446	2087	75		2300	3
MW-20A	171989	9977446	2087	110		2500	

Figure 8 below shows the location of some of the drilled wells within the Menengai geothermal field. Most of these wells have been discharge tested while some are still heating up.

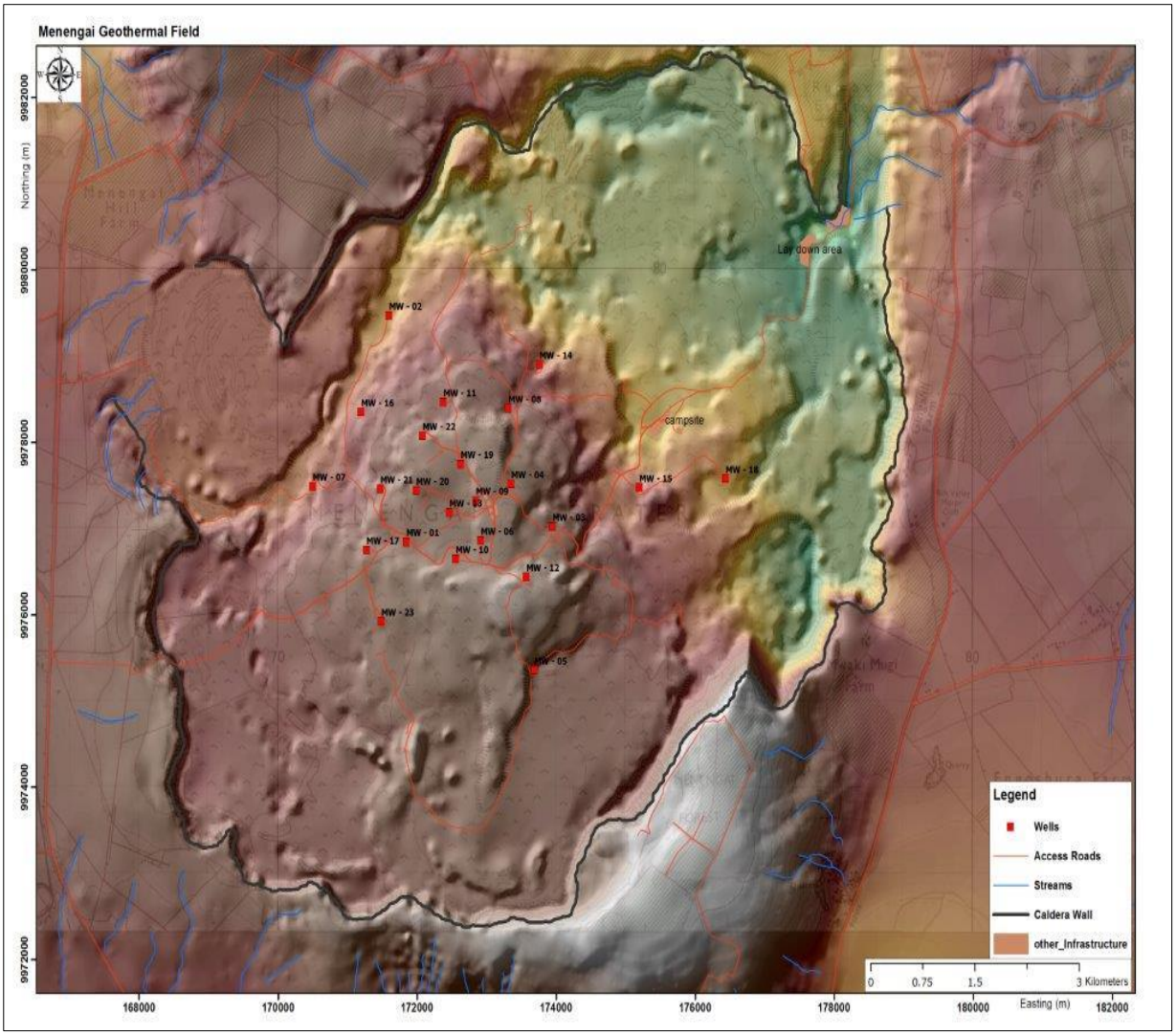

Figure 10: Some of the wells in Menengai geothermal field

4.1.2 Digital elevation matrix

Variable topology distance transforms runs on digital elevation model (DEM) producing distances on a 3-D landscape. The DEM for Menengai is used in the variable topology distance transform as the input file and constraints set so as to be obtained the desired route based on the expected flow type in the pipeline. The output from the distance transform (the pipeline route and length) form the input to topology design, flow modelling and cost analysis.

4.1.3 Weather data

The summary of weather data used in this study for the Menengai geothermal project are summarised in Table 5.

Table 5: Menengai weather data

Climate and geographical characteristics	
Average wet bulb temperature	10^{o}C
Atmospheric pressure	0.8 bar-a
Wind speed	40 m/s
Seismic coefficient	0.2 g
Average elevation	2050 m

4.1.4 Pipe material

The properties of the pipe material used in this project are summarised in Table 6 below. The pipe material is ASTM A53 Gr B.

Table 6: Pipe material properties

Material parameter	**Value**
Young's modulus	200 X 10^{9} Pa
Corrosion allowance	3 mm
Pipe roughness	0.046 mm

4.2 Results

4.2.1 Pipeline route selection

Results from variable topology distance transform are shown in Figure 11 and Figure 12 below. Two phase pipelines are restricted to 1% of the maximum slope upwards while single phase (mainly steam) restricted to about 2% maximum slope upwards. No go zone areas are defined in a matrix and implemented in distance transform so that the pipeline route do not cross those areas. This is important since Menengai geothermal field is located inside a forest reserve with many plant and animal species that must be protected. Man- made obstacles may also be present along the route and must be avoided in the pipeline route.

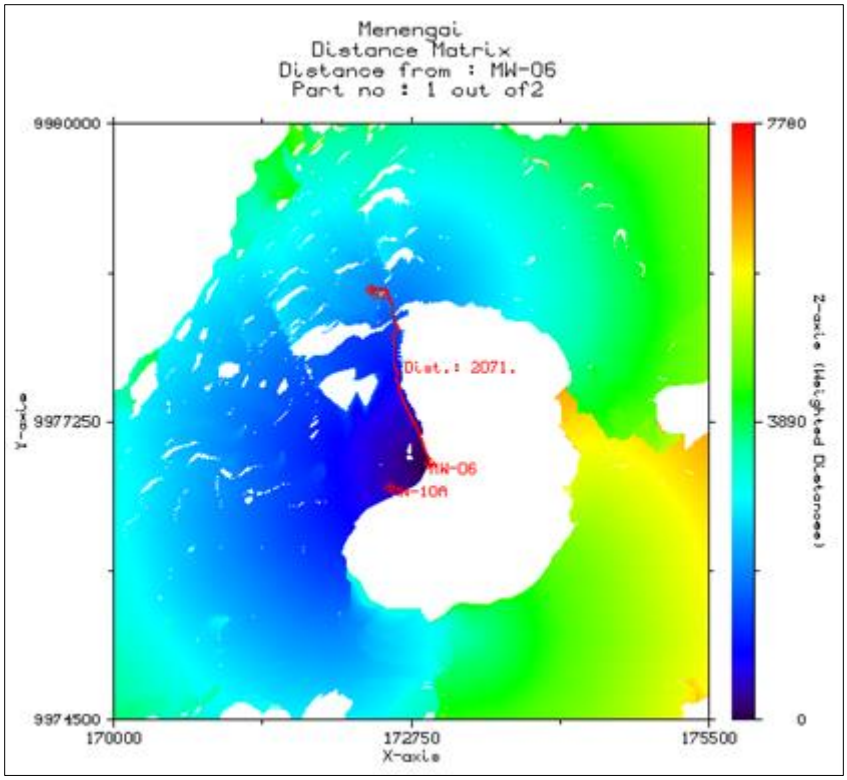

Figure 11: Pipeline route from MW-06 to Area B (MW-11). Blue colour represents areas with lowest weighted distance, red colour indicates areas with highest weighted distance and white colour indicates areas that the pipe route cannot pass through.

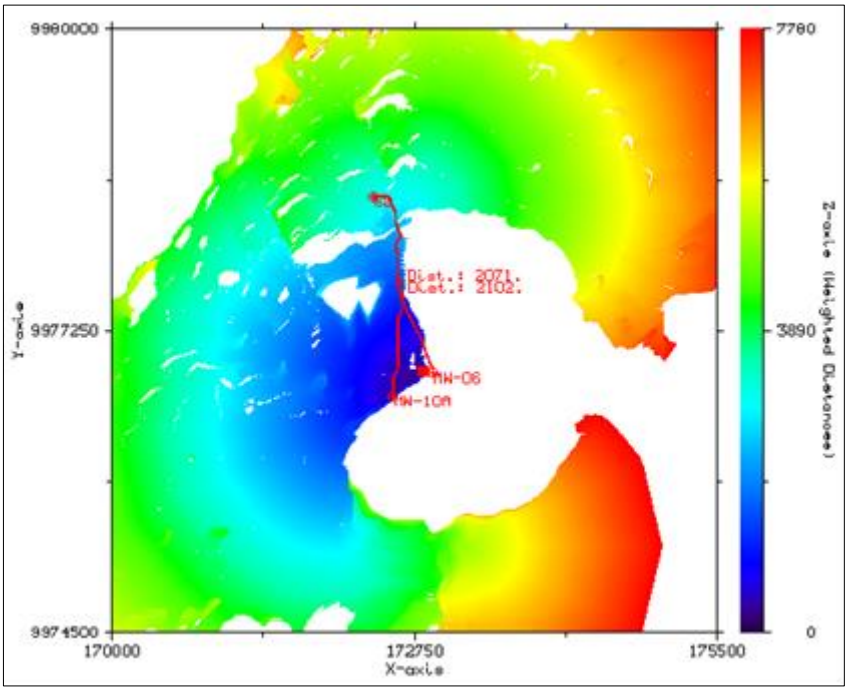

Figure 12: Pipeline route from MW-10A to Area B (MW-11). Blue colour represents areas with lowest weighted distance, red colour indicates areas with highest weighted distance and white colour indicates areas that the pipe route cannot pass through.

When an obstacle is defined, an alternative route is found and in most cases, the pipe lengths are longer than if no obstacle is in place. The Figure 13 below shows pipeline route when an

obstacle is placed along the way. Obstacles can be natural or man-made, barriers or areas that pipeline or other construction activities should not interfere with.

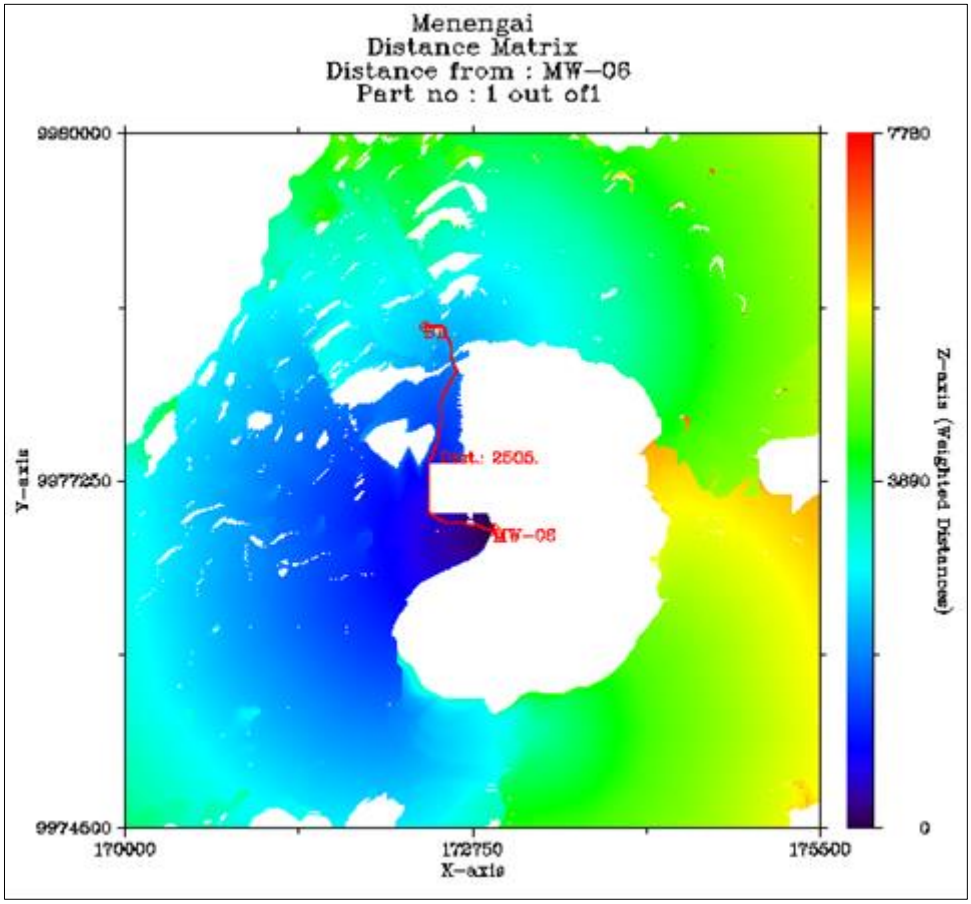

Figure 13: Pipeline route with obstacle on the way. Blue colour represents areas with lowest weighted distance, red colour indicates areas with highest weighted distance and white colour indicates areas that the pipe route cannot pass through.

The overall pipeline length with an obstacle is greater than the length without any obstacle. Pipe length increases from 2071 m to 2506 m when obstacle is placed along the route for MW-06. Some results for the route selection are attached in the appendix.

4.2.2 Pipeline topology design

Different scenarios for pipe topology are presented below. In each scenario, pipelines carrying two-phase, brine and steam are analysed for the case of central separator station and individual separator stations. The total pipeline lengths for all the arrangements and flow in each pipe is obtained. The results for pipeline length for the scenarios presented using type of fluid flowing in each pipe. Topology design helps reduce total pipeline length as opposed to if all the pipelines from different platforms are run directly to separator station, power plant or re-injection well. This optimization helps in overall reduced project cost due to shorter pipelines. Pipeline lengths for common separator and power plant located in area A are summarised in Table 7. Figure 14 show the pipeline layout that gives the minimum total length for common separator when power plant is located in area A. This layout gives the minimum total distance between the wells, arrows shows the direction of flow. Results for other power plant locations are attached in appendix.

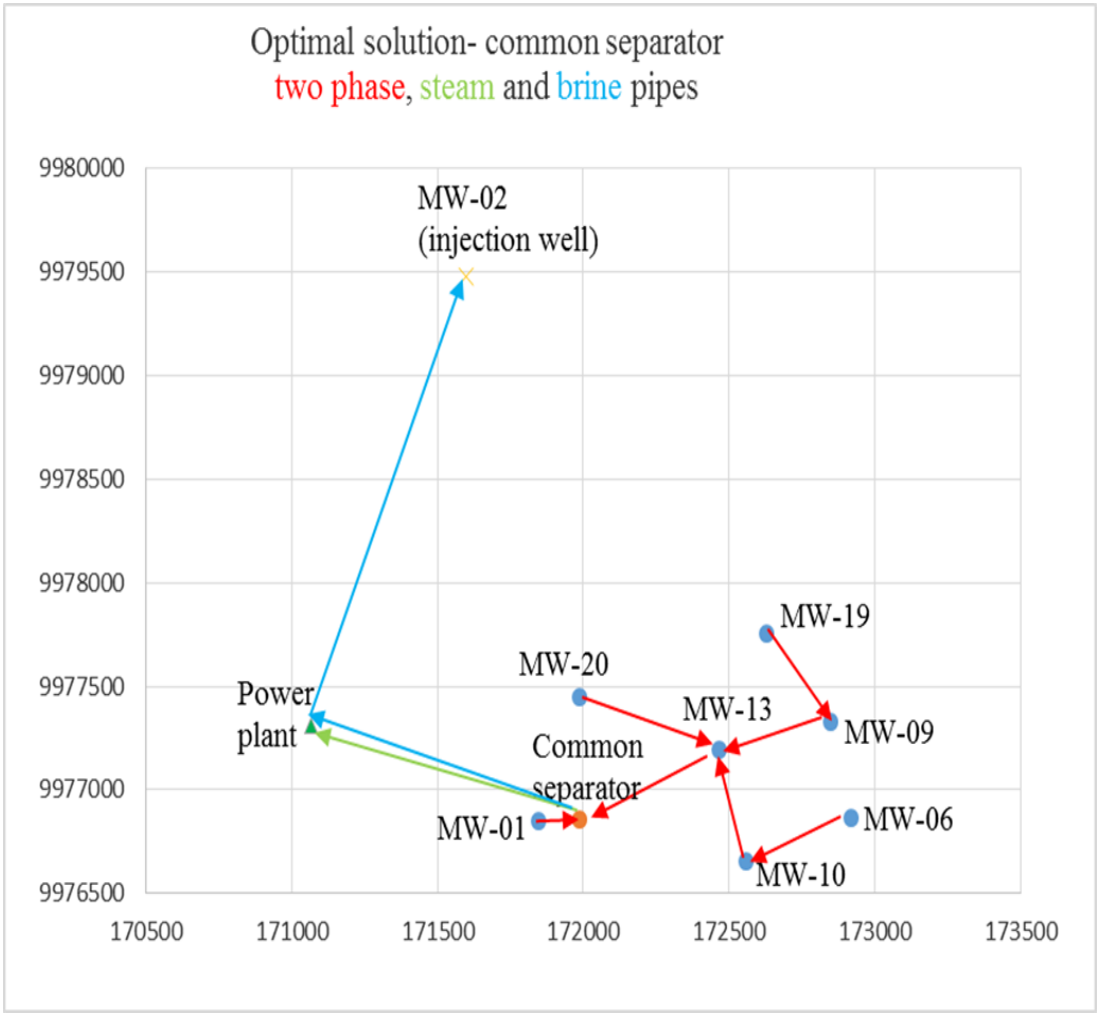

Figure 14: Optimal solution for pipelines with central separator for power plants located in area A. Red arrows represents two-phase pipelines, green arrow represents steam pipe line and blue arrows represents brine pipelines.

Table 7: Pipeline lengths for common separator and plant located in area A.

Pipe ID	**Fluid type**	**Length (m)**	**Arrangement**
MW-01 to common separator	Two-phase	231	1 X 1100 mm
MW-19 to MW-09	Two-phase	486	1 X 700 mm
MW-06 to MW-10	Two-phase	425	1 X 600 mm
MW-09 to MW-13	Two-phase	411	1 X 1100 mm
MW-10 to MW-13	Two-phase	560	1 X 700 mm
MW-20 to MW-13	Two-phase	265	1 X 800 mm
MW-13 to common separator	Two-phase	586	2 X 1100 mm
Common separator to plant	Steam	1045	3 X 1100 mm
Common separator to plant	Brine	1045	1 X 350 mm
Plant to re-injection well (MW-02)	Brine	1957	1 X 450 mm

In this case, all the production wells used in this study have common separator station (Figure 14) and the pipe line lengths are computed based on the distances of wells from that common

separator. The results for brine and steam pipelines when individual separator is assumed are shown below. The optimal solutions for steam pipes topology is shown in Figure 15 and the distances summarised in Table 8.This are results obtained when the power plant is located in area A. This scenario is achieved assuming individual separator scenario.

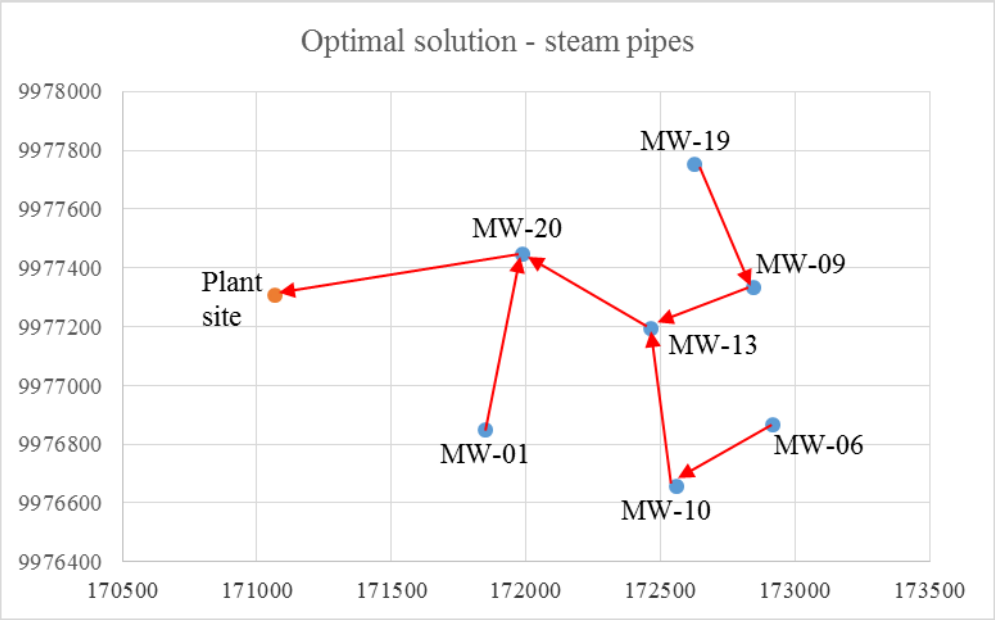

Figure 15: Optimal solution for steam pipelines with individual separator and power plant located in area A

Table 8: Pipeline lengths for steam pipes

Pipe ID	**Length (m)**	**Arrangement**
MW-01 to MW-20	602	1 X 1100 mm
MW-19 to MW-09	486	1 X 600 mm
MW-06 to MW-10	425	1 X 700 mm
MW-09 to MW-13	411	1 X 1100 mm
MW-10 to MW-13	560	1 X 800 mm
MW-13 to MW-20	265	2 X 1100 mm
MW-20 to power plant	948	3 X 1100 mm

Solution for brine pipelines when power plant is located in area A are shown in Figure 16 and the distances between wells summarised in Table 9.

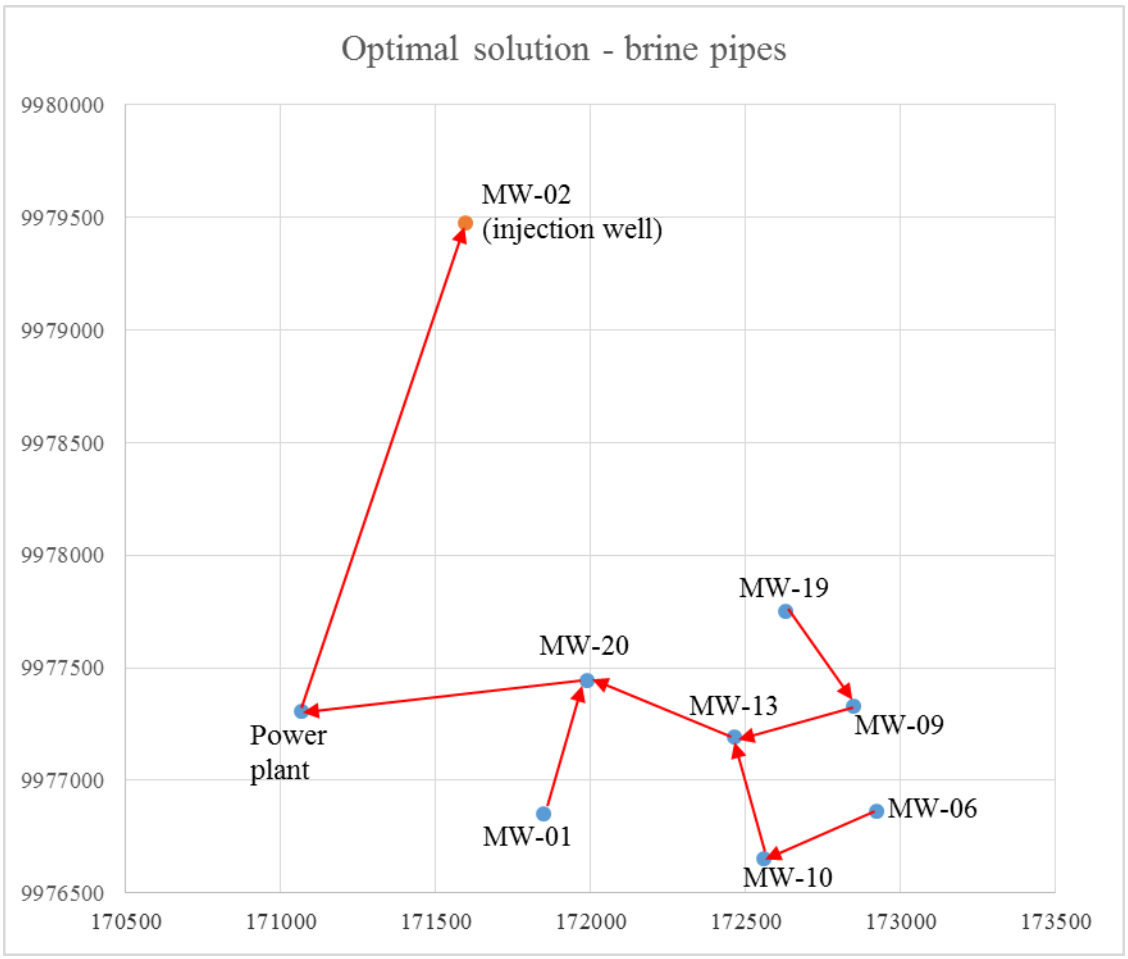

Figure 16: Optimal solution for brine pipelines with individual separator and power plant located in area A

Table 9: Pipeline lengths for brine pipes

Pipe ID	**Length (m)**
MW-01 to MW-20	602
MW-19 to MW-09	486
MW-06 to MW-10	425
MW-09 to MW-13	411
MW-10 to MW-13	560
MW-13 to MW-20	265
MW-20 to power plant	948
Power plant to MW-02	1957

4.2.3 Pipe diameter optimization

Brine pipelines

Optimum diameter selected is the one with minimum total updated cost. In this case, a 450 mm nominal diameter pipe is the one with the minimum updated cost. Figure 17 shows the

optimum diameter for water (brine) pipeline. This pipeline have a total length of 1957 m and runs from power plant site to injection well at MW-02 as shown in Figure 16.

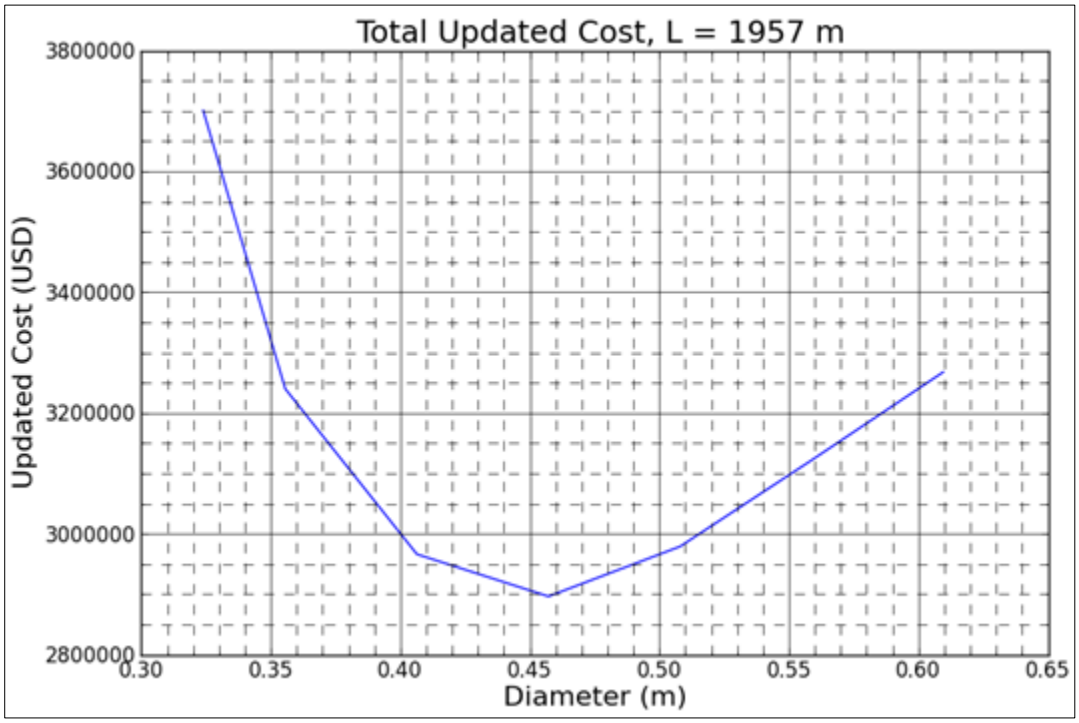

Figure 17: Brine pipe diameter selection. Optimum nominal diameter is 450 mm

Figure 18 shows variation of pump power and pipe diameter for pipe line running from power plant located in area A to re-injection well at MW-02. The total length of the pipeline is 1957 m and energy cost used is 0.22 USD/kWh. 20 KW pump is required for pumping fluid to the re-injection well for the 450 mm optimum diameter.

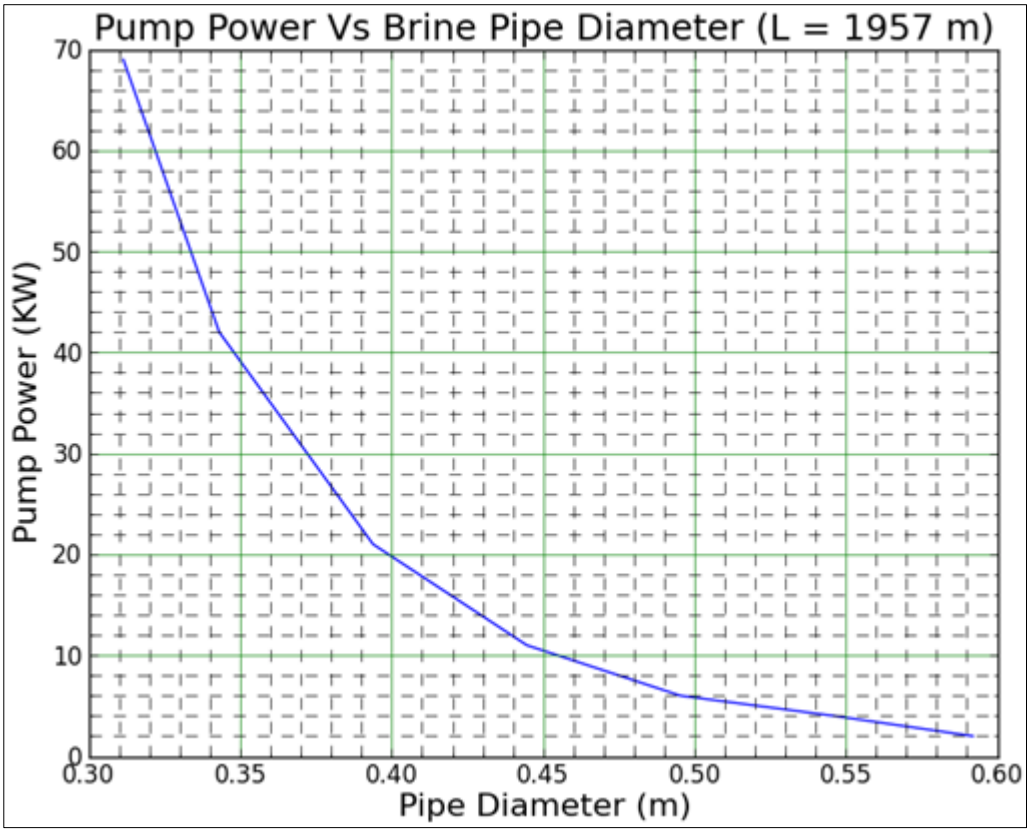

Figure 18: Pumping power for brine pipeline from area A to re-injection well MW-02. Energy cost is 0.22 USD/kWh

Steam pipelines

Using Figure 15 to show diameter selection, pipeline form MW-20 to power plant is analysed for cost and pressure drop. Total pipe line cost and pressure drop have to be considered for diameter selection for steam pipes. Based on pressure drop shown in Figure 20, the diameter with pressure drop of about 0.2 bar is 1100 mm nominal pipe diameter. This pipe diameter has a cost of 3 million USD. Three such pipes are needed to carry all steam form the central separator station. The total cost for steam pipes will therefore be around 9 million USD.

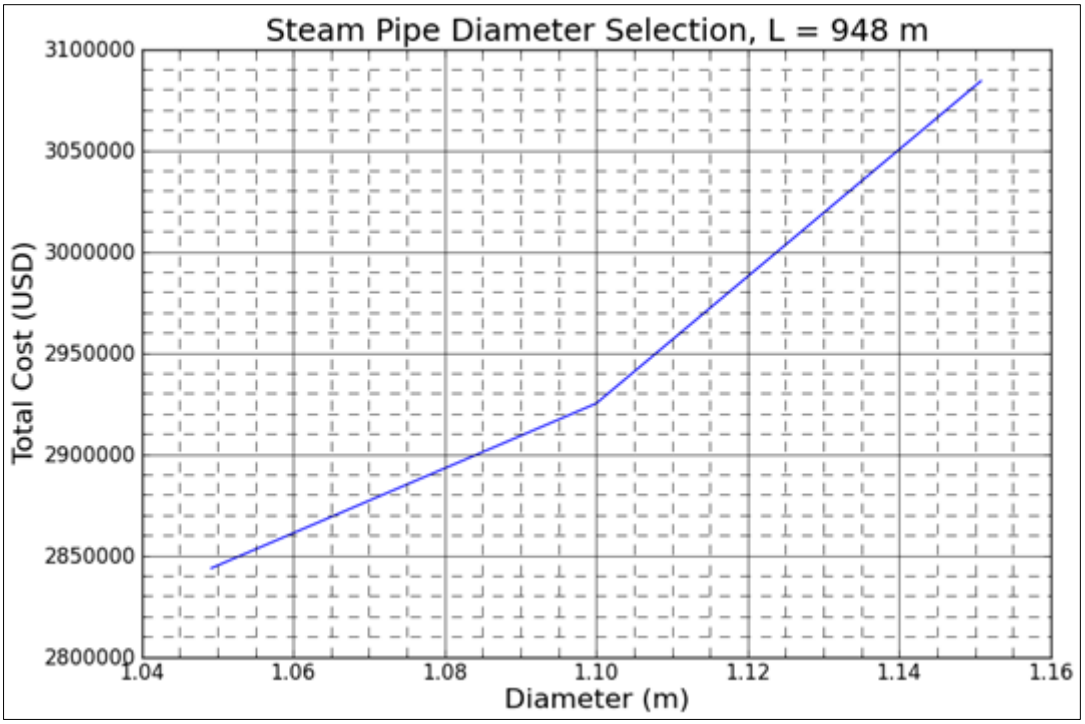

Figure 19: Steam pipe diameter selection (Pipe line from MW-20 to power plant as shown in Figure 15)

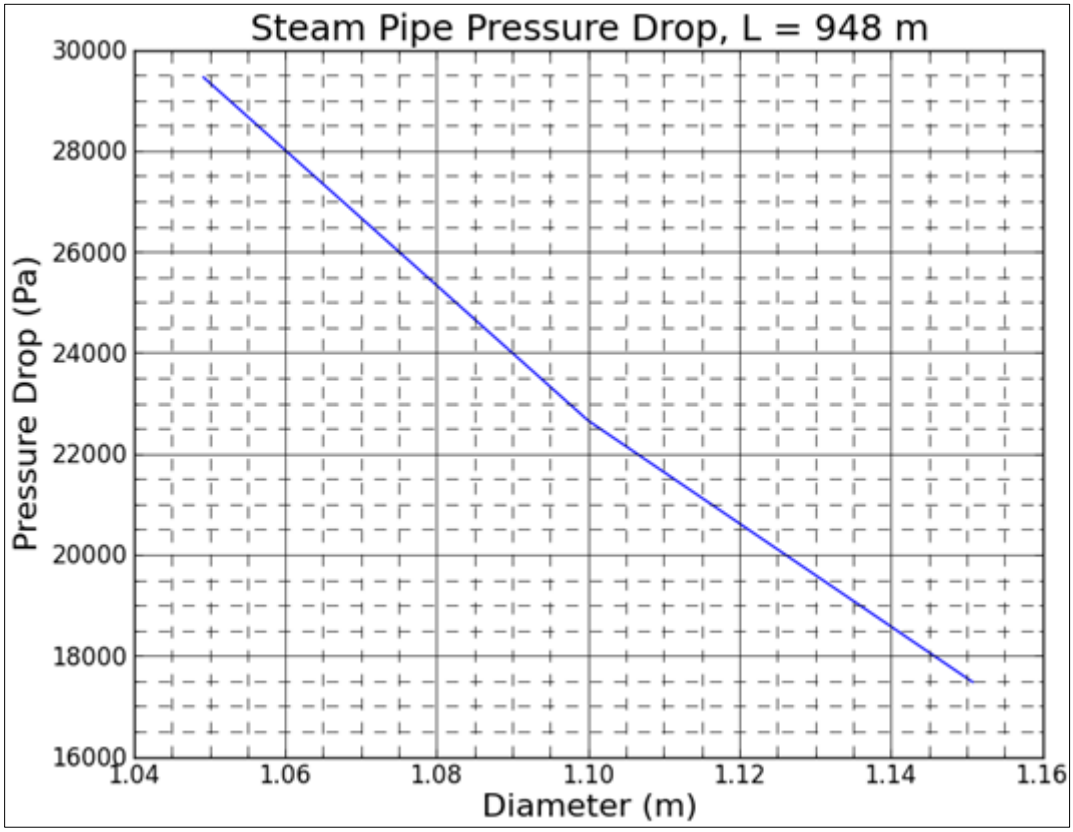

Figure 20: Pressure drop in steam pipe (Pipe line from MW-20 to power plant as shown in Figure 15)

Two phase pipelines

Pipe diameter with lowest cost and reasonable pressure drop (less than 0.2 bar) is selected. Figure 21 shows a plot of pipe diameter and cost for pipelines carrying two phase fluids. In Figure 22 , pressure drop of the same pipeline is presented. This is the pipeline that runs from MW-10 to MW-13 and can be seen in Figure 14. Diameter is selected considering both cost and pressure drop. Most correlations predict less than 0.2 bar pressure drop and hence any pipe diameter can be selected in this case.

Figure 21: Cost of two phase pipeline (Pipe line from MW-10 to MW-13 as shown in Figure 14)

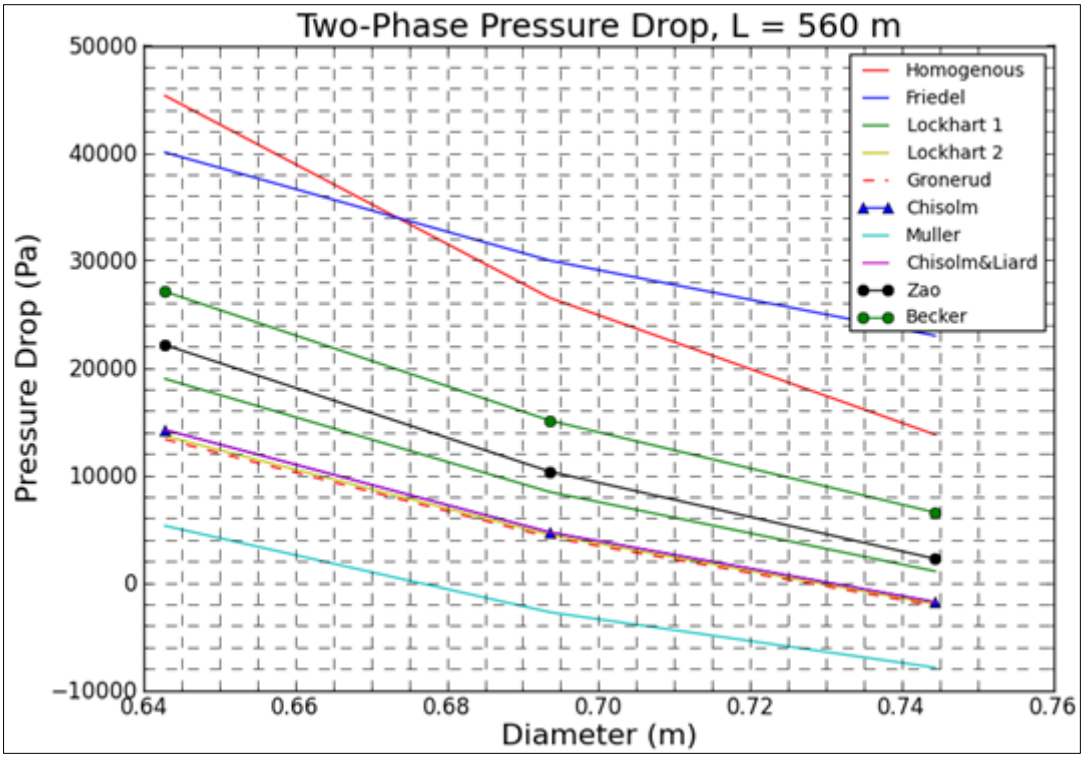

Figure 22: Total two phase pressure drop for two phase pipe (Pipe line from MW-10 to MW-13 as shown in Figure 14).

4.2.4 Two phase pressure loss

Different correlations for pressure loss gave different results but most of the results are not far apart. Pressure drop of about 0.2 bar used for selecting optimum diameter.

Void fraction correlation models

The models results are relatively similar for quality greater than 40%. Since quality of most wells in Menengai geothermal field is greater than 30 %, any of these models can be used to estimate void fraction for two phase flows for Menengai geothermal system. The model by Tuner gives the lowest value for the void fraction for a wide range of mass quality. Figure 23 are the results for void fraction correlations.

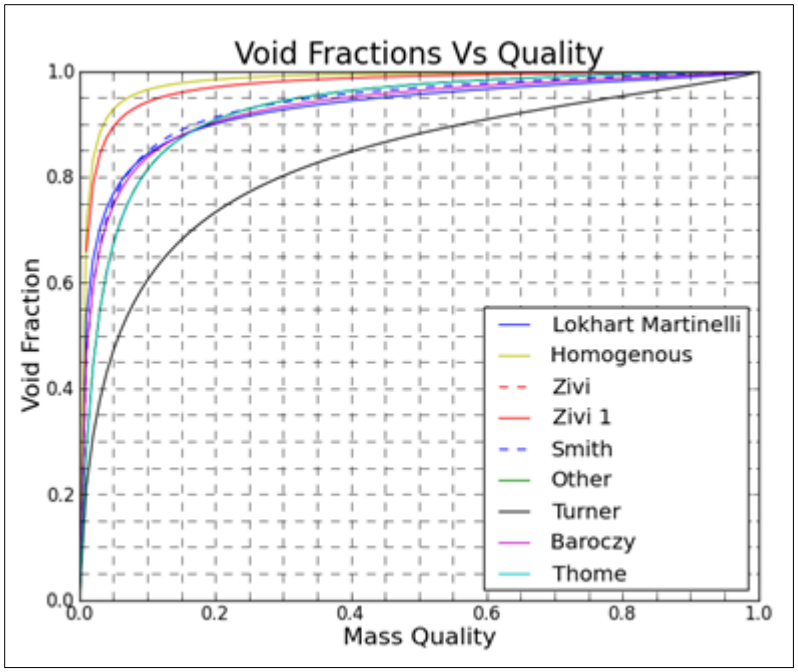

Figure 23: Results of void fraction correlations

Two phase pressure loss models

The results for two phase frictional pressure drop estimations are presented in Figure 24 below. Seven out of eleven models have close values but in general all the eleven correlations have good results. ZAO, homogenous and Chalwa models gives the lowest values for friction pressure drops.

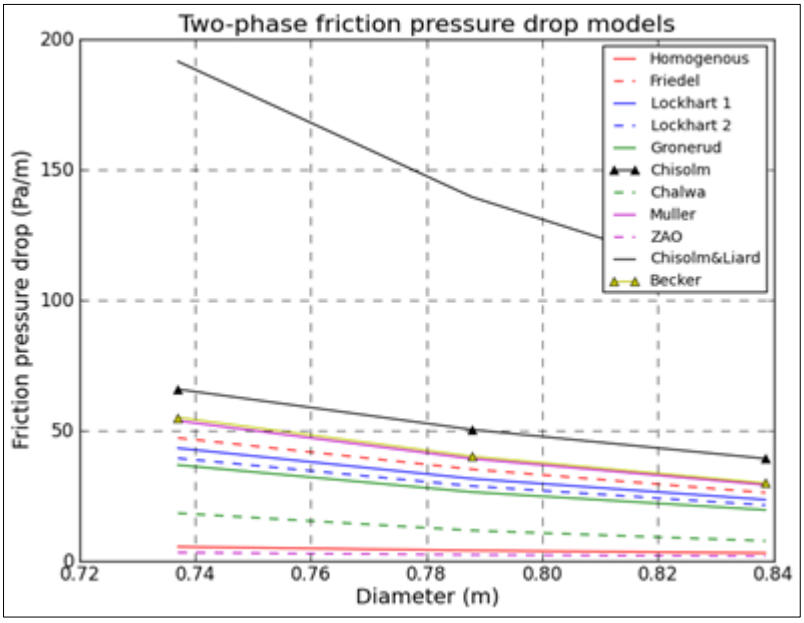

Figure 24: Frictional pressure drop models

Figure 25 shows topology design for two phase pipelines. Pressure drop in some of the pipelines are presented based on the figure. It shows the optimal solution for all the two phase wells.

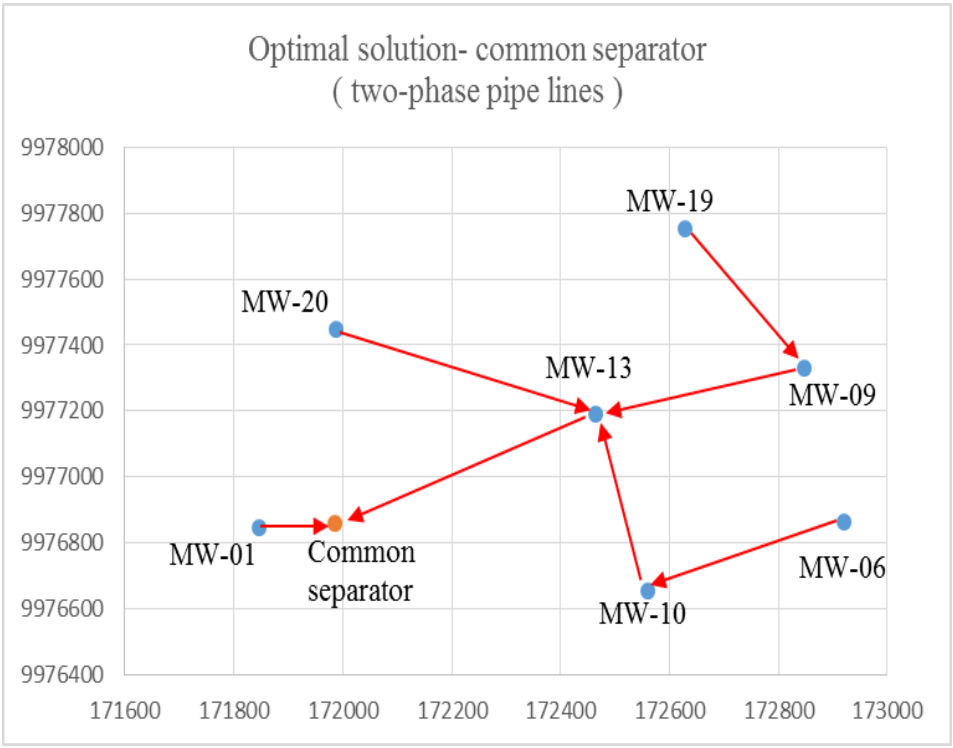

Figure 25: Topology design for two phase pipelines. Common separator located close to MW-01.

Total two phase pressure drop are calculated using several models and the results are as shown in Figure 27 and Figure 27 below. The results are obtained by using different pipeline lengths and some are shown here below. Figure 27 is obtained for pipe length of 265 m, this is the pipe line form MW-20 to MW-13 as shown in Figure 25. In Figure 27, the pipe length is 586 m, this is pipe line from MW-13 to MW-01. Most of the models predict relatively close values for total two phase pressure drop. Other results are attached in the appendix.

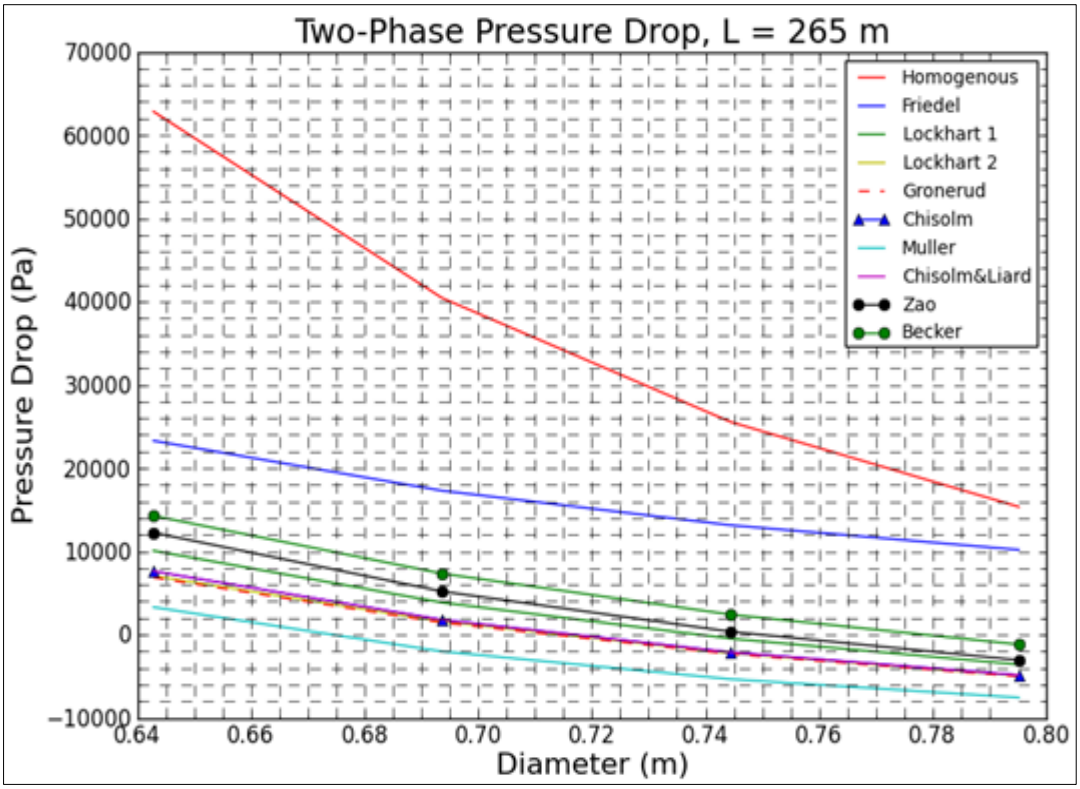

Figure 26: Total two-phase pressure drop (MW-20 to MW-13)

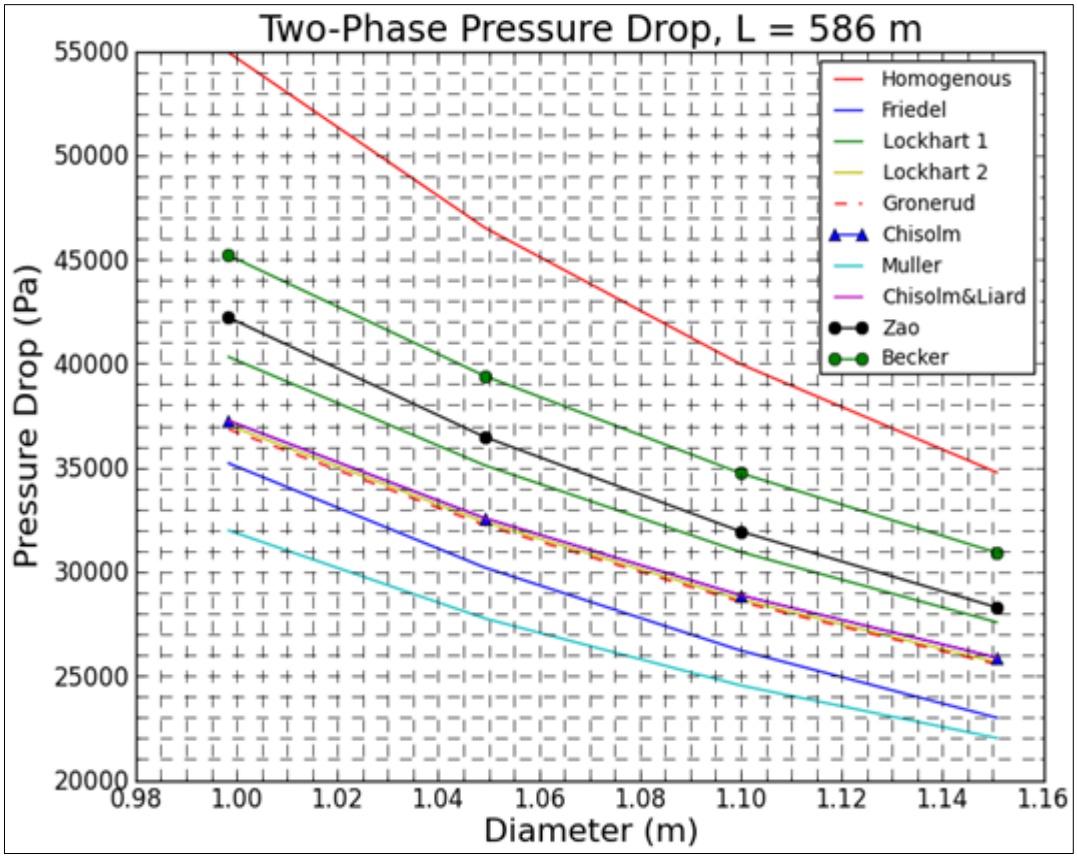

Figure 27: Total two phase pressure drop (MW-13 to MW-01)

4.2.5 Separator placement and design

The best separator location for a group of wells are done using variable topography distance transform using by including weights into the distance transform. The locations are arrived using different weights based on pipe length, mass flow and quality. The results presented here are obtained when different weight factors are used. Two phase wells are given weights given between 0 and 1. The higher the value, the higher the chance the separator is located closer to that well.

Separator placement

The results for separator location using weighted distance for all wells used in this study is shown in Figure 28. All wells have common separator location closer to MW-01. This is the only optimal place based on the restrictions used in the weighted variable topography algorithm. The location is marked with the red box in Figure 28.

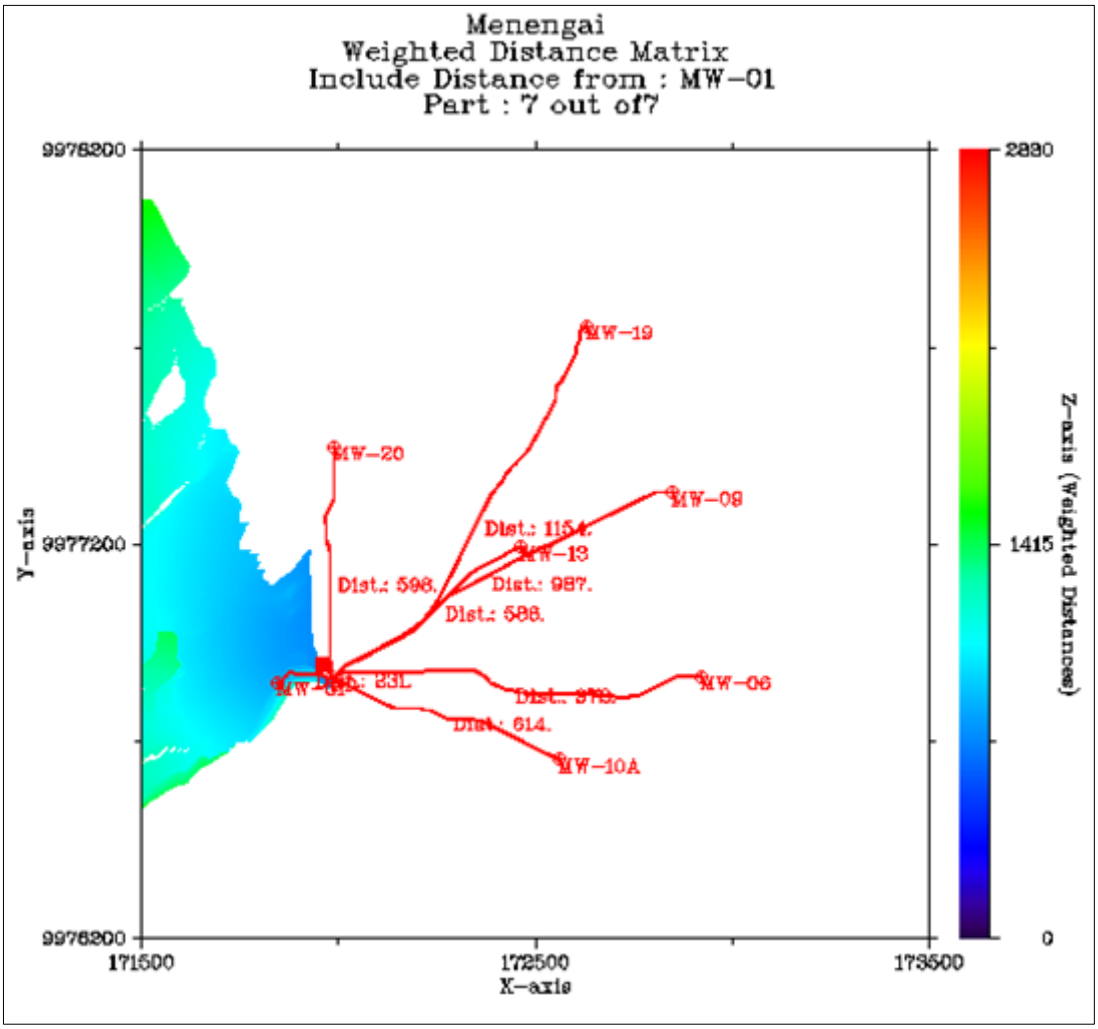

Figure 28 : Optimal location for separator station for all wells. Blue colour indicate areas with the lowest weighted distances from the separator, white areas indicate regions where the separator cannot be placed for the group of wells considered.

A clear picture can be seen in Figure 29, this shows the best location when separator location is sought using only two wells (MW-01and MW-20). From the colour scale, blue areas

shows areas with lowest weighted distances and red are areas with the highest weighted distance. The red box in Figure 29 is the optimal location when two wells are used.

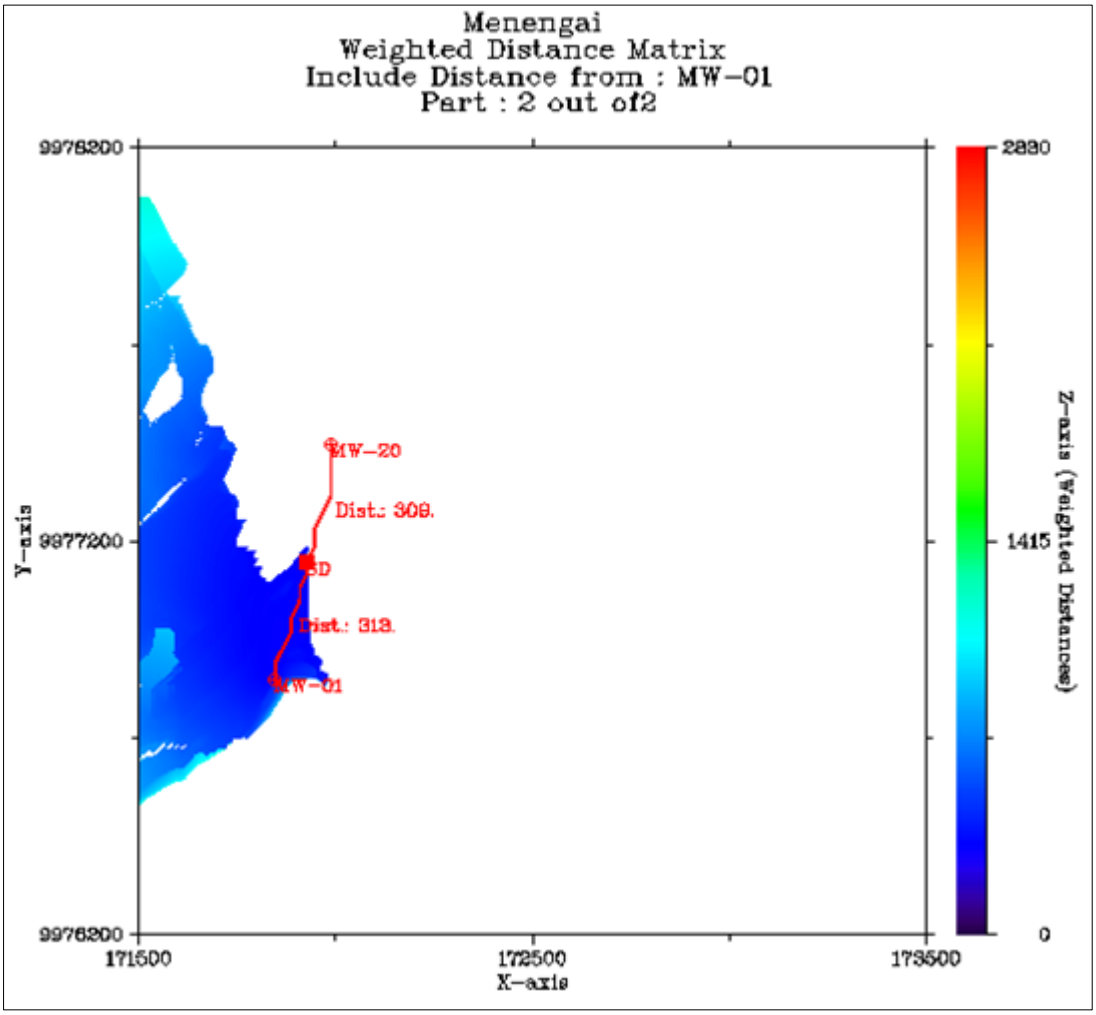

Figure 29 : Separator station location for two wells. Blue colour indicate areas with the lowest weighted distances from the separator, white areas indicate regions where the separator cannot be placed for the group of wells considered.

Result for weighted mass flow

Wells with larger mass flow are given more weights than those with less total mass output. The results of this adjustment give the locations of the separator station for the wells as shown in Figure 30. The location shifts from the location obtained using weighted distance by up to 59 m in x direction and 169 m in y direction. This however is considered to have no major influence as the two locations are more or less the same area. Effort should be made to find how the shift in location affect the overall pipeline length.

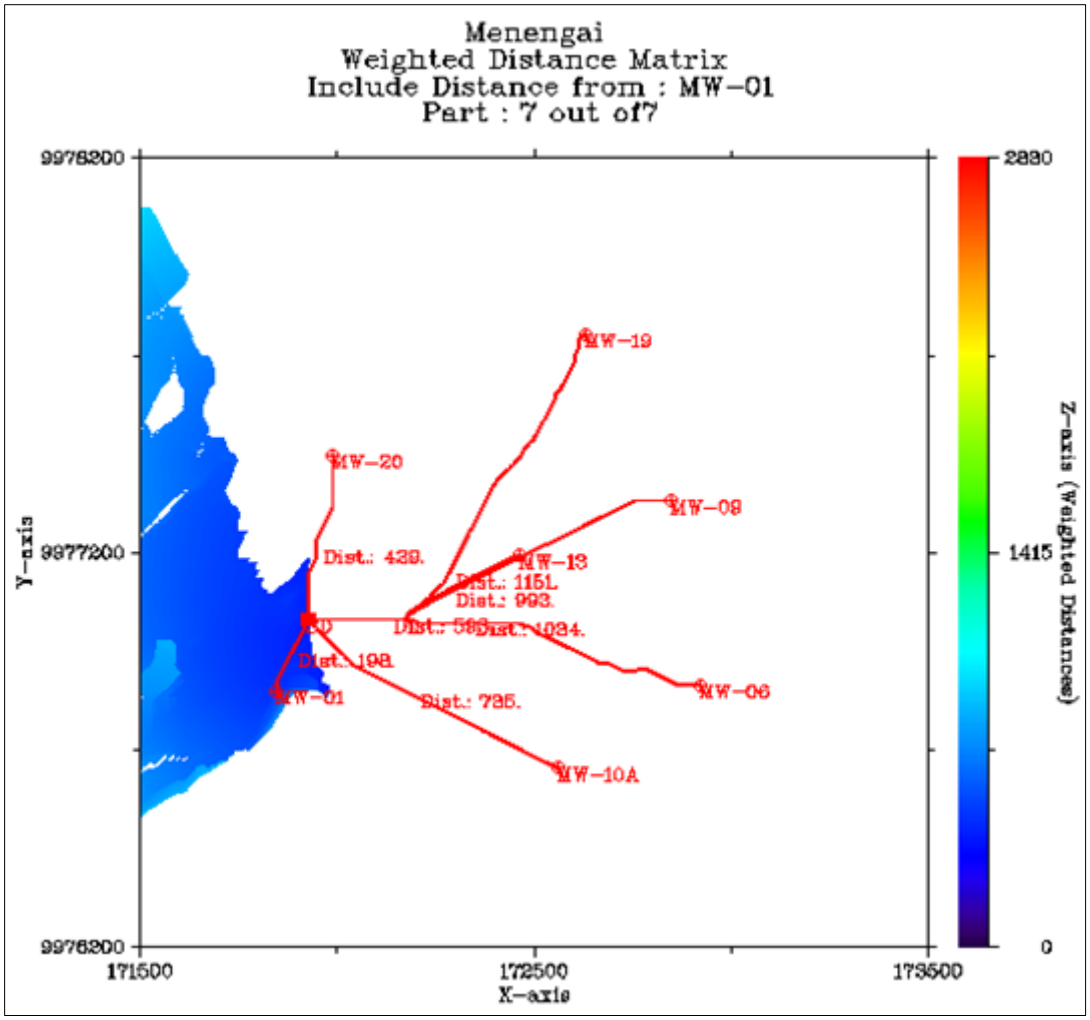

Figure 30: Separator station location using weighted mass flow. Blue colour indicate areas with the lowest weighted distances from the separator, white areas indicate regions where the separator cannot be placed for the group of wells considered.

Result for steam quality

Wells with low steam quality implies that water phase exceeds steam phase in a pipe. Separator should be located closer to such like wells. Wells with low steam quality are given higher weights than those with high steam quality. Figure 31 shows possible location of the separator when steam quality is used to set the weight values. The location shifts by around 26 m in x direction and 34 m in y direction from the first location obtained using weighted distances.

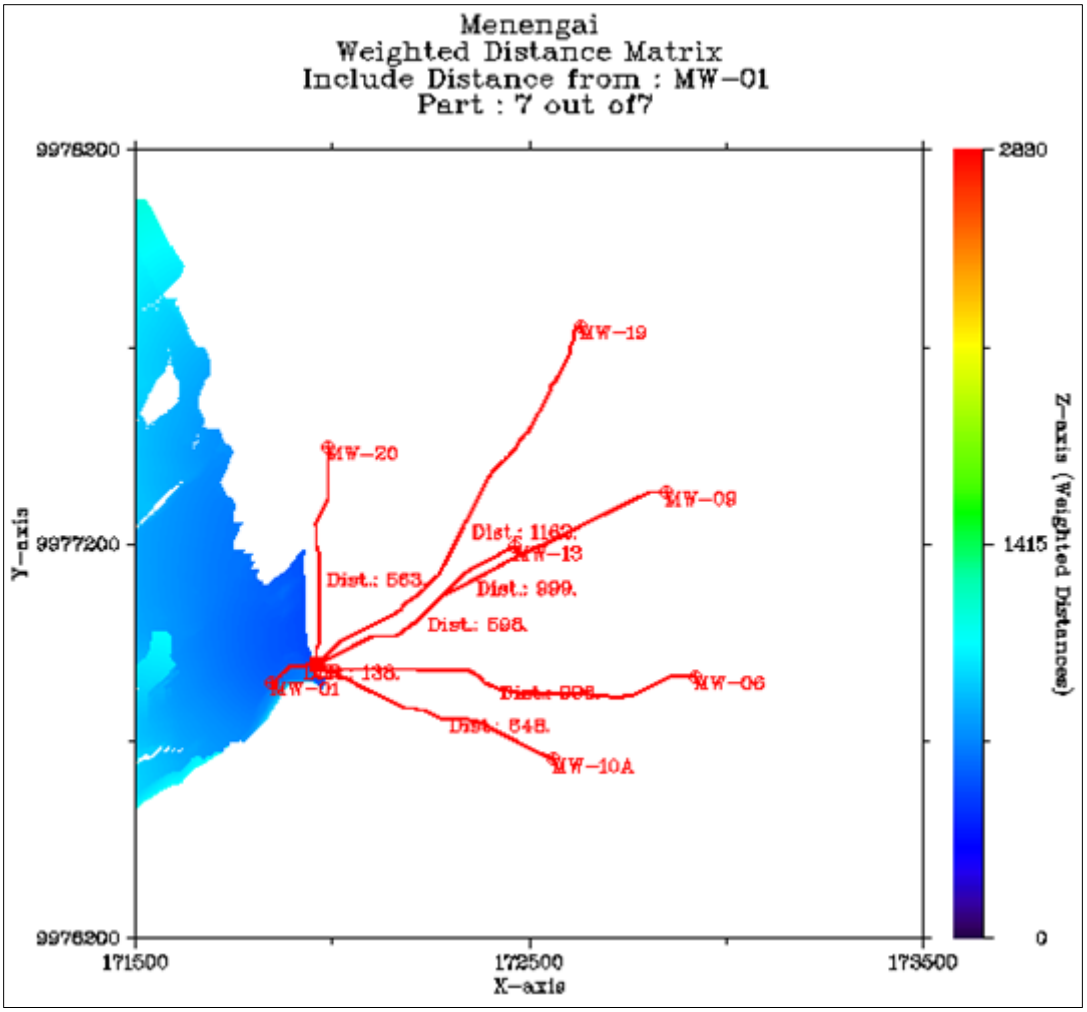

Figure 31: Separator station location using steam quality. Blue colour indicate areas with the lowest weighted distances from the separator, white areas indicate regions where the separator cannot be placed for the group of wells considered.

From the results, the optimal separator location can be obtained with or without additional weights as weights are seen not to adversely affect the overall optimal location for the separator station. The plots for different locations for the separator using the three weights used above is shown in Figure 32.

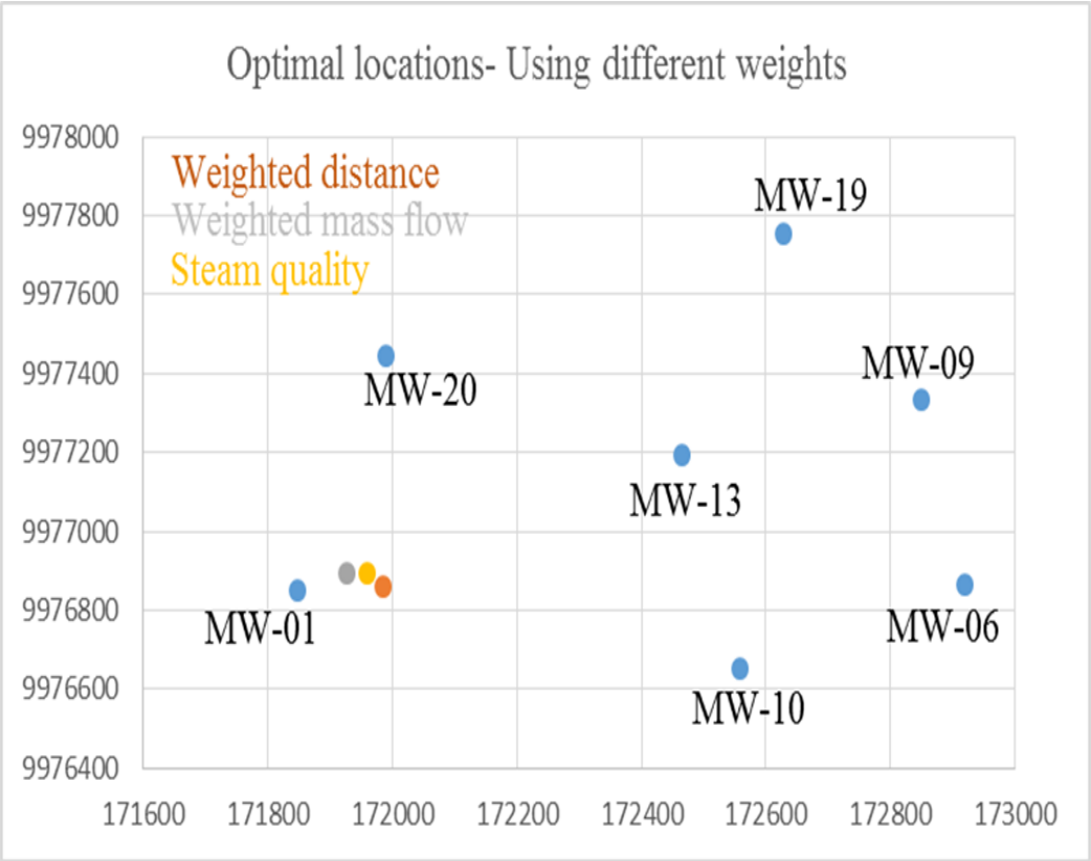

Figure 32: Location of separator based on different weight criteria. Orange shows location using weighted distances, yellow shows location using steam quality and grey shows location using weighted mass flows for the wells used.

Separator design

The results for separator sizing and cost are as summarised in Table 10. All the three design approaches are presented in the results. The separation efficiency and outlet steam quality are maintained as high as possible for the selected sizes. It is not possible to have single separator vessel for all the mass for two phase flow. The results are there for three separator vessels. The average enthalpy for all wells used for determining the fluid properties

Table 10: Vessel size and cost for common separator station

Item	**Bangma**	**Lazalde**	**Spiral**
Inlet pipe diameter (m)	0.84	1.05	1.05
Outlet pipe diameter (m)	0.84	1.05	1.05
Inlet velocity (m/s)	36.67	36.67	36.67
Diameter (m)	3.15	3.46	3.10
L_t (m)	7.35	6.80	7.14
L_b (m)	4.73	7.14	5.15
Height (m)	12	14	12
η (%)		99.99	
Number of separators	3	3	3
Unit cost (USD)	498,278	592,690	490,404
Total Cost (USD)	**1,494,834**	**1,778,070**	**1,471,212**

From Table 10 above, spiral design gives the cheapest design. Spiral design gives the best design and should be adopted for Menengai field. Cost values are not actual since they are derived from estimates of volume of material required to fabricate the separator vessel. The cost for individual separator per every well platform is also summarised in Table 11. The average enthalpy for wells in each well pad used for calculation of the fluid properties.

Table 11: Vessel size and cost for individual separators scenario

Pad ID	**Item**	**Bangma**	**Lazalde**	**Spiral**
S1	Diameter (m)	2.85	3.13	2.80
	Height (m)	11	12	11
	Cost	354,732	425,507	348,846
S2	Diameter (m)	1.80	1.98	1.77
	Height (m)	7	7	7
	Cost	90,045	99,010	88,551
S3	Diameter (m)	2.55	2.80	2.51
	Height (m)	10	10	10
	Cost	258,166	283,868	253,882
S4	Diameter (m)	0.90	0.99	0.89
	Height (m)	3	4	4
	Cost	9,647	14,144	12,650
S5	Diameter (m)	1.65	1.81	1.62
	Height (m)	6	7	6
	Cost	64,854	83,195	63,778
S6	Diameter (m)	1.80	1.98	1.77
	Height (m)	7	7	7
	Cost	90,045	99,010	88,551
S7	Diameter (m)	2.25	2.48	2.21
	Height (m)	9	9	9
	Cost	180,894	198,904	177,893
Total Cost		**1,048,383**	**1,203,638**	**1,034,151**

The cheapest cost for individual separator scenario is spiral design. Lazalde design however have the highest cost. The central separator scenario have the highest costs compared to individual separator per well pad.

4.2.6 Power plant placement optimization

The chosen location for plant location may not be the best as the weights used in analysis are based on decision of few people. However, it should be noted that the chosen location is entirely based on this study and the method used. Other methods may give different location as the best plant location. Table 12 shows the ranking of each Areas A, B and C for different criteria.

Table 12: Criteria matrix for the three alternatives

	Land availability	Distance to production wells	Distance to re-injection wells	Pipe line cost	Number of production wells
Area A	0.0738	0.5870	0.6434	0.5870	0.3312
Area B	0.6434	0.3324	0.2828	0.3324	0.5492
Area C	0.2828	0.0806	0.0738	0.0806	0.1196

Area B scores highest on land availability and distance from production wells. Area A ranks first on distance from production wells, distance from re-injection wells and pipeline cost. Area C ranks last on four criteria and only second on only one criterion. The best overall was found by multiplying the criteria matrix by it preference vector and the best location for the power plant is determined to be area A with a score of 0.5108 followed by area B with a score of 0.3797. Table 13 shows the results for the three areas considered.

Table 13: Final score for best plant location

Option	Score
Area A	**0.5108**
Area B	0.3797
Area C	0.1094

The best place for power plant location is area A, this is area between MW-01 and MW-07. This location is purely chosen based on Analytical Hierarchy Process (AHP) using weights that are attached in the appendix.

4.2.7 Cost comparison for different pipeline arrangement scenarios

In a bid to show how this tool can be used to compare different arrangement for pipelines, the cost of pipelines for all the possible plant locations are calculated and presented. A case is analysed for common separator for all the wells and also assuming individual separator for all the wells for all the possible power plant locations. Costs for different areas are compared based on the fluid type.

Two phase pipeline costs

The cost for individual separator station is the same for all power plant sites considering two phase pipelines. This is due to the fact that a constant pipe length of 50 m is used for the distance from the well to the separator. The cost for common separator is lowest for area B and C and highest for area A for common separator system. Figure 33 shows the percentage cost for common and individual separator arrangements for different power locations, the cost is similar for all plant locations for individual separator arrangements.

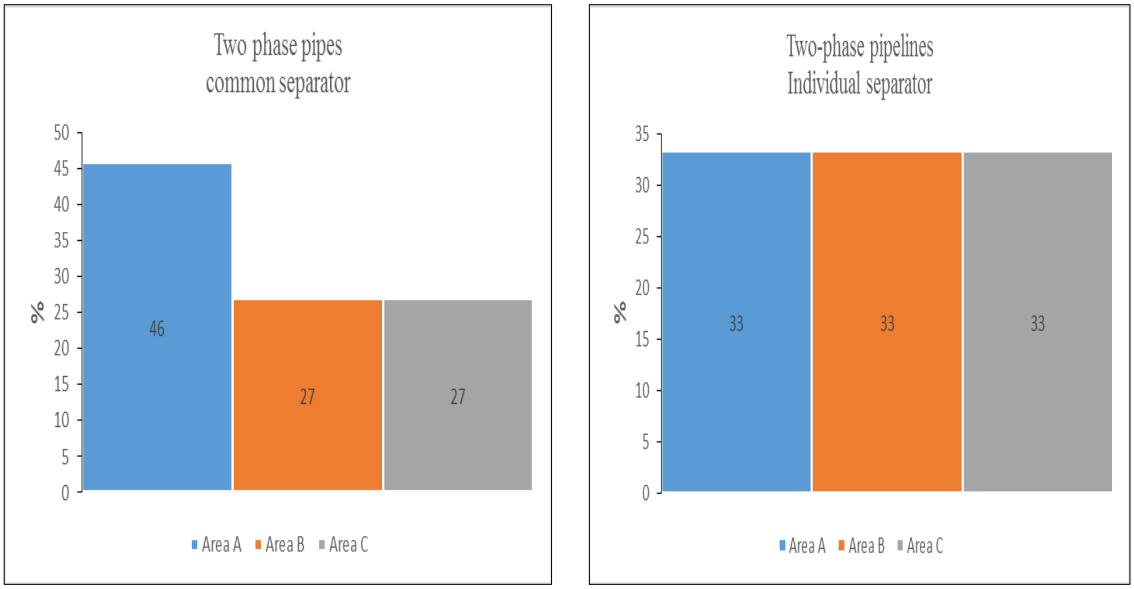

Figure 33: Cost comparison for two phase pipelines, common separator on left and individual separator on the right. Cost for common separator is 19.9 million USD and cost for individual separator is 2.1 million USD.

Steam pipeline costs

Locating plant in area A have lowest cost for both individual and common separator. For common separator scenario, cost of steam pipelines almost doubles that of area A if the plant is located in area B and is more than four times when plant is in area C. Figure 34 shows cost of steam pipe lines for different locations for the power plants.

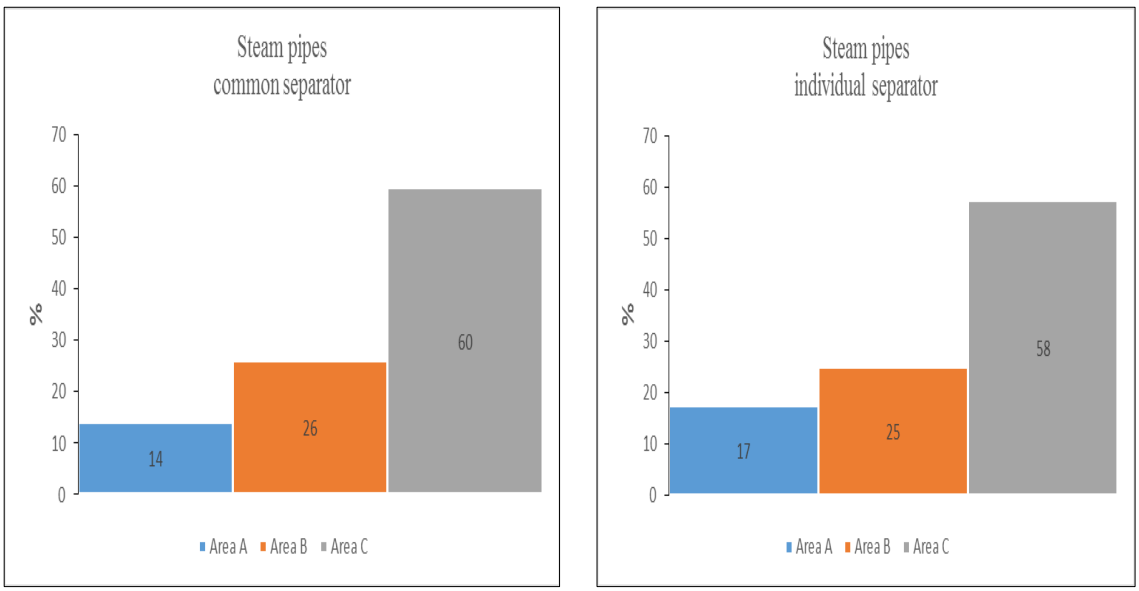

Figure 34: Cost comparison for steam pipes, common separator on left and individual separator on the right. Cost for common separator is 72.6 million USD and cost for individual separator is 97.8 million USD.

Brine pipeline costs

The cost for brine pipes is relatively low compared to steam and two-phase pipeline due to the fact that brine pipes are smaller in diameter (less capital cost) and pumping is not required in most cases (negative hydrostatic head). Brine pipes have lowest cost for Area A and highest cost for area C considering both individual and common separator station placement scenarios. Figure 35 shows the summary for the three possible power plant locations considering common and individual separation. The cost for brine pipes is lowest for area A and highest for area C due to longer pipelines.

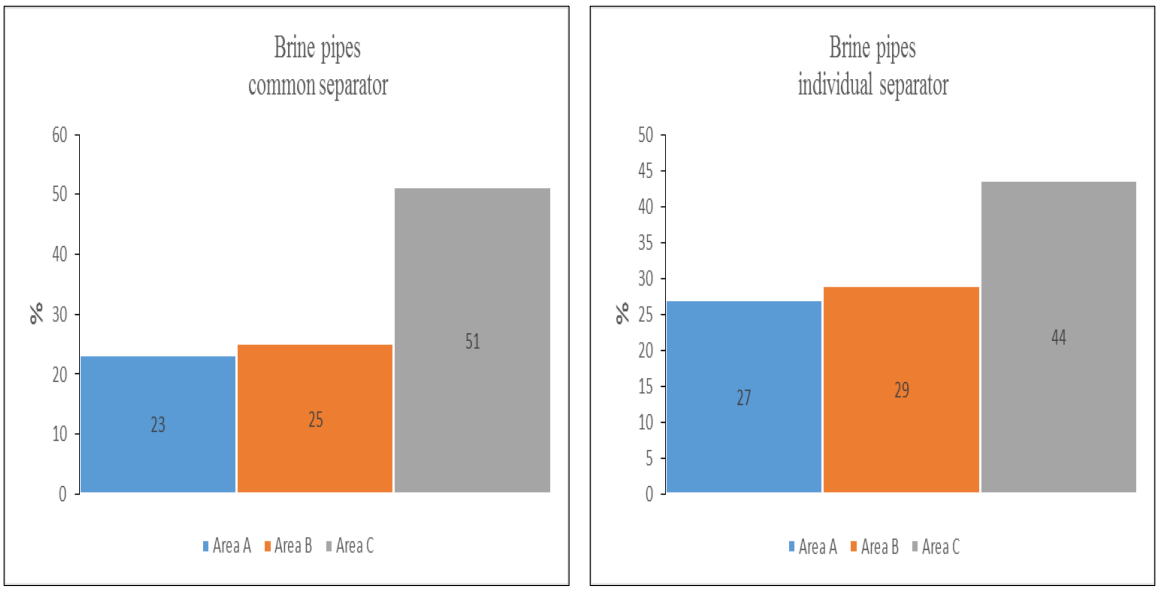

Figure 35: Cost comparison for brine pipes, common separator on left and individual separator on the right. Cost for common separator is 17.7 million USD and cost for individual separator is 21.9 million USD.

Total pipeline cost

Comparing the three possible plant sites based on pipeline cost, area A have the lowest cost for the total pipelines cost. Figure 36 shows cost summary for plant in site A, two-phase pipelines cost 39% of the total pipeline cost for common separator station and 3 % when individual separators are used. The total pipeline for area A is 23 million and 24 million USD for common separator and individual separator respectively.

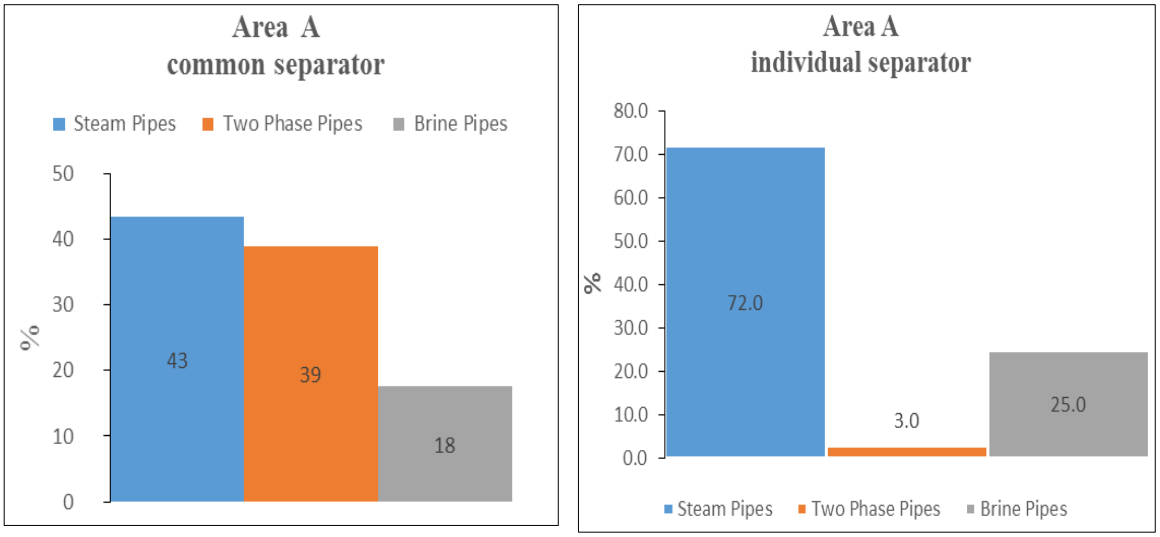

Figure 36: Common separator and individual separator for plant at Area A. Cost for common separator is 23 million USD and individual separator is 24 million USD.

For power plant in area B, steam pipes have the highest costs at 66 % and 78 % for common separator and individual separator stations respectively. Figure 37 shows the graphical summary by fluid type for both central and individual separators. The total pipeline for area B is 29 million and 32 million USD for common separator and individual separator respectively.

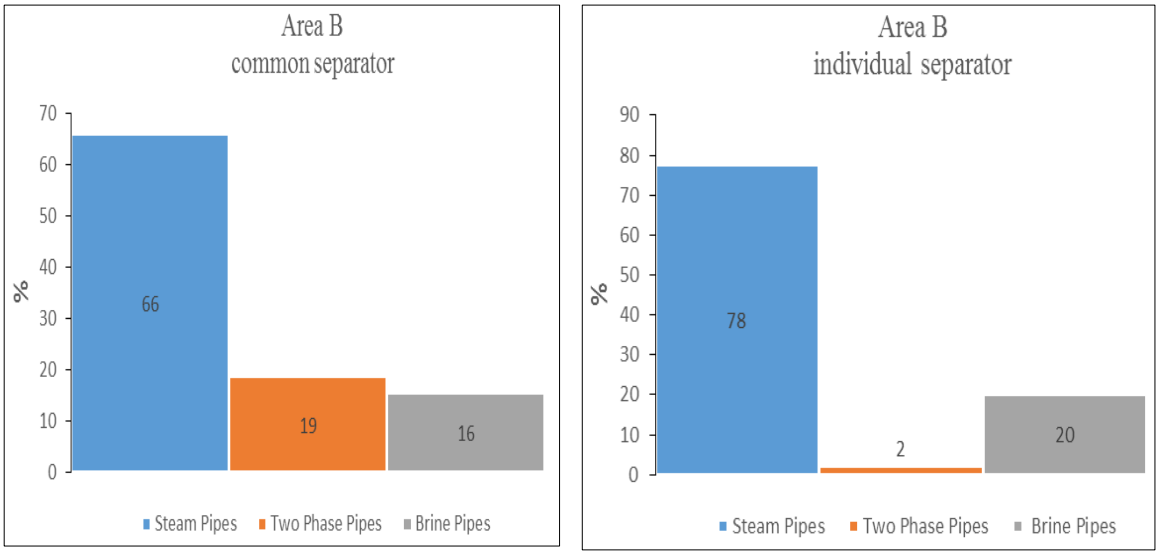

Figure 37: Common separator and individual separator for plant at Area B. Cost for common separator is 29 million USD and individual separator is 32 million USD.

For plant in area C, steam pipes have the highest costs at 75 % and 85 % for common separator and individual separator stations respectively. Figure 38 shows summary by fluid for location C. The total pipeline for area C is 58 million and 67 million USD for common separator and individual separator respectively.

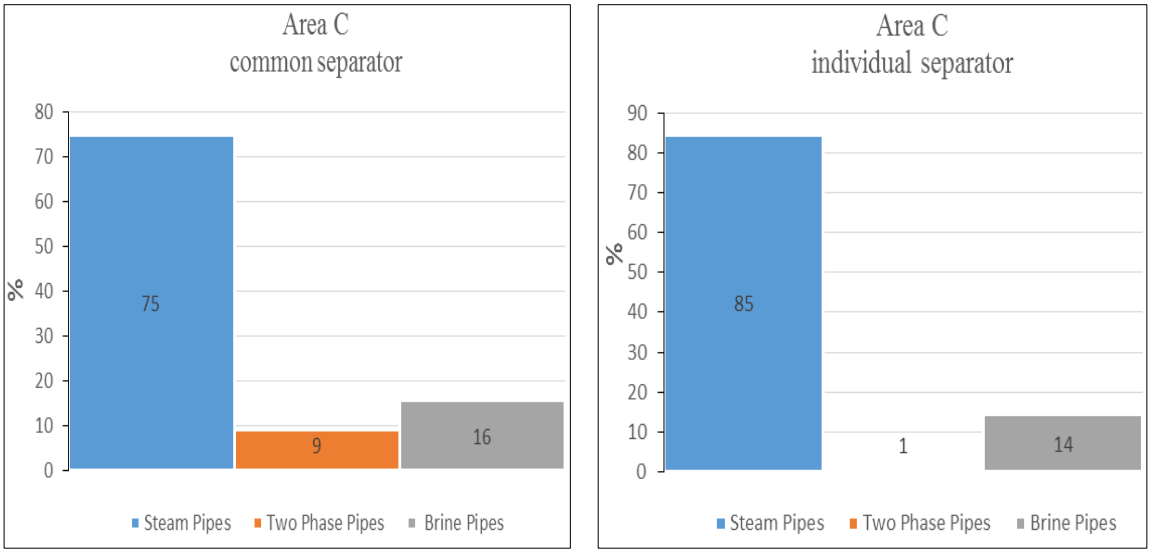

Figure 38: Common separator and individual separator for plant at Area C. Cost for common separator is 58 million USD and individual separator is 67 million USD.

5 Discussions

Route design employed in this study gives good results and optimises the route based on the given constraints. Obstacles can easily be defined and included into the distance transform algorithm. Variable topography distance transform offers a good approximation of distances using digital elation matrix for Menengai geothermal field. The constraints employed for maximum incline and height difference ensure that the pipe do not cross areas with rough terrain as it is the case with some parts in Menengai due to lava flows. The coordinates of the route are printed by the algorithm and can be used to carry out detailed route planning.

Topology optimisation reduces the overall pipe length for a given distance between wells. This ensures reduced overall pipeline cost. This method is however only considered when working with wells that can be connected together, due to fluid pressure or fluid type difference. Topology design results using evolutionary algorithms in excel solver optimises both pipe network arrangement, flow in each pipeline and elevation difference between start and end of each pipe.

Pressure loss models for two phase friction pressure drop provides results that are not far apart and using the models to predict two phase pressure drop for Menengai pipelines may give an indication on the magnitude of pressure loss though only measurements can show the actual pressure drop. Total pressure loss in two phase pipelines and steam pipelines is limited to 0.2 bar for this study, however some steam pipelines are selected with higher pressure drop due to longer pipelines.

Optimum diameter for brine pipes is selected using total updated cost method while for steam and two-phase pipelines, the optimum diameter is selected by considering both pressure drop and cost. Velocity of steam is restricted to between 25 m/s and 40 m/s while water velocity restricted to 1-3 m/s. Only pipelines that are within those velocity ranges are considered for selection based on total cost and or pressure drop.

Area A gives the lowest cost for both individual and central separator station followed by area B while area C have the highest cost. Both area A and B can thus be considered for power plant construction. The best arrangement for separator station is common separator station layout, it gives the lowest cost for pipelines, this may help reduce the overall cost for steam field development. Use of multiple weights based on total two phase flow and steam quality gives different locations for separator placement. The results however give areas that are basically not far apart from each other hence can suitably be used to find the best separation location for a group of wells.

The best location for power plant location based on data and assumptions used in this study is area A. It has the lowest total pipeline cost for both common separator and individual separator layout scenarios. This area is followed closely by area B while area C should only be considered as the last resort. Area A also have the highest score based on analytic

hierarchy process. The method however can give different location from area A if different evaluating criteria is used on the three alternatives or if another alternative is defined.

The total cost for steam gathering system is lowest for area A using common separator station. The cost is however high for areas B and C due to longer pipeline lengths. The cost of steam gathering system is seen to be largely dependent on the location of power plant which influences the overall pipeline length and in turn the cost. The choice of power plant location site should therefore be considered and evaluated carefully using many criteria and criteria weighting to also done carefully to find the best location for future wells drilled in Menengai geothermal field.

6 Conclusions and recommendations

A tool for designing steam gathering system has been developed and tested using data from Menengai geothermal field. This tool will go in a long way to help in decision making for the gathering system design for Menengai geothermal field and any other field that will be developed by GDC.

Distance transform give good results for pipeline route with or without constraints or obstacles. The routes can provide preliminary data before detailed route survey is carried out.

Topology design should be done for all future pipe networks in Menengai geothermal field to achieve optimum total pipeline length. The method selects which pipes that can join each other within the network and also helps optimise the flow in each pipe.

Total pressure drop for all pipelines lengths and arrangements are within reasonable limits. Majority of pipelines carrying two phase and steam have pressure drop of less than 0.2 bar. Placement of separators in Menengai using distance transform will prove beneficial for cases where common separator stations will be considered necessary.

The best place to locate power plant for Menengai geothermal field is area A. This is however based on the data available and other options may rank high if more well production data become available. Power plant should be located in area A with common separator station close to MW-01, this arrangement gives the lowest cost for the gathering system based on the available data.

Digital elevation matrix with smaller resolution (3-5 m) should be used in distance transform algorithm so as to provide more detailed topographical features and better results in route selection. The price for steel used in this study are estimates and using actual prices for steel can help give relatively reliable cost figures for different pipeline scenarios analysed.

Studies on the existence of sensitive plant and animal habitats within the project area should also be considered. The selection of pipeline routes and design should take into account such areas to ensure sustainable development.

References

ASME, 1974: *ASME boiler and pressure vessel code.* American Society of Mechanical Engineers.

Chisholm, D., 1983: *Two-phase flow in pipelines and heat exchangers*. The Institution of Chemical Engineers, NY, 304 pp.

DiPippo, R., 2007: *Geothermal power plants. Principles, applications, case studies and environmental impact* (2nd ed.). Butterworth Heineman, Elsevier, 493 pp.

Foong, K.C., 2005: *Design concepts for more efficient steam-water separator,* Proceedings at WGC.

Heimisson, I., 2014: *Head loss in two phase flow of water and steam in geothermal gathering pipes system*. University of Iceland, Reykjavik, 75 pp

Henriquez, J.L.M and Aguirre, A.L., 2011: *Piping design, the fundamentals, Geothermal training in El Salvador*. UNU-GTP and LaGeo.15 pp

Jónsson M.T., 2014: *An approach to optimum route and site selection of steam gathering system for geothermal power plants using multiple weight distance transform*. University of Iceland, Reykjavik, 7 pp.

Kellogg, M.W., 1956: *Design of piping systems* (rev. 2nd edition). John Wiley & Sons, Inc., NY, USA, 385 pp.

Kjærnested, S.N., 2011: *A comparative study of geothermal pipeline route selection methods with visual effects optimization*. University of Iceland, Reykjavik, 57 pp.

Lazalde-Crabtree, H., 1984: Design approach of steam-water separators and steam dryers for geothermal applications. *Geothermal Resour. Council, Bulletin, Sept. 1984,* 11-20.

Mundakir, A., Lee, K.C : *Geothermal two-phase pressure loss in a bend*. Geothermal institute, University of Auckland.

Mohitpour,M., Golshan, H., and Murray, A., 2000:*Pipeline design and construction, a practical approach*. ASME, NY, USA, 654 pp

Munggang, H.P, Sadiq,J.Z and John, E.C, 2012: *CFD modelling of two-phase flows inside geothermal steam-water separators*. 34th Newzeland Geothermal workshop proceedings. University of Auckland.

Ofwona, C.O., 2004 : *Heat loss assessment of Menengai – Olbanita geothermal prospect*. KenGen, Kenya, internal report, 19 pp.

Onyango, S.O., 2012: Preliminary design of the Menengai geothermal phase I steam gathering system. . Report 26 in: *Geothermal training in Iceland 2012*. UNU-GTP, Iceland, 601-641.

Palson, H., 2014: *Geothermal Power Plants*. Haskoli Islands, Iceland, unpublished lecture notes.

Þorleikur, J., and Yngvi,G., 2014: *Mechanical Design of Geothermal Power Plants*. Haskoli Islands, Iceland, unpublished lecture notes.

Saaty, T.L., 1980: *The analytic hierarchy process*. McGraw-Hill, New York.

Smith, M., 2005. *Determination of gradient and curvature constrained optimal paths*. London: University College.

Thome, J. (ed.), 2006: Engineering data book III. Wolverin Tube Inc., Lausanne, Switzerland.

10 year power sector expansion plan 2014-2024, Kenya government report. June 2014

Appendices

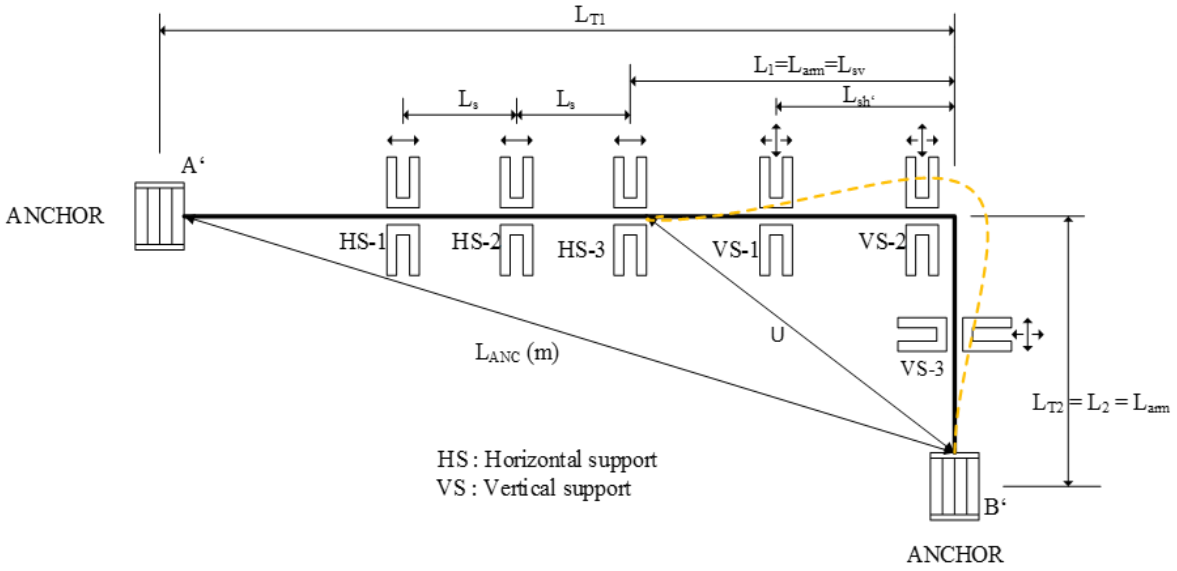

Appendix 1: Change of direction expansion loop

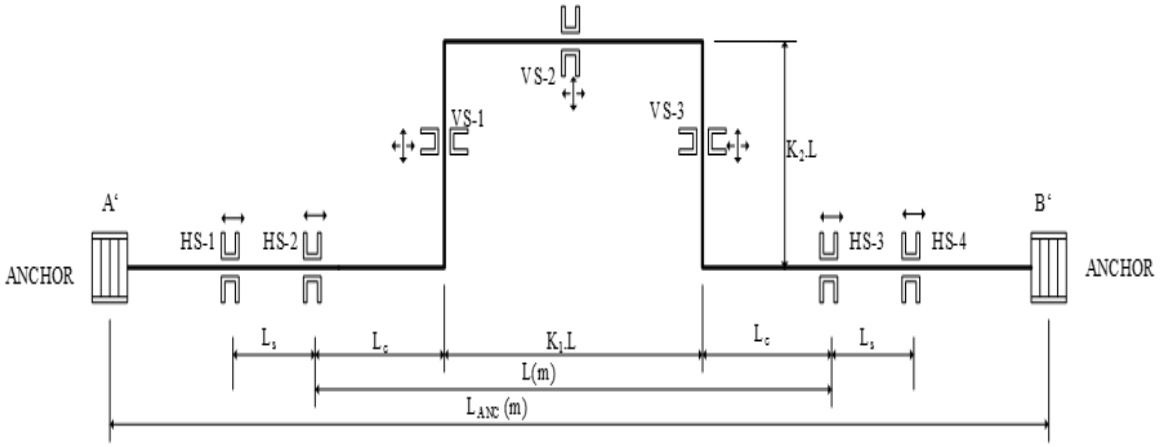

Appendix 2: U-shape expansion loop

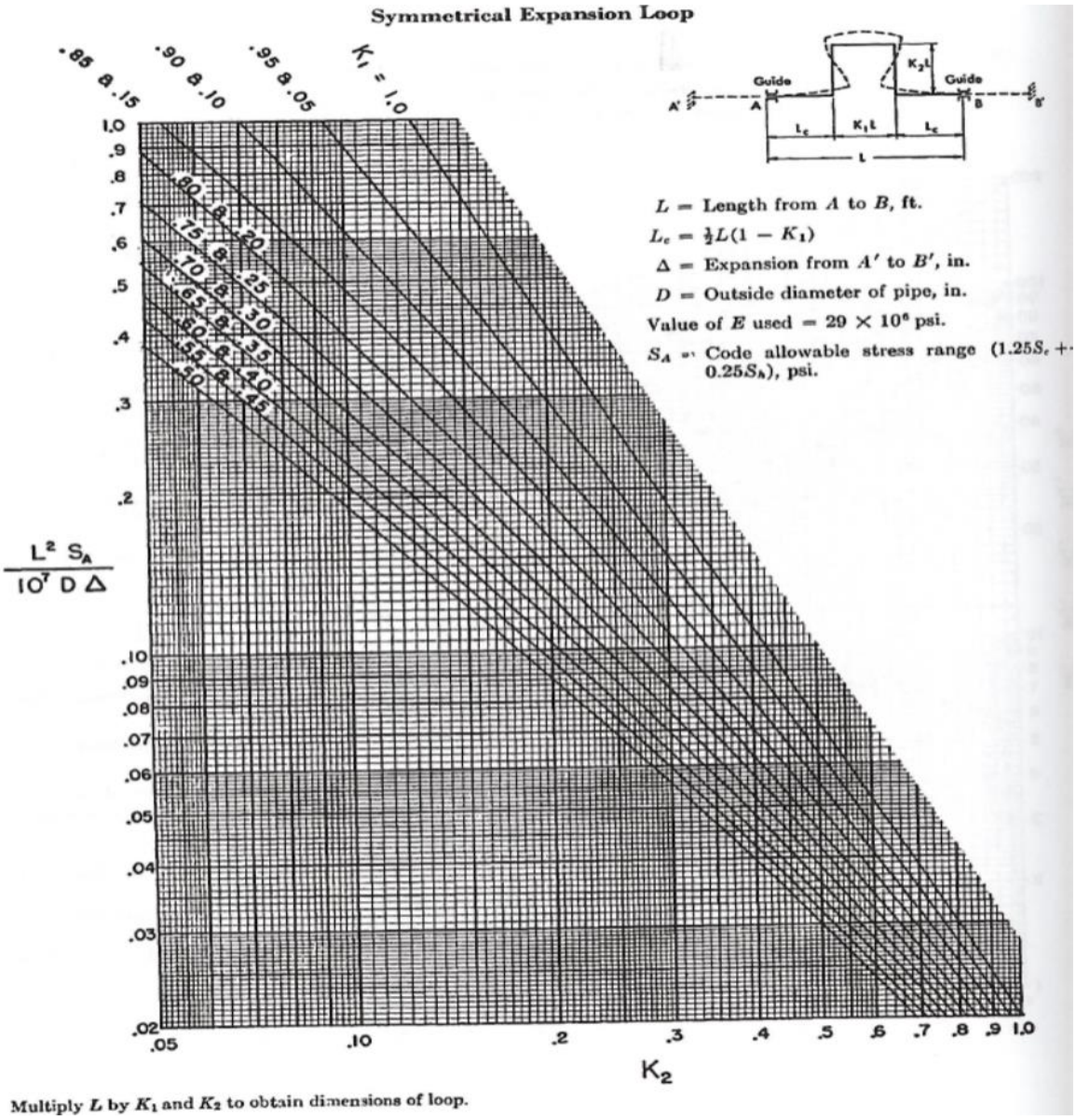

Appendix 3: MW Kellogg chart

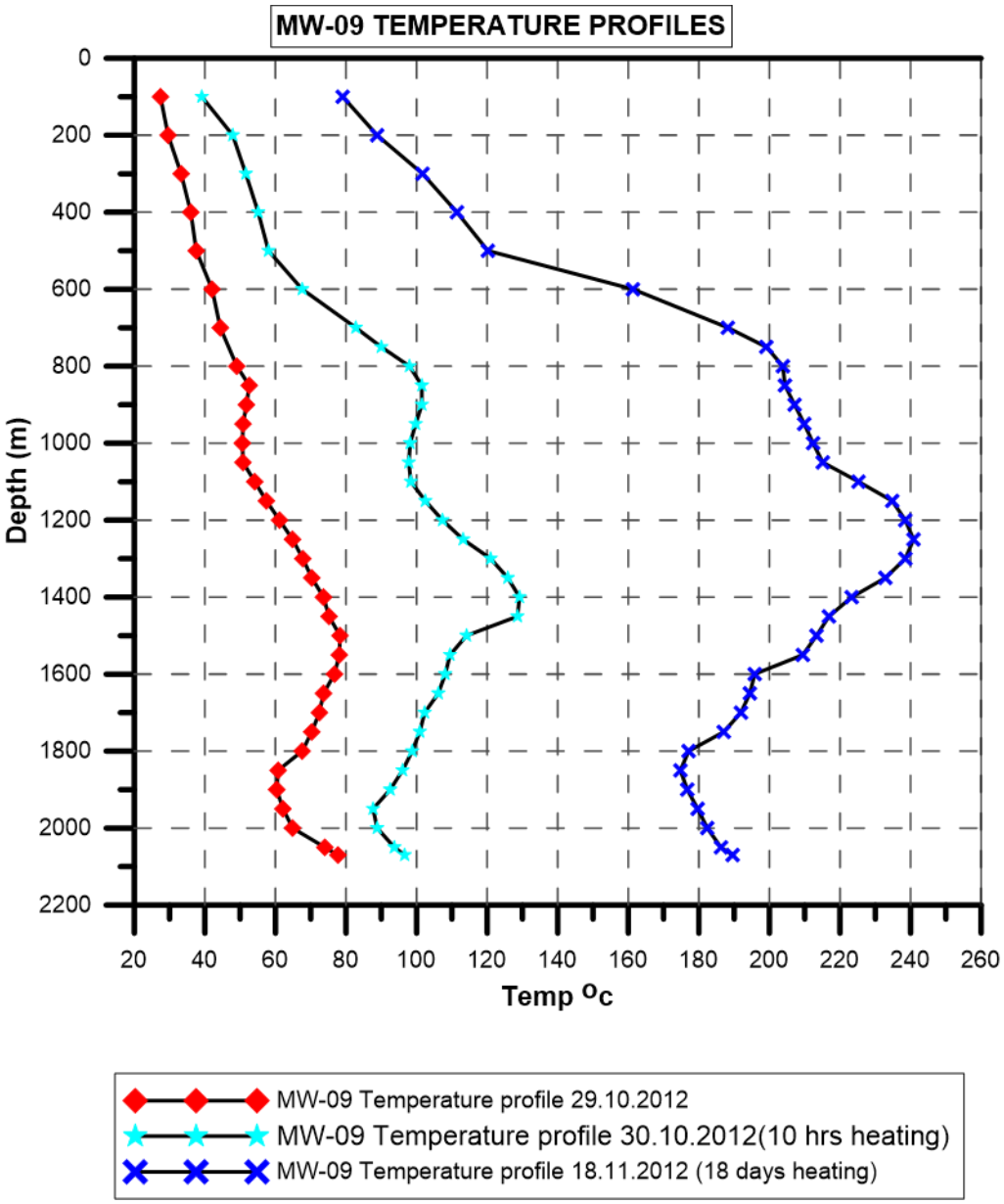

Appendix 4: MW - 09 Temperature profile

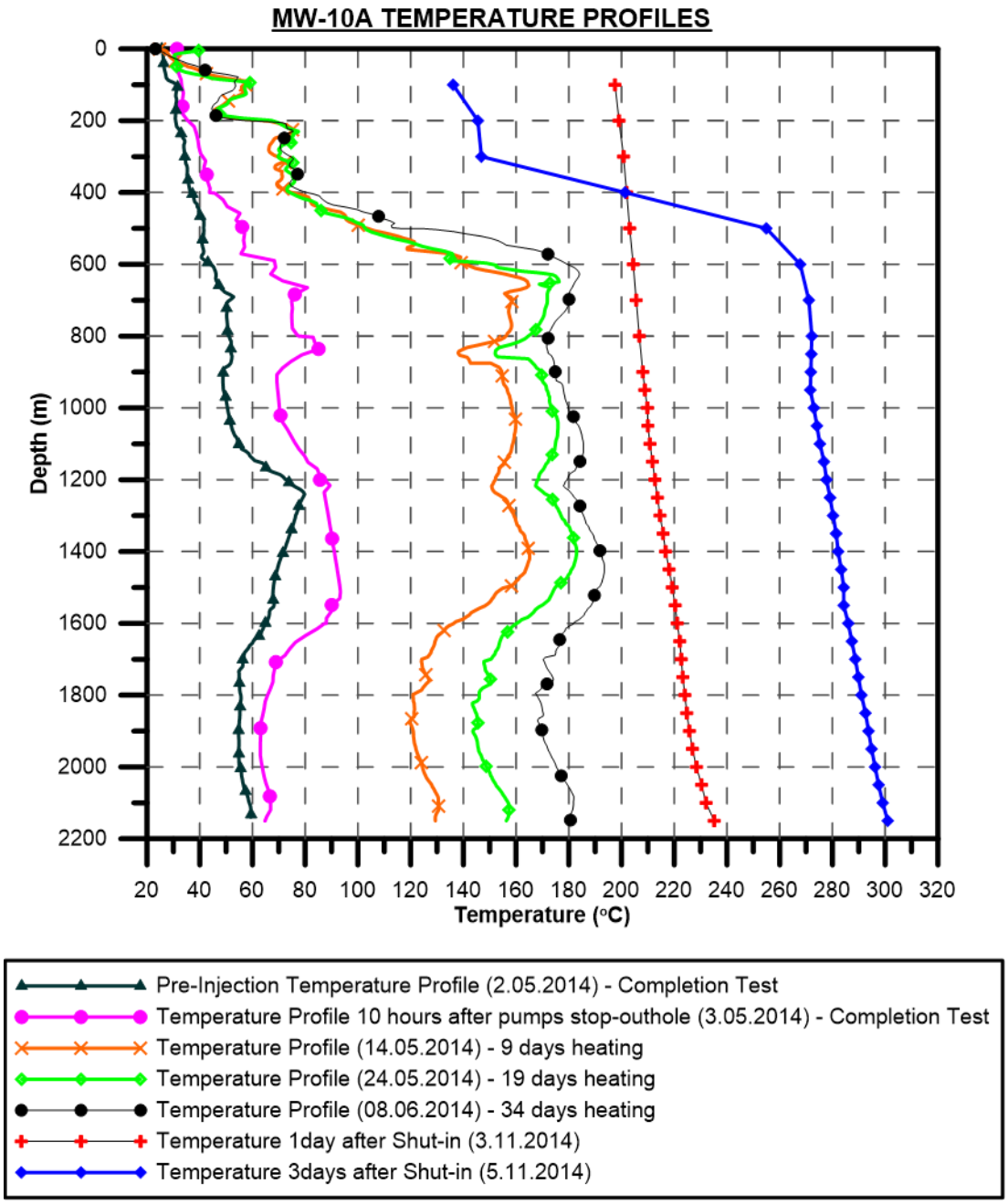

Appendix 5: MW - 10A Temperature profile

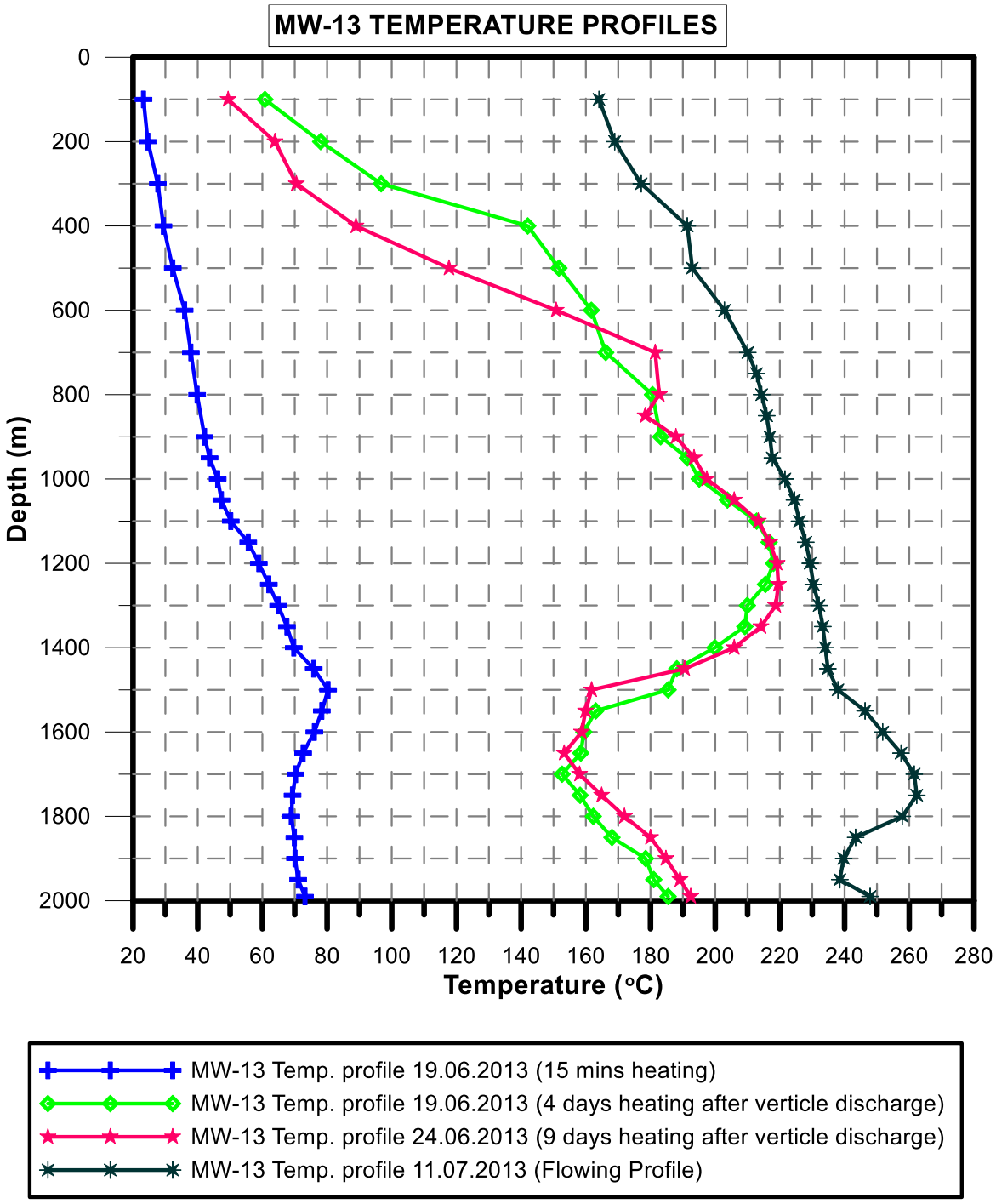

Appendix 6: MW- 13 Temperature profile

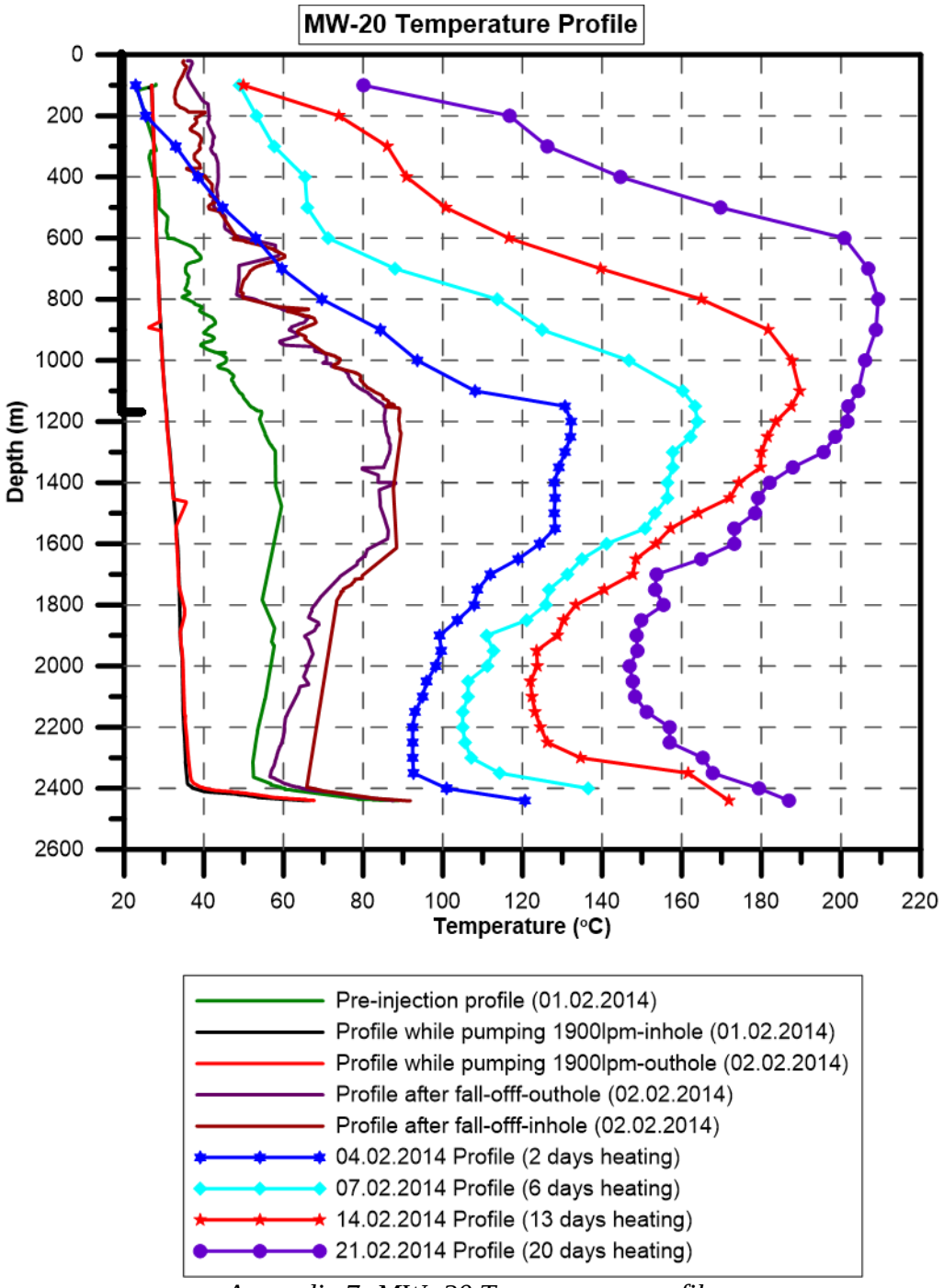

Appendix 7: MW- 20 Temperature profile

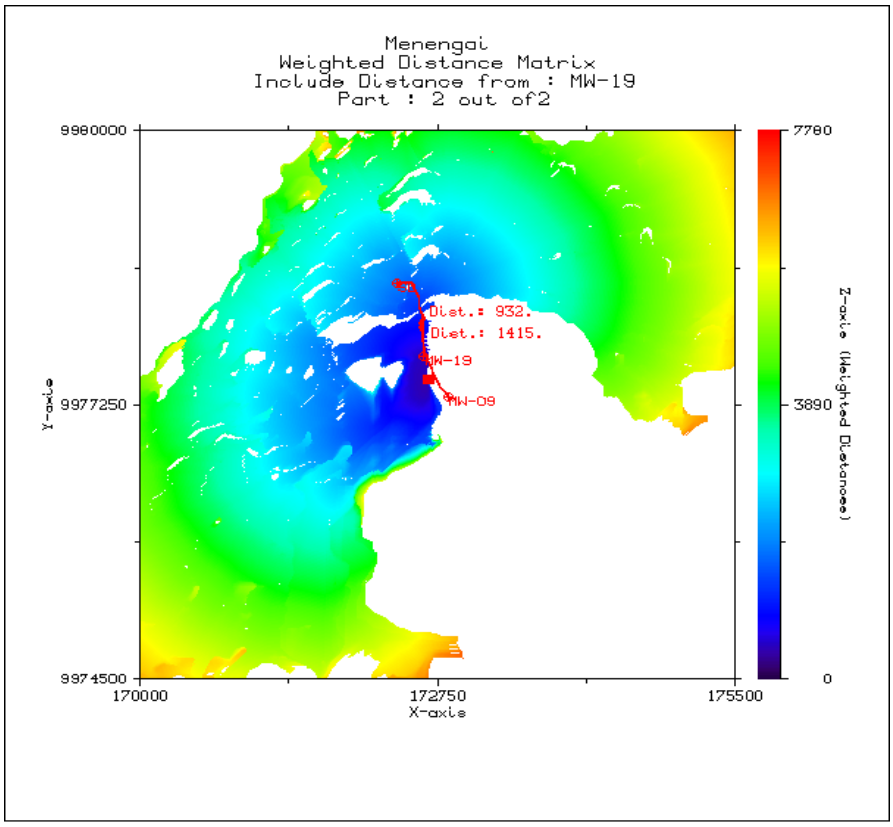

Appendix 8: Pipe route for MW-09 and MW-19 to area B

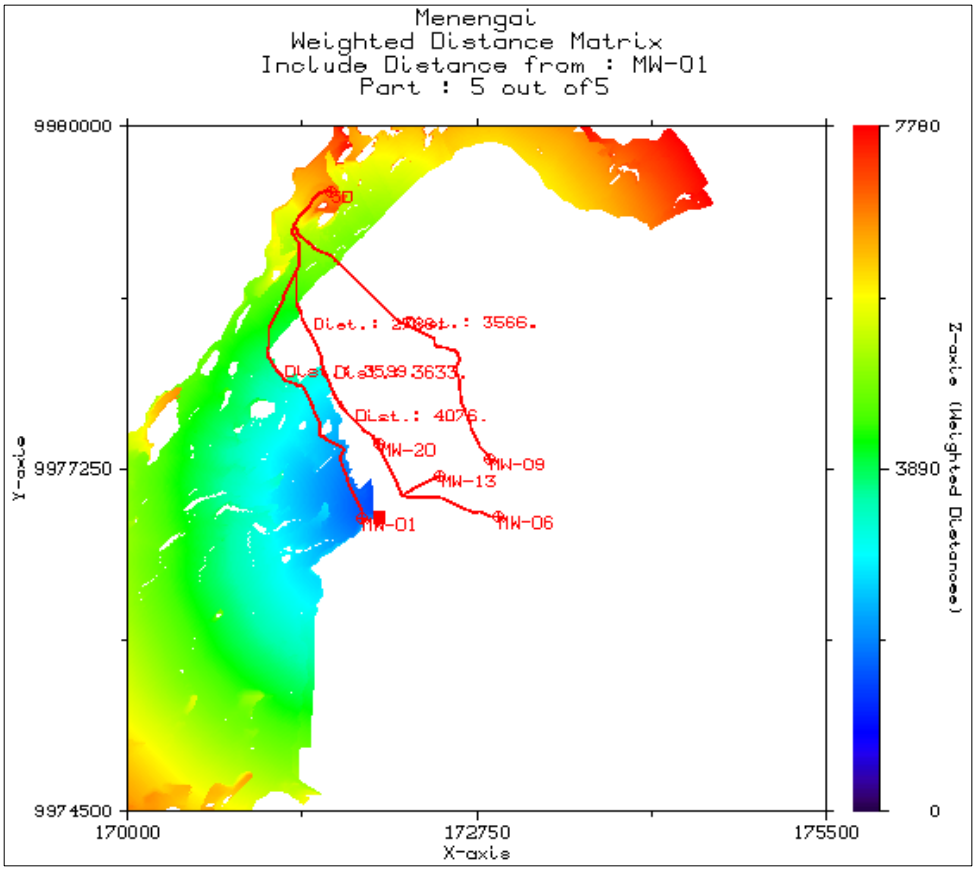

Appendix 9: Example of five wells run to MW-02

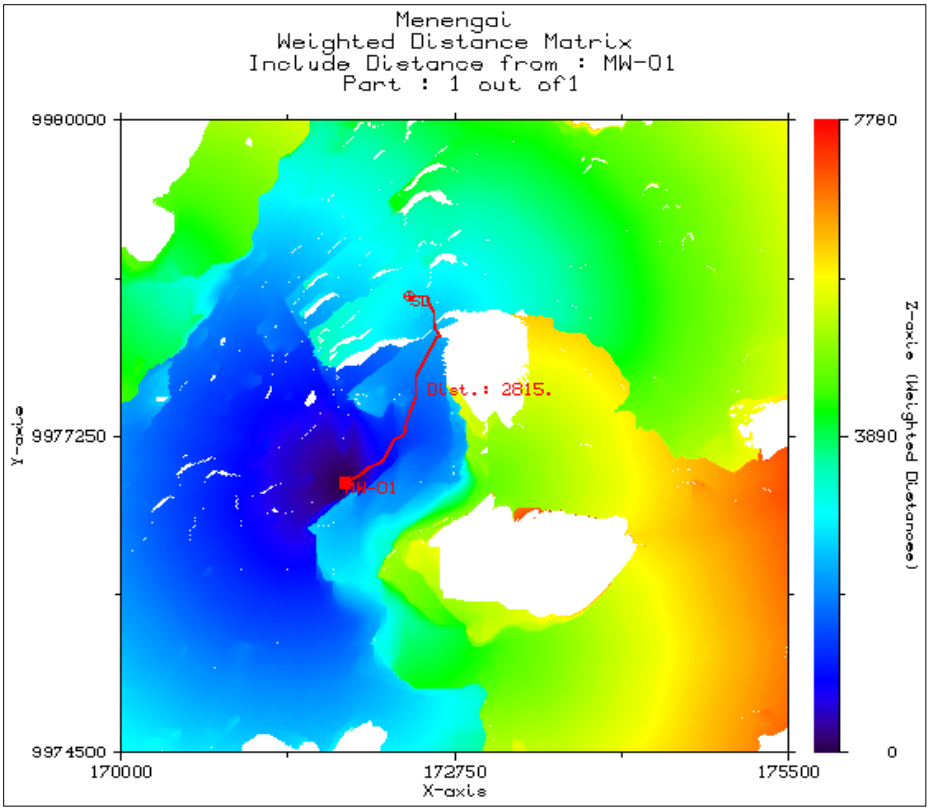

Appendix 10: Pipe route from MW-01 to area B

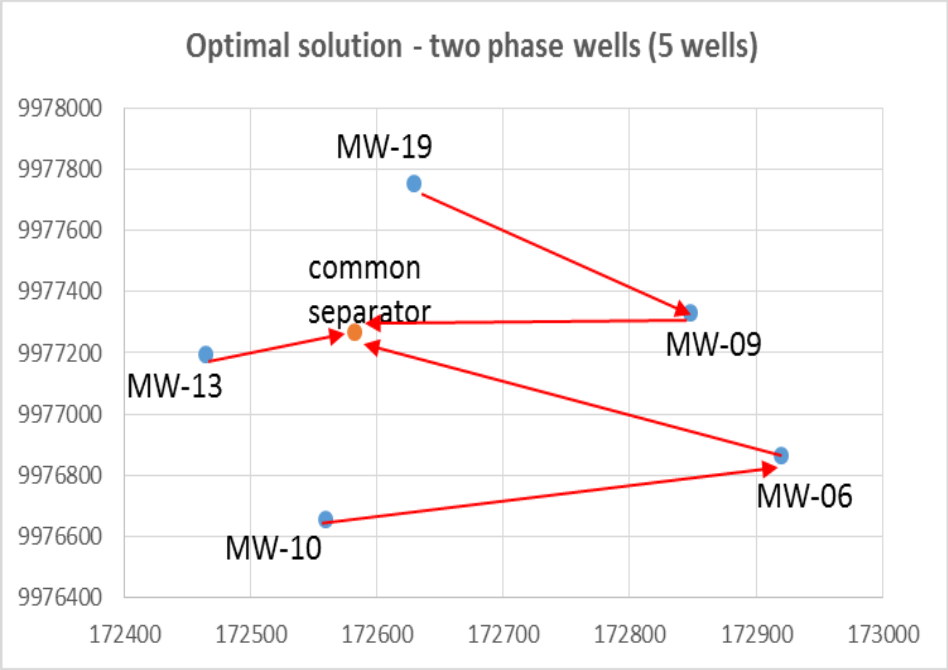

Appendix 11: Topology design for two phase pipelines, 5 wells

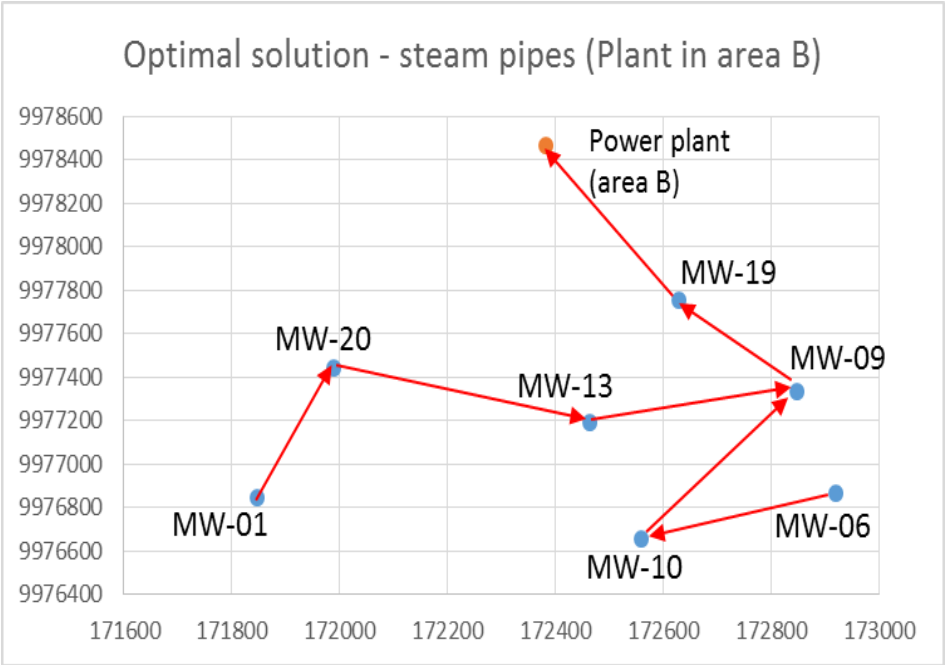

Appendix 12: Topology design for steam pipelines, power plant located in area B

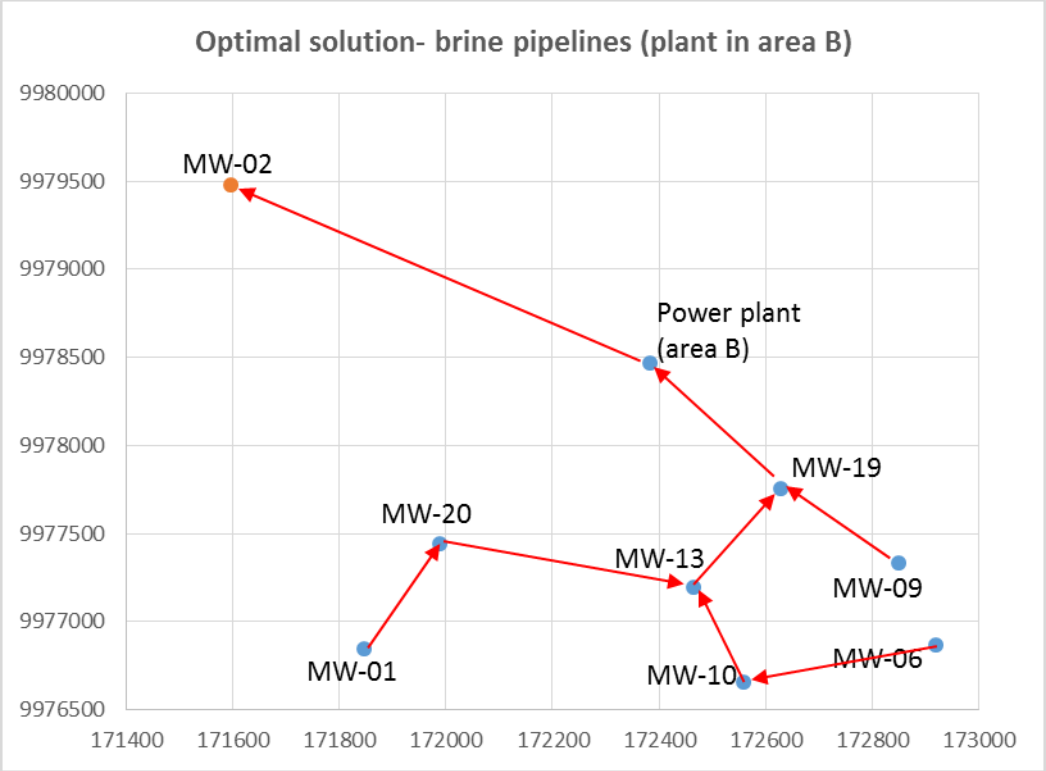

Appendix 13: Topology design for brine pipelines, power plant located in area B

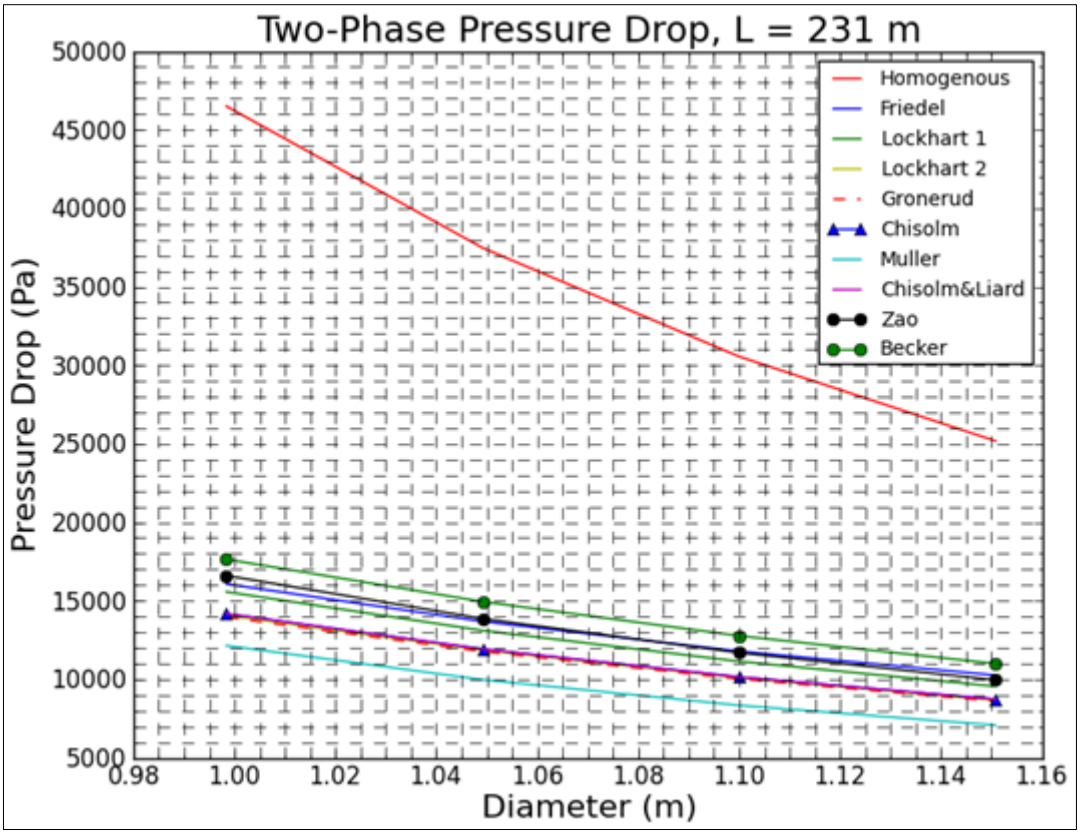

Appendix 14: Total two-phase pressure drop (MW-01 to common separator)

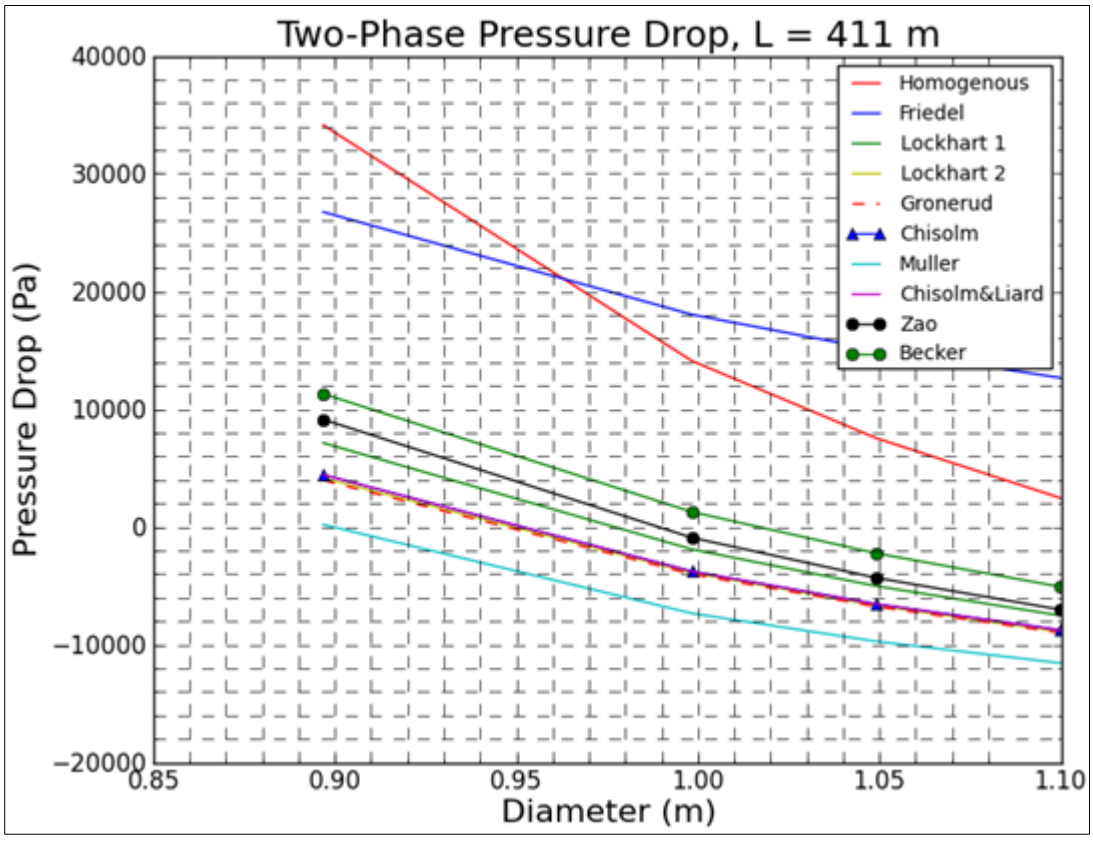

Appendix 15: Total two-phase pressure drop (MW-09 to MW-13)

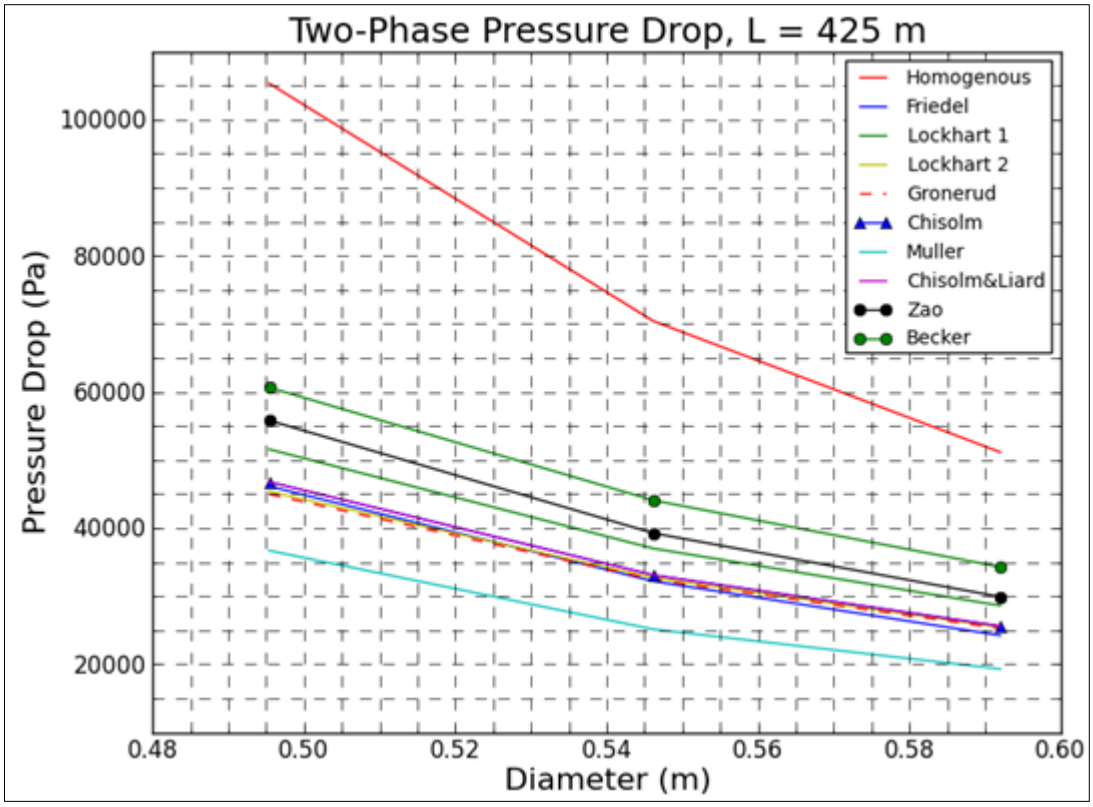

Appendix 16: Total two-phase pressure drop (MW-06 to MW-10)

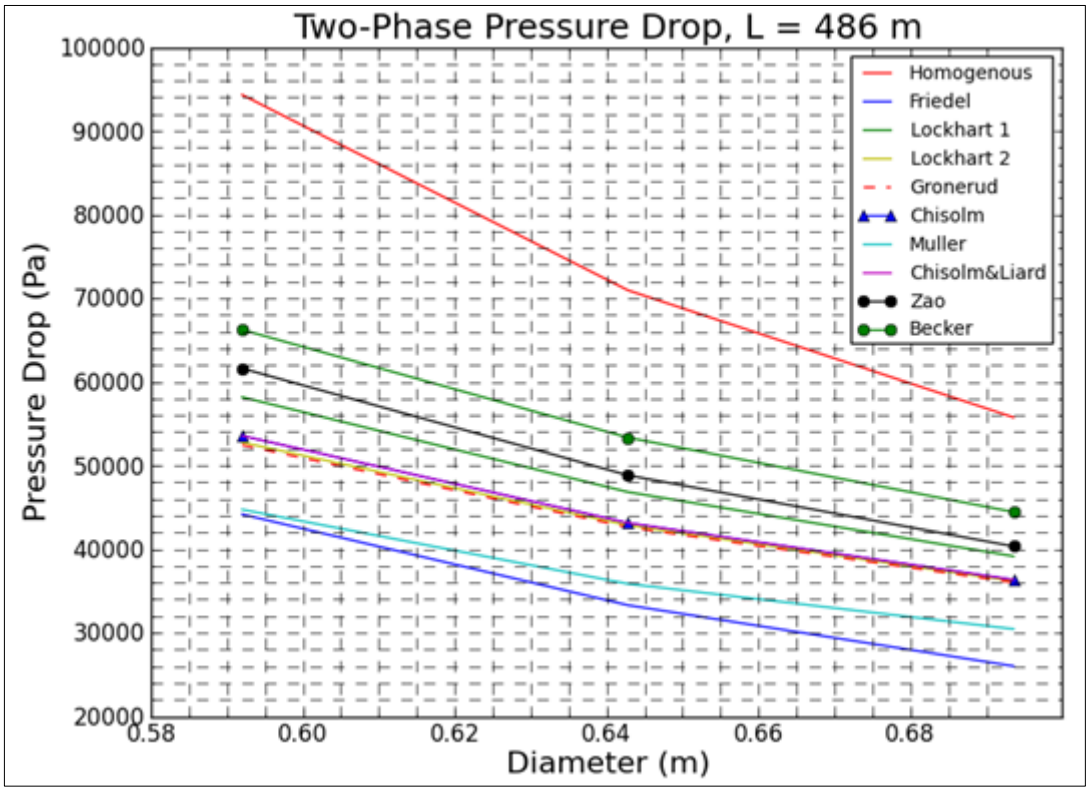

Appendix 17: Total two-phase pressure drop (MW-19 to MW-09)